Gersonde, R., Hodell, D.A., Blum, P., et al., 1999
Proceedings of the Ocean Drilling Program, Initial Reports Volume 177

6. SITE 1091[1]

Shipboard Scientific Party[2]

BACKGROUND AND OBJECTIVES

Site 1091 (proposed site TSO-5C) is located on the western flank of the Meteor Rise at a water depth of 4363 m near magnetic Anomalies 24–25 (early Eocene–late Paleocene), which represents the oldest oceanic crust between the Meteor Rise and the Mid-Atlantic Ridge (MAR). Oceanic crust began to form between the MAR and Meteor Rise as a result of a jump in the spreading center from the fossil ridge axis in the Agulhas Basin to the Meteor-Islas Orcadas Rises at ~62 Ma (Fig. **F5,** p. 39, in the "Leg 177 Summary" chapter). Site-survey *Thompson* Cruise TTN057 collected single-channel seismic profiles in the region surrounding Site 1091 (Fig. **F1**). Seismic profiles indicate a thick (~1200 m) package of sediment overlying normal oceanic crust (Fig. **F2**). We surveyed two areas that appeared promising on the basis of Parasound profiles collected by the *Polarstern*. The region to the southwest was deemed superior by virtue of its higher sedimentation rates and relatively uniform upper stratigraphic succession. A 13-m piston core (TTN057-10-PC3) recovered in the vicinity of Site 1091 contains latest Pleistocene sediments deposited at an average sedimentation rate of 80 m/m.y. The lithology consists of alternating diatom and calcareous ooze representing glacial and interglacial periods, respectively.

Site 1091 is located in the central Polar Front Zone (PFZ), ~2° north of the present-day position of the Polar Front (PF), ~2° south of the Subantarctic Front, and ~7°–8° south of the Subtropical Front (Fig. **F1,** p. 35, in the "Leg 177 Summary" chapter). Because of the close proximity to the PF, the sedimentary environment at Site 1091 is highly sensitive to changes of the frontal position. During glacial periods, opal accumulation rates increased markedly whereas carbonate export production and preservation declined. During the last glaciation, maximum biological productivity occurred within the PFZ and probably was fueled by iron fertilization of surface water, when iron was

F1. Track line and shotpoints for the site survey of Site 1091, **p. 19.**

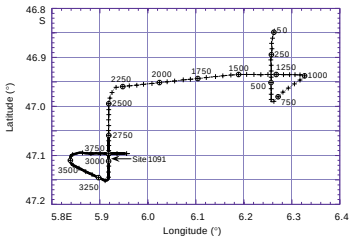

F2. Seismic profile showing the location and penetration depth of Site 1091, **p. 20.**

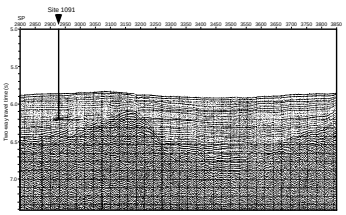

[1]**Examples of how to reference the whole or part of this volume.**
[2]**Shipboard Scientific Party addresses.**

Ms 177IR-106

possibly delivered by enhanced eolian dust input from periglacial Patagonian deserts (Kumar et al., 1995). However, a part of the glacial increase in accumulation rates can be attributed to lateral advection and sediment focusing (Frank et al., in press; Diekmann et al., in press). Site 1091 will be an important site for reconstructing the history of PFZ movement and for testing hypotheses related to glacial–interglacial changes in biological productivity and nutrient cycling in the Southern Ocean.

The high sedimentation rates at Site 1091 complement the record at Site 1089 (41°S) in the northern Subantarctic Zone and Sites 1093 and 1094 in the Antarctic Zone to the south. The north-south transect of high-resolution sites drilled during Leg 177 will be used to reconstruct past movement of the PFZ and Antarctic sea-ice field. Site 1091 will provide a high-resolution record in the northern PFZ and will permit the study of climate variability at orbital and suborbital (millennial) time scales. The record at Site 1091 can also be compared with lower sedimentation-rate signals obtained at Site 1092 and Ocean Drilling Program (ODP) Site 704 (Hodell and Venz, 1992; Hodell, 1993), located only ~60 km to the east of Site 1091 on the crest of the Meteor Rise. The water depth of Site 1091 (4363 m) places it within lower Circumpolar Deep Water (CDW) (Fig. F2, p. 36, in the "Leg 177 Summary" chapter). Together with Site 704 (2532 m) and Site 1092 (1988 m), Site 1091 forms a depth transect that can be used to study the history of middle to upper North Atlantic Deep Water (NADW) and lower CDW, respectively.

The primary objective of Site 1091 was to recover a high-resolution sequence within the PFZ that could be used to study

1. The Pliocene–Pleistocene history of migration of the PFZ and Antarctic sea-ice field;
2. Glacial–interglacial changes in biological productivity and dust flux to the Southern Ocean;
3. The history of millennial scale climate oscillations of the Southern Ocean region and its relation to climate records from the North Atlantic and polar ice cores;
4. The melting history of the Antarctic ice sheet and associated meltwater plumes during glacial–interglacial cycles of the late Pleistocene; and
5. Changes in lower CDW and Antarctic Bottom Water properties and their response to changes in the flux of NADW to the Southern Ocean during the Pliocene–Pleistocene Epochs.

OPERATIONS

Moderate winds from the west-northwest prevailed for the transit to Site 1091 on the western flank of the Meteor Rise. The 281-nmi transit was made in 30 hr, with an average speed of 9.3 kt. The positioning beacon was launched at 1845 hr on 1 January 1998.

Hole 1091A

Predicted severe weather (other than cold rain showers) failed to develop. Hole 1091A was spudded at 0445 hr on 2 January with the bit positioned at 4369 meters below rig floor (mbrf). The first core recovered 6.9 m and placed the seafloor depth at 4371.6 mbrf. Continuous

advanced hydraulic piston corer (APC) cores were recovered, with Cores 3H and 16H requiring a second wireline trip when the APC failed to actuate. Orientation began with Core 3H. A growing swell caused increasing pitch and vessel heave while coring was in progress, and a second swell added rolls of as much as 7°. For the safety of the drill string, knobby drilling joints were used from Core 17H, which was the first use of knobbies for APC coring in ODP's history.

Weather and motion conditions moderated, and the six knobby drilling joints were removed after Core 29H. Four additional cores were taken to 310.9 meters below seafloor (mbsf), when coring was terminated. The APC refusal point had not been reached, as cores were achieving full stroke and the maximum withdrawal overpull had been 60 kips. Most of the scientific objectives had been reached, however, and the forecast of imminent and exceptionally severe weather prompted the decision to pull out of the hole. The seafloor was cleared at 0315 hr on 4 January to end Hole 1091A.

Hole 1091B

The severe weather did not develop. The vessel was offset 10 m and the bit was positioned 3 m higher than it had been for Hole 1091A. Hole 1091B was spudded with the first APC core at 0455 hr on 4 January. Orientation began with Core 4H but was discontinued after Core 13H because the paleomagnetic data from Hole 1091A did not warrant the additional operating time.

By the morning of 5 January, wind gusts were approaching 40 kt and swells exceeded 20 ft in height. The severe heave conditions affected core recovery adversely and seemed to increase the frequency and severity of core-liner failures. Coring continued to the target depth of 274 mbsf, but recovery fell to ~60% for the final 10 cores.

Hole 1091C

The rig was offset by 10 m for a repeat section. A seafloor core was shot from 4372 mbrf, 3 m deeper than the original Hole 1091A mudline core. The driller's pressure gauge showed a mechanical actuation of the APC that significantly reduced prospects for a high-quality core, and it was requested that the interval be re-cored.

Hole 1091D

Normal actuation was indicated as a new hole was spudded from the same pipe depth (4372 mbrf). The severe weather and motion conditions persisted for the first few hours of coring but began improving rapidly in the evening hours of 5 January. Core recovery improved with depth as weather conditions moderated. When the target depth of 203 mbsf had been reached, the drill string was again pulled above the seafloor for a final attempt to fill gaps in the upper stratigraphic section.

Hole 1091E

The vessel was positioned 10 m north of Hole 1091B and Hole 1093E was spudded at 1440 hr on 6 January. Again the bit depth was 4372 mbrf because an important sediment gap existed in the uppermost core interval. Environmental operating conditions were favorable as six APC cores were taken to a depth of 51.7 mbsf. However, recovery was again

limited to ~61%. Nearly every core experienced some degree of core-liner failure, and some of the failures contributed directly to the reduced recovery.

Coring operations at Site 1091 were terminated as the allotted operating time expired. The drill string was recovered and the drill ship was underway at 0545 hr on 7 January.

LITHOSTRATIGRAPHY

Overview

Site 1091 was drilled to a total depth of 311 mbsf (325 meters composite depth [mcd]). Sediments from this site constitute one lithologic unit, are of Pleistocene and late Pliocene age, and consist of light to olive green diatom-rich ooze, with minor and varying amounts of nannofossils, foraminifers, and mud (Fig. F3). Smear-slide analysis (see the "Core Descriptions" contents list) shows that diatom abundance typically varies from 30% to 90%, total carbonate components (nannofossils + foraminifers) typically range from 0% to 40%, whereas mud exceeds 20% of the total composition only near the base of the section in Cores 177-1091A-30H through 33H. X-ray diffraction (XRD) analysis reveals similar trends in major lithologic components (Fig. F4; Table T1, also in ASCII format in the TABLES directory). Diatom-rich intervals are pronounced between 91 and 262 mcd. About 10 very thin (5–25 cm) and often calcareous-rich beds provide stratigraphic correlation among the three deeper holes (1091A, 1091B, and 1091D) drilled at this site.

Diatoms are the dominant lithologic component at this site, with lesser amounts of nannofossils, foraminifers, and mud (Fig. F4). A distinctive characteristic of the diatom-rich sediments is the presence of diatom mats, marked by a rough spongy surface texture that was observed after scraping the split cores (Fig. F5). The diatom assemblages observed are often dominated by a few species or contain near-monospecific assemblages of *Fragilariopsis kerguelensis, Thalassiothrix* sp., or *Actinocyclus ingens*. Although the sediments are classified mainly as diatom oozes and nannofossil-, foraminifer-, and/or mud-bearing diatom oozes, diatom nannofossil oozes occur in several sections, with nannofossil abundance as much as 90%. Total carbonate percentages obtained from smear-slide analysis (typically 0%–40%) are higher than percent $CaCO_3$ determined by coulometry, which is typically less than 20 wt% (see "Geochemistry," p. 13). In previous sites drilled during this leg, the carbonate concentrations determined by these two techniques were comparable. The discrepancy at this site may be caused by overestimation of the minor carbonate fraction in smear slides against the background of a dominant opal fraction. Foraminifer abundance obtained from smear-slide analysis in some cases exceeded 50%, and was especially high in the upper intervals (typically 10 m) of all holes. Mud content was uniformly low except in the basal sediments from this site, where mud exceeded 40% of the total composition and sedimentation rates were lower (~30 m/m.y.) than rates in the sediments above (~145 m/m.y.).

A variety of lithostratigraphic features, including paler carbonate and distinctive diatom horizons, were used to develop a sedimentological interhole correlation (Fig. F6). This information complemented multisensor track (MST) data (see "Chronostratigraphy," p. 6; "Physical Properties," p. 15) and aided in the preparation of a composite section

F3. Lithologic summary of Site 1091, p. 21.

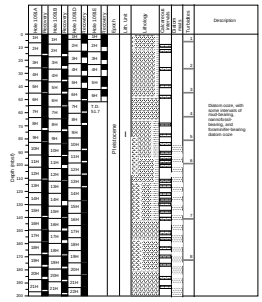

F4. Lithologic summary of carbonate, diatom, and mud contents at Site 1091, p. 23.

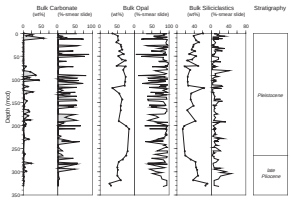

T1. X-ray diffraction data for Site 1091, p. 52.

F5. Diatom mats (interval 177-1091D-14H-2, 30–70 cm), p. 24.

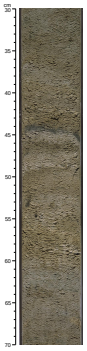

F6. Core correlation diagram for Site 1091, p. 25.

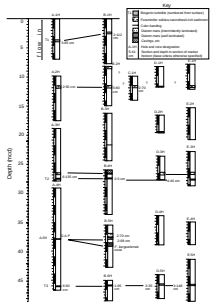

that, in turn, allowed placing cores within their proper stratigraphic context in terms of the mcd scale (Fig. F6). One lithologic unit was recognized at this site.

Description of Lithostratigraphic Unit

Unit I

Intervals: 177-1091A-1H through 33H (0–310.9 mbsf; 324.61 mcd); 177-1091B-1H through 29H (0–273.8 mbsf; 281.21 mcd); 177-1091D-1H through 22H (0–203.1 mbsf; 218.67 mcd); 177-1091E-1H through 6H (0–51.7 mbsf; 56.30 mcd)
Age: Pleistocene to Pliocene

The unit consists of Pleistocene and upper Pliocene medium green to olive diatom ooze, nannofossil-, foraminifer-, and mud-bearing diatom ooze, and diatom nannofossil ooze. Several intervals are essentially carbonate free, with the exception of the discrete carbonate-ooze horizons indicated on Figure F3 and several of the thin marker beds (Fig. F6). Carbonate is a minor but significant component of the sediment in intervals 0–9, 67–78, 111–140, 165–175, and 206–215 mbsf (all depths correspond to Hole 1091A; Fig. F3). Intervals of intermittently laminated diatom mats occur between 85 and 210 mbsf (Fig. F3), with minor layers above and below this interval. Color mottling is present throughout the unit and is manifested as brighter green and tan irregular layers, but specific ichnofossils are rare. Millimeter-scale laminations are intermittent, are purple and white in color with various textures (Fig. F7), and in many cases are present below diatom-mat layers. Small dropstones (1–2 cm) are scattered throughout the cores, and one large dropstone is present in Core 177-1091A-13H (Fig. F8). The bottom three cores of Hole 1091A are uniformly diatom rich and display a darker green color and more extensive bioturbation than the cores above. These cores are also quite mud rich (Fig. F4) and indicate lower sedimentation rates for the late Pliocene section (see "Chronostratigraphy," p. 6).

A number of distinctive 7- to 34-cm-thick marker beds occur at Site 1091 (Table T2; Fig. F6) and were used for interhole correlation among Holes 1091A, 1091B, 1091D, and 1091E. The beds are of two types: autochthonous carbonate-rich deposits likely related to peak interglacials (see "Chronostratigraphy," p. 6), and allochthonous deposits. The allochthonous beds have a number of common features, including marked color and textural differences with the surrounding sediment (including lack of bioturbation and absence of diatom mats), sharp lower contacts, and grading with 3- to 10-mm-thick basal layers of foraminifers and up to ~5% well-sorted, very fine-grained sand. Some beds appear to display cross-lamination at the base (Fig. F9), whereas others display little internal structure (Fig. F10). Several of these calcareous layers are enclosed within carbonate-free sediment and some contain reworked older nannofossils (Table T2; see "Chronostratigraphy," p. 6). Evidence of sedimentary structures indicating current activity combined with their carbonate contents suggests that these beds represent turbidity-current deposits, perhaps derived from the Meteor Rise to the east of Site 1091. The relatively high carbonate values associated with some of these beds may favor the interpretation of downslope transport of this material by turbidity currents (from above the carbonate compensation depth) rather than lateral transport by contour currents.

F7. Laminated bedding (interval 177-1091A-6H-1, 68–88 cm), p. 30.

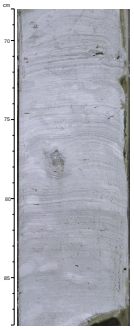

F8. Large diorite dropstone (interval 177-1091A-13H-1, 75–105 cm), p. 31.

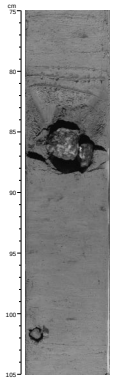

T2. Locations, descriptions, and characteristics of marker beds, p. 53.

F9. Thin marker bed (interval 177-1091B-27H-2, 140 cm, to 27H-3, 10 cm), p. 32.

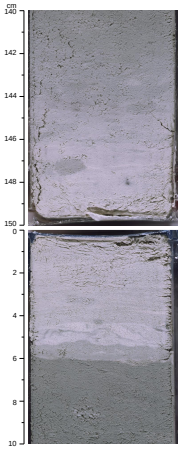

However, any genetic interpretation of these deposits is ambiguous until more detailed studies of grain-size distribution and geochemistry are performed.

CHRONOSTRATIGRAPHY

Composite Depths

MST and color reflectance data (650–750 nm) collected from Holes 1091A–1091E were used to determine depth offsets in the composite section. Magnetic susceptibility, gamma-ray attenuation (GRA) bulk density, and color reflectance measurements were the primary parameters used for core-to-core correlation at Site 1091. GRA and magnetic susceptibility data were collected at 2- to 4-cm intervals on cores recovered from Holes 1091A–1091E. Color reflectance data were collected at 4- to 6-cm intervals on cores from Holes 1091A, 1091B, 1091D, and 1091E (see **"Physical Properties,"** p. 15).

The composite data show that the cores from Site 1091 provide a nearly continuous overlap to 234 mcd (base of Core 177-1091A-23H). The data used to construct the composite section and determine core overlaps are presented on a composite depth scale in Figures **F11, F12,** and **F13**. The depth offsets for cores from Holes 1091A–1091E are given in Table **T3** (also in ASCII format in the **TABLES** directory).

Stretching and compression of sedimentary features in aligned cores indicate distortion of the cored sequence. Because much of the distortion occurred within individual cores on depth scales of <9 m it was not possible to align every feature in the MST and color reflectance records accurately by simply adding a constant to the mbsf core depth. Postcruise processing will be required to align sedimentary features within individual cores. Only after allowing variable adjustments of peaks within each core can a more precise estimate of core gaps be made.

Following construction of the composite depth section for Site 1091, a single spliced record was assembled for the aligned cores over the upper 234 mcd, primarily by using cores from Holes 1091A, 1091B, and 1091D. The composite depths were aligned so that splice tie points between adjacent holes occurred at exactly the same depths in mcd. Intervals having significant disturbance or distortion were avoided if possible. The Site 1091 splice (Table **T4,** also in ASCII format in the **TABLES** directory) can be used as a sampling guide to recover a single sedimentary sequence between 0 and 234 mcd. Spliced records of magnetic susceptibility, GRA bulk density, and color reflectance (Oregon State University Split Core Analysis Track [OSU-SCAT] data only, see **"Lithostratigraphy,"** p. 5, in the "Explanatory Notes" chapter) are shown in Figure **F14**.

One known gap exists between the base of Core 177-1091B-1H and the top of Core 2H. Correlation of MST data sets between Site 1091 and site-survey cores TTN057-10 and 11 suggests only about 0.5 m of section is missing across this gap. A second gap in the composite section may exist between the base of Core 177-1091A-8H and the top of Core 177-1091B-9H. None of the MST or color reflectance data sets could unambiguously verify the existence of an overlap.

At Site 1091, a relatively large number of splice tie points (about one-third) could not be based on prominent features identified in more than one of the MST and/or color reflectance data sets. In some cases, the splice tie points between cores could only be constructed using the

F10. Thick marker bed (interval 177-1091D-16H-2, 100–145 cm), **p. 33.**

F11. Smoothed magnetic susceptibility data from Site 1091, **p. 34.**

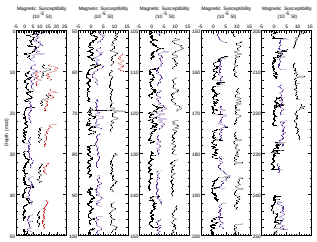

F12. Smoothed color reflectance data from Site 1091, **p. 35.**

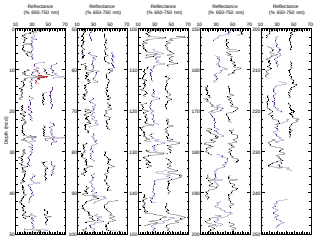

F13. Smoothed GRA bulk density data from Site 1091, **p. 36.**

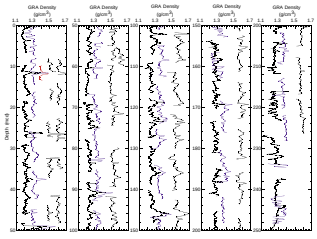

T3. Composite depths for Site 1091, **p. 54.**

known core-section depth of laterally correlative lithologic features such as biogenic turbidites, color banding, and diatom mats. We have identified these problematic splice tie points in Table T4.

T4. Site 1091 splice tie points, p. 56.

Biostratigraphy

Calcareous Nannofossils

Sediments recovered from Site 1091 provide a nearly continuous record of the Pleistocene–Pliocene interval. Calcareous nannofossil assemblages are characterized by common to rare abundances and medium to poor preservation. Several barren intervals mark the Pliocene–Pleistocene record and nannofossil events are, therefore, poorly defined. The biozones of Martini (1971) and Okada and Bukry (1980), as well as some additional events defined by Raffi et al. (1993) and Wei (1993) (see "Biostratigraphy," p. 10, in the "Explanatory Notes" chapter), were recognized within the Pleistocene interval. Figure F15, and Tables T5 and T6 (both also in ASCII format in the TABLES directory), summarize the main calcareous nannofossil biostratigraphic results.

F14. Spliced magnetic susceptibility, GRA bulk density, and color reflectance at Site 1091, p. 37.

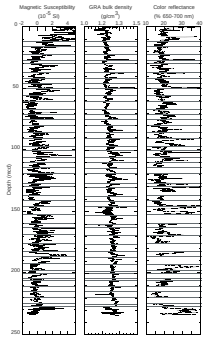

F15. Bio- and magnetostratigraphic correlations and age designations for Site 1091, p. 38.

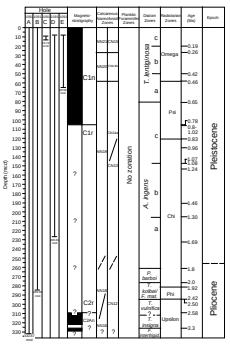

Pleistocene

The Pleistocene interval is represented from 0 to ~260 mcd (Fig. F15). The first occurrence (FO) of medium *Gephyrocapsa* (4–5.5 µm) approximates the Pliocene/Pleistocene boundary between 231.6 and 233.9 mcd (Fig. F15). The FO of *Emiliania huxleyi* is found from 26.34 to 27.58 mcd (base of Zone NN21). The last occurrence (LO) of *Pseudoemiliania lacunosa* is placed between 57.44 and 60.41 mcd, defining the base of Zone NN20. *Reticulofenestra asanoi* is recognized in Hole 1091A from 123.48 to 147.60 mcd, although specimens of this species are recorded in scattered samples to a depth of 45.72 mcd and are interpreted as reworked (Table T5). The reentrance of medium *Gephyrocapsa* is present between 127.62 and 132.37 mcd. Large *Gephyrocapsa* (>5.5 µm) are observed from 158.06 to 188.83 mcd in Site 1091. The LO of *Calcidiscus macintyrei* is not identified in Hole 1091A because this species is very rare or absent (Tables T5, T6).

T5. Main calcareous nannofossil species in Hole 1091A, p. 57.

Pliocene

The presence of *Pseudoemiliania lacunosa* (FO within Zones NN14/NN15 according to Rio et al., 1990) as well as the absence of other typical cosmopolitan and relatively dissolution-resistant lower Pliocene species, such as *Reticulofenestra pseudoumbilicus* (LO at the top of Zone NN15) (Table T5), allow us to assign the lower part of Hole 1091A (below 260.0 mcd) to the late Pliocene. This is in agreement with other biostratigraphic information (Fig. F15). However, characteristic dissolution-resistant and relatively warm-water upper Pliocene markers (e.g., *Discoaster brouweri* and *Discoaster pentaradiatus*) are absent in the analyzed samples and prevent a more accurate zonal assignment.

T6. Biostratigraphic age assignments for Site 1091, p. 60.

Planktic Foraminifers

At Site 1091, the abundance of planktic foraminifers varies considerably between the studied core-catcher (CC) samples (Table T7, also in ASCII format in the TABLES directory). All samples were either dry-sieved at 150 µm (Samples 177-1091A-1H-CC, 9–14 cm [6.84 mbsf], through 12H-CC, 0–10 cm [109.25 mbsf]) or wet-sieved at 63 and 150 µm (starting with Sample 177-1091A-13H-CC, 6–16 cm [121.08 mbsf]).

T7. Major planktic foraminifer species at Site 1091, p. 63.

Although, in many cases, the abundance of planktic foraminifers is low in the examined CC samples, the number of specimens present (almost always *Neogloboquadrina pachyderma* [sinistral]) is high enough for stable isotopic analyses in most cases. It should be noted, however, that the abundance estimates given in Table T7 are based on a sample volume of ~20 cm^3. The preservation of planktic foraminifers at Site 1091 is good to moderate and fragmentation is low. The low abundance of planktic foraminifers recorded in many of the studied CC samples seems mainly to be the result of dilution by siliceous microfossils or low productivity rather than dissolution of carbonate. Alternatively, dissolution might have reached the state where fragments start to dissolve. Even in samples with extremely few planktic foraminifers, however, there are no signs of corrosion on the foraminifer tests. Hence, it is likely that the relatively high sedimentation rate at this site has kept dissolution of calcium carbonate to a minimum.

Generally, *N. pachyderma* (sinistral) dominates the planktic foraminifer assemblages and this species is present in all foraminifer-bearing CC samples. Additional species present in the >150-µm fraction are *Globigerina quinqueloba, Globigerina bulloides, Globigerinita glutinata, Globigerinita uvula, Globorotalia inflata, Globorotalia puncticulata, Globorotalia puncticuloides, Globorotalia truncatulinoides,* and *N. pachyderma* (dextral).

Benthic Foraminifers

At Site 1091, benthic foraminifers are generally not very abundant and vary considerably in their state of preservation. Problems were encountered with picking benthic foraminifers from the highly abundant, needle-shaped remains of the diatom genus *Thalassiothrix* in the >63-µm fraction. Under the given time constraints it was necessary to wet-sieve sediment samples at >150 µm after Sample 177-1091A-12H-CC had been processed. The change in sieve size is clearly apparent in Table T8 (also in ASCII format in the TABLES directory). The general absence of small tests of *Alabaminella weddellensis* and marked increase in large, robust *Melonis pompiliodes* below 109.25 mbsf in Hole 1091A are clearly an artifact of this change in sample preparation. A cursory examination of the 63- to 150-µm fraction residues confirms the presence of *A. weddellensis* in most samples.

T8. Benthic foraminifers at Site 1091, p. 65.

Although highly variable, benthic foraminifers typically constitute between 5% and 10% of the total foraminifer fauna from the >150-µm fraction studied. Absolute foraminifer abundances are variable and low, reaching a maximum of 21 specimens/cm^3 in Sample 177-1091B-1H-CC, 9–14 cm. Low benthic foraminifer abundances may be explained by the relatively high sedimentation rates (see "Stratigraphic Summary," p. 12). Several barren intervals (5 out of 62 samples) suggest that a continuous benthic foraminifer isotopic record from this site will be difficult to obtain. However, *Cibicidoides* spp. and *Oridorsalis umbonatus* are recorded in 33 of the 62 samples examined and, given sediment volumes >20 cm^3, it may be possible to generate a combined benthic stable isotopic record from these taxa at Site 1091.

Quantitative estimates of relative species abundance were made from Holes 1091A and 1091B, with counts of up to 315 specimens per sample. Species richness is variable, with a maximum of 29 taxa recorded in Sample 177-1091A-27H-CC, 11–16 cm, and a minimum of 1 taxon recorded in a number of samples (Table T8). Not all of this variability can be accounted for by sample size (see "Biostratigraphy," p. 10, in the "Explanatory Notes" chapter), but may be a function of generally

poor preservation and selective loss in certain intervals. However, low sample abundance and poor foraminifer preservation are not well correlated. Closer sampling intervals and well-constrained age-depth models on millennial time scales will be required to determine whether or not benthic foraminifer production, dilution, or preservation best explains this variability.

The most common benthic taxa recorded at Site 1091 include *A. weddellensis, Cibicidoides* aff. *wuellerstorfi, Eggerella bradyi, M. pompiliodes, O. umbonatus, Pullenia bulloides, Pullenia quinqueloba,* and *Pullenia subcarinata*. The assemblages present are mostly dominated by infaunal taxa and presumably responded to the high primary productivity in the surface waters above this site.

Diatoms

In addition to the CC samples obtained from all holes, we have examined smear slides from sections in Hole 1091A (Table **T9,** also in ASCII format in the **TABLES** directory). All diatom stratigraphic information from the four holes was combined and converted to the mcd scale (Tables **T6, T10**, both also in ASCII format in the **TABLES** directory). Diatoms are abundant in almost all the samples studied above ~270 mcd at Site 1091. In the lowermost part of Site 1091, characterized by low sedimentation rates below 270 mcd, diatom abundance varies between few and abundant. The preservation of diatom assemblages is generally moderate or good (Fig. **F16;** Table **T9**). During examination of the diatom assemblages, we also encountered silicoflagellates in trace numbers, as well as sporadic *Actiniscus* specimens and sponge spicules (Table **T9**).

T9. Diatom, silicoflagellate, ebridian, *Actiniscus*, sponge spicule, and phytolith occurrence, Site 1091, **p. 67.**

T10. Control points used to calculate sedimentation rates at Site 1091, **p. 73.**

F16. Diatom abundance and preservation of significant diatom taxa at Site 1091, **p. 39.**

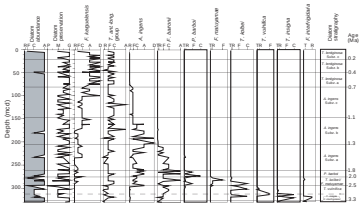

Biostratigraphy

The *Thalassiosira lentiginosa* Subzone b, which ranges from the top of marine isotope Stage (MIS) 7 to the base of MIS 11, is placed between 21.0 and 49.50 mcd (Fig. **F15**). This indicates that peak values in color reflectance (650–700 nm) recorded at 26.5, 38, and 49 mcd (Fig. **F14**) are associated with the climatic optima of MISs 7, 9, and 11, respectively. This interpretation is supported by calcareous nannofossil stratigraphic events, such as the FO of *Emiliania huxleyi* at 27 mcd and the LO of *Pseudoemiliania lacunosa* at 58.9 mcd that occur in MISs 8 and 12, respectively (Table **T10**). The top of the *Actinocyclus ingens* Zone, marked by the LO of *A. ingens*, can be placed at ~80.7 mcd. Below this, the *A. ingens* Subzone b ranges between 147.9 and 205.8 mcd. Assemblages assigned to the upper Pliocene *P. barboi* Zone, which underlies the *A. ingens* Zone and corresponds with the Olduvai Subchron of the Matuyama Chron, were found between 262 and 277 mcd. Below this interval, the *Thalassiosira kolbei–Fragilariopsis matuyamae* Zone, which ranges between 2 and 2.5 Ma, is recognized. In this interval, the age-depth model indicates a drop in sedimentation rates to ~30 m/m.y. (Table **T10**). The relatively short *T. kolbei–F. matuyamae* Zone at Site 1091 may indicate the presence of one or more short hiatuses. The *Thalassiosira vulnifica* Zone, which ranges between 2.5 and 2.6 Ma, has been identified between 294.8 and 312.1 mcd. The range of the *T. vulnifica* Zone straddles the boundary between the Matuyama and Gauss Chrons at 2.58 Ma. This is consistent with the interpretation of the magnetostratigraphic data obtained at this site (see **"Paleomagnetism,"** p. 11; Fig. **F15**). This interval is underlain by only a few meters (312.1–316.4 mcd) containing assemblages assigned to the upper

Pliocene *Thalassiosira insigna* Zone, which ranges between 2.6 and 3.3 Ma. This assignment is based on the co-occurrence of *Fragilariopsis weaveri, T. vulnifica,* and *T. insigna*. According to Harwood and Maruyama (1992), the LO of *F. weaveri* can be placed at ~2.7 Ma and thus falls in the upper portion of the *T. insigna* Zone. On the basis of this stratigraphic sequence of the marker taxa in the *T. insigna* Zone, we suggest that the upper portion of this zone is not represented at Site 1091 because of a hiatus (Fig. **F15;** Table **T10**). The base of Site 1091, only recovered in Hole 1091A, is assigned to the *Fragilariopsis interfrigidaria* Zone, which ranges between 3.26 and 3.8 Ma. We note the co-occurrence of the nominate taxon and *F. weaveri*, which has its FO in the uppermost part of the *F. interfrigidaria* Zone (Harwood and Maruyama, 1992).

Paleoceanographic Implications

The abundance distribution of diatoms and specific diatom taxa can be used to interpret the general paleoenvironmental evolution at Site 1091 since the early late Pliocene. The transition from diatom-rich sediments, deposited at high sedimentation rates, to sediments with lower diatom contents, deposited at lower sedimentation rates, may indicate a drastic change in opal export productivity rates in the latest Pliocene, at ~2 Ma. This change is possibly related to the establishment of water-mass distributions and oceanic frontal systems that allowed enhanced biosiliceous export rates. Mass deposition of taxa such as *Fragilariopsis kerguelensis* led to high opal sedimentation in the late and mid-Pleistocene, whereas *Actinocyclus ingens* and *Thalassiothrix longissima* were prominent contributors of high opal accumulation rates during the early Pleistocene (Fig. **F16**). This led to the formation of so-called diatom mats (see **"Lithostratigraphy,"** p. 4). A similar distinct acme of *A. ingens* was also found between ~165 and 225 mcd in the *A. ingens* Subzones b and a. An *A. ingens* acme at about the same time as that observed at Site 1091 has been described by Gersonde and Bárcena (1998) from piston cores recovered in the Subantarctic area of the Atlantic sector of the Southern Ocean. The great abundance of the genus *Hemidiscus* within the *F. interfrigidaria* Zone (Core 177-1091A-33H) suggests warm surface waters during the mid-Pliocene.

Radiolarians

Radiolarian biostratigraphy at Site 1091 is based on the examination of 36 CC samples (Table **T11,** also in ASCII format in the **TABLES** directory). All samples yielded well preserved, abundant Pleistocene to late Pliocene radiolarians. The radiolarian assemblages recovered are mostly of an Antarctic origin, and all existing Antarctic Pliocene to Pleistocene radiolarian zones from the Upsilon to the Omega Zone (Lazarus, 1992) are found at this site.

T11. Main components of the radiolarian assemblages at Site 1091, **p. 74.**

In Hole 1091A, the boundary of the Omega and Psi Zones (0.46 Ma) is recognized between Samples 177-1091A-3H-CC, 12–17 cm (25.4 mbsf, 27.63 mcd), and 5H-CC, 9–15 cm (44.09 mbsf, 46.46 mcd). The boundary of the Psi and Chi Zones (0.83 Ma) can be placed between Samples 177-1091A-14H-CC, 16–21 cm (130.54 mbsf, 139.2 mcd), and 16H-CC, 11–16 cm (148.34 mbsf, 162.25 mcd). However, the LO of *Pterocanium trilobum,* which defines the top of the Chi Zone, is found in Sample 177-1091B-9H-CC, 11–16 cm (82.88 mbsf, 83.6 mcd) (Table **T11**). This depth corresponds to the middle part of the Psi Zone in Hole 1091A, suggesting reworking of *P. trilobum* in Hole 1091B. Conse-

quently, the boundary of the Psi and Chi Zones is placed at ~120 mcd between Samples 177-1091A-12H-CC, 0–10 cm (109.25 mbsf, 116.51 mcd), and 177-1091B-13H-CC, 10–15 cm (122.09 mbsf, 124.20 mcd) (Table T10). Likewise, the boundary of the Chi and Phi Zones (1.92 Ma) is recognized between Samples 177-1091B-28H-CC, 20–25 cm (255.60 mbsf, 275.43 mcd), and 29H-CC, 11–16 cm (268.87 mbsf, 285.04 mcd), although the latter sample contains reworked specimens of *Helotholus vema,* which defines the underlying Upsilon Zone. Finally, the boundary of the Phi and Upsilon Zones (2.42 Ma) is placed between Samples 177-1091A-28H-CC, 22–27 cm (263.22 mbsf, 285.69 mcd), and 30H-CC, 10–15 cm (281.43 mbsf, 303.90 mcd). The first appearance datum (FAD) of *Cycladophora davisiana* at 2.58 Ma is recognized in the Upsilon Zone between Samples 177-1091A-30H-CC, 10–15 cm (281.43 mbsf, 303.90 mcd), and 32H-CC, 30–35 cm (299.17 mbsf, 321.64 mcd) (Table T10; Fig. F15).

Boundaries of all the aforementioned zones are defined by the last appearance datum of marker species rather than the more reliable FAD. In addition, abundances of marker species, especially *Stylatrctus universus* and *Pterocanium trilobum,* are rare to few in the assemblages examined. Additional work will, therefore, be required to determine the precise zonal boundaries at this site.

Paleomagnetism

Archive halves of APC cores recovered at Site 1091 were measured using the shipboard pass-through magnetometer. Measurements were made at 5-cm intervals. Sections obviously affected by drilling disturbance were not measured. Core 177-1091A-1H was measured after alternating-field (AF) demagnetization at peak fields of 0 (natural remanent magnetization [NRM]), 5, 10, 15, and 20 mT. Cores 177-1091A-2H through 10H were measured after peak fields of 0, 10, 20, and 25 mT. Core 177-1091A-11H was measured after peak fields of 0, 10, 20, 25, 30, and 35 mT. Cores 177-1091A-12H through 33H and 177-1091B-1H through 2H were measured after peak fields of 0, 10, 20, 25, and 30 mT. Cores 177-1091B-3H through 29H were measured after peak fields of 0, 10, 20, and 30 mT, and Cores 177-1090E-1H through 14H were measured after peak fields of 0, 20, and 30 mT.

NRM intensities are about 1×10^{-2} A/m at the top of each hole, decrease through the upper 20 mbsf to ~1×10^{-3} A/m, and remain fairly uniform thereafter for most of the cored interval. In Hole 1091A, NRM intensities >1×10^{-2} A/m were found below 250 mbsf. After AF demagnetization at peak fields of 25 to 30 mT, intensities generally decreased to ~3.5×10^{-4} A/m above 250 mbsf and to ~3×10^{-3} A/m below. NRM inclinations are typically steep down as a result of a magnetic overprint, probably largely attributable to the drill string. The drill-string remagnetization was largely removed at peak demagnetization fields in excess of 10 mT; the resulting inclination values, however, are highly scattered (Figs. F15, F17; Table T10). Magnetization directions attributed to the Matuyama Chron are particularly inconsistent, probably as a result of normal polarity magnetic overprints associated with (1) drilling-related core deformation and (2) magnetite dissolution and growth of iron sulfides in a reducing diagenetic environment.

The Brunhes/Matuyama boundary can be identified in the 95.50- to 102.40-mbsf interval of Hole 1091A. The Matuyama/Gauss boundary is tentatively identified in the 285.80- to 288.70-mbsf interval of Hole

F17. Inclination of the remanent magnetization after AF demagnetization at Holes 1091A, 1091B, and 1091D, p. 40.

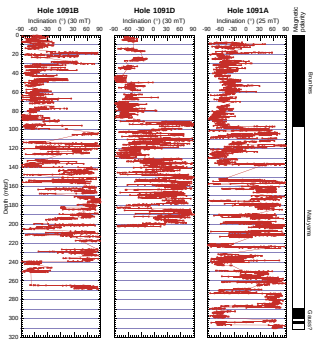

1091A (Fig. F17). No other polarity transitions can be identified with any confidence.

Stratigraphic Summary

A 310.9-m-thick (332.87 mcd) sedimentary section was recovered at Site 1091. Holes 1091A–1091E were cored with the APC to 310.9, 273.8, 4, 203.1, and 51.7 mbsf, respectively. The combined MST and color reflectance data provide a nearly continuous section to 234 mcd (base of Core 177-1091A-23H) (Figs. F10, F11, F12, F13). One known gap exists (~0.5 m) between the base of Core 177-1091B-1H and the top of Core 2H. A second gap in the composite section may exist between the base of Core 177-1091A-8H and the top of Core 177-1091B-9H. At Site 1091, a relatively large number of splice tie points could not be defined on the basis of prominent features identified in more than one of the MST and/or color reflectance data signals.

The age of the recovered section at Site 1091 is Holocene to late Pliocene, displaying high sedimentation rates in the Pleistocene interval (~145 m/m.y.; Fig. F18). Although the lithology at Site 1091 is dominated by siliceous microfossils (diatoms and radiolaria), the sediments contain enough calcareous nannofossils for the establishment of a combined biosiliceous/calcareous biostratigraphy, particularly in the thick Pleistocene interval. Unfortunately, the shipboard pass-through magnetometer measurements indicate strong disturbances and normal polarity overprints of the magnetization record, probably related to core deformation, magnetite dissolution, and post-sedimentary growth of iron sulfides. This results in highly scattered inclination values that only allow the identification of the Brunhes/Matuyama and Matuyama/Gauss boundaries (Table T10; Fig. F17). Marine isotope stages can be identified for the last 700 k.y. by using a combination of physical properties variations that reflect glacial–interglacial variability in carbonate and opal content, the abundance pattern of the diatom *Hemidicus karstenii,* and radiolarian and calcareous nannofossil biostratigraphic events. This preliminary interpretation must be confirmed by postcruise stable isotopic measurements of planktic and benthic foraminifers that occur in sufficient numbers throughout the Site 1091 record.

All biostratigraphic datums, magnetostratigraphic results, and interpretation of physical properties records yield consistent age assignments throughout the record at Site 1091. The climatic optima of MISs 7, 9, and 11 have been identified at 26.5, 38, and 49 mcd, respectively (Fig. F14). This indicates average sedimentation rates of ~120 m/m.y. for the last 0.42 m.y. The average sedimentation rates during the Pleistocene, which has its base at ~261 mcd, were ~145 m/m.y. This is consistent with the common occurrence, especially in the early Pleistocene, of so-called diatom mats (see "Lithostratigraphy," p. 4) that mainly consist of *Actinocyclus ingens* or diatoms belonging to the *Thalassiothrix antarctica-longissima* group. A distinct drop in sedimentation rates is seen below ~285 mcd in upper Pliocene sediments assigned to the *T. kolbei/F. matuyamae* diatom Zone and the Phi radiolarian Zone. The decrease in diatom abundance may indicate that at least part of this drastic drop in sedimentation rates is related to a change in opal export rates, probably caused by changes in hydrographic conditions that controlled biosiliceous production. However, it cannot be ruled out that the presence of the relatively thin sedimentary section in the lowermost Matuyama Chron might also be caused by one or more hiatuses in

F18. Age-depth plot of biostratigraphic and paleomagnetic events at Site 1091, p. 41.

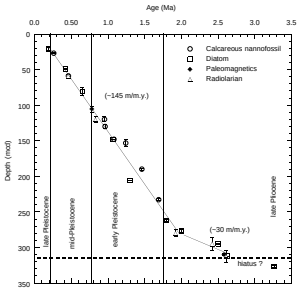

this interval. A distinct change in sedimentation rates at ~2 Ma was also reported for Site 704, drilled on Meteor Rise east of Site 1091. Hodell and Venz (1992) proposed that the increase in sedimentation rates between the late Pliocene and Pleistocene was related to a northward expansion of nutrient-rich Antarctic water masses.

The absence of diatom assemblages representing the upper portion of the *Thalassiosira insigna* Zone suggests a possible hiatus at ~311 mcd. This zone is correlated to the upper portion of the Gauss Chron (see "Biostratigraphy," p. 10, in the "Explanatory Notes" chapter) and the hiatus may span a time interval ranging at least from 2.6 to 2.7 Ma. The oldest sediments recovered at Site 1091, belonging to the upper *Fragilariopsis interfrigidaria* diatom Zone and the Upsilon radiolarian Zone, are somewhat older than 3.3 Ma. Thus, the normal polarity magnetic interval observed at the base of Hole 1091A may represent part of C2An.3n in the Gauss Chron.

GEOCHEMISTRY

Volatile Hydrocarbons

As a part of the shipboard safety and pollution program, volatile hydrocarbons (methane, ethane, and propane) were measured in the sediments of Site 1091 from every core in Hole 1091A using the standard ODP headspace sampling techniques. Results are presented in Table T12 and Figure F19. Headspace methane concentrations were generally low (2–22 parts per million by volume [ppmv]) throughout the sedimentary sequence at Site 1091. Ethane, propane, and other higher molecular weight hydrocarbons were not observed.

Interstitial Water Chemistry

Shipboard chemical analyses of the interstitial water from Site 1091 followed the procedures for Sites 1088–1090. The results from the shipboard analyses (Table T13; Fig. F20) were obtained from 33 interstitial water samples from Hole 1091A to a depth of 307 mbsf. Interstitial water samples were taken from every core throughout the entire section.

Unlike previous sites, Site 1091 has relatively low calcium carbonate ($CaCO_3$) content (except in a few narrow horizons; see Fig. F21; "Solid Phase Analysis," p. 15; "Lithostratigraphy," p. 4) and very abundant diatom opal. This distinct sedimentary composition results in subtle, but observable, differences from previous sites in the interstitial water profiles of chemical species determined by shipboard analyses. First, the chlorinity maximum, possibly associated with the last glacial period, is somewhat more pronounced (with a single high value of 571 mM) and is located at a deeper depth (50 mbsf) than at Sites 1088–1090. The salinity maximum is also observed clearly in the Na^+ profile at Site 1091 because of the lack of significant gradients in the upper part of the section for the major cations and anions other than Cl^- (Na^+ was calculated by charge balance). There is a slight minimum in Cl^- of 565 mM at 127–137 mbsf. These same features are reproduced in more detail at Site 1093. At present, it is not clear why the Cl^- profiles at Sites 1091 and 1093 are so distinct from those of previous sites, but there are two important sedimentological characteristics that might affect the diffusion process. First, the sedimentation rate is fairly high (the aver-

T12. Concentrations of methane at Site 1091, p. 76.

F19. Concentration of methane vs. depth at Site 1091, p. 42.

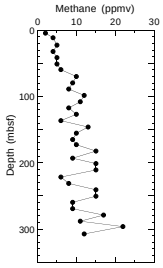

T13. Interstitial water chemistry at Site 1091, p. 77.

F20. Interstitial water chemistry profiles vs. depth at Site 1091, p. 43.

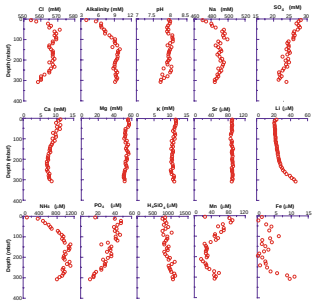

F21. $CaCO_3$, TOC, TN, TS, and TOC/TN vs. depth at Hole 1091A, p. 44.

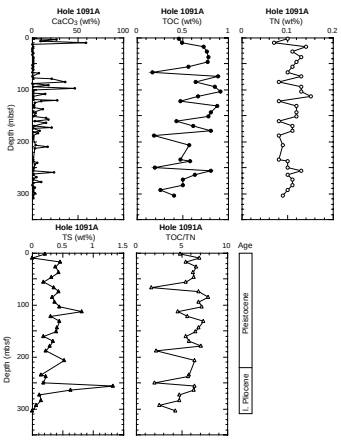

age is ~100 m/m.y. in the upper 100 m), perhaps resulting in an accumulation that was rapid enough to deepen the Cl^- maximum. Second, numerous diatom mats are present between 85 and 230 mbsf (see "Lithostratigraphy," p. 4) that may restrict diffusion enough to preserve a lower salinity signal from previous interglacial periods. Of course, it is inappropriate to speculate further without additional shore-based measurements of $\delta^{18}O$ and diffusional modeling. Also, given the limitations of shipboard analyses, there is little that can be said about the decrease in Cl^- below 250 mbsf, except that it presumably results from the influence of lower salinity waters deeper in the sediment.

The low $CaCO_3$ content of Site 1091 sediments produces Ca^{+2}, Mg^{+2}, and Sr^{+2} profiles that show little or no evidence of carbonate diagenesis. Ca^{+2} concentrations are essentially constant at near-bottom-water concentrations (~10.5 mM) down to ~90 mbsf and then decrease slightly to concentrations of ~7 mM in a broad minimum from 200 to 250 mbsf. The decrease in Ca^{+2}, which is not accompanied by any apparent change in Mg^{+2} concentrations, may reflect authigenic calcite precipitation resulting from the increase in alkalinity. Mg^{+2} and Sr^{+2} concentrations are essentially constant throughout the section within the analytical uncertainty of these determinations.

K^+ concentrations are also constant throughout the section at near-bottom-water concentrations of ~10.4 mM, suggesting little net interaction of K^+ with clay minerals or basement (which is at ~1200 mbsf at Site 1091). Li^+ does show some evidence for small decreases from bottom-water concentrations in the uppermost 150 m, possibly connected to authigenic calcite precipitation. Below 250 mbsf, Li^+ increases steeply as a result of a deep source, perhaps a higher concentration of volcanic detritus in deeper sediments or interaction with basement. Because basement is at ~1200 mbsf at Site 1091, the steep increase in Li^+ is more likely related to the composition of deeper sediments, as indicated by the increased mud content and significantly lower sedimentation rates at the bottom of the section (see "Lithostratigraphy," p. 4; "Chronostratigraphy," p. 6).

The redox characteristics of Site 1091 sediments can be classified as reducing based on the observation of dissolved H_2S (by scent, although often faint) in Cores 177-1091A-3H through 31H. However, sulfate concentrations decrease only modestly from near-bottom-water concentrations of ~28 mM at 4 mbsf to ~22 mM around 300 mbsf. Numerous observations of pyrite in smear slides throughout the section (see "Lithostratigraphy," p. 4), as well as the moderately high total organic carbon (TOC) and total sulfur (TS) contents (see Fig. F21; "Solid Phase Analysis," p. 15), suggest that sulfate concentrations may not reflect the long-term redox character of these sediments (see below). Furthermore, downhole sulfate reduction rates must be relatively slow, considering the observed maximum alkalinity and ammonium concentrations of ~10 and 1 mM, respectively, at ~150 mbsf.

Both Sites 1089 and 1091 have similar TOC content (~0.5 wt%), but the fact that sulfate concentrations decrease to near zero by 50 mbsf at Site 1089 and only decrease by about 20%–25% by 300 mbsf at Site 1091 reflects a fundamental difference in the nature of organic-matter degradation. The difference in diffusion and burial rates between Sites 1091 and 1089 could conceivably only explain part of the difference in sulfate profiles. One possible explanation stems from the observed downhole variations in alkalinity, ammonium, and phosphate (Fig.

F20) at Site 1091. Alkalinity and ammonium increase gradually to maxima around 150 mbsf, whereas the maximum in phosphate is observed between 20 and 30 mbsf. The phosphate maximum probably reflects more labile bulk organic matter that is oxidized in the upper 30 to 40 m of sediment. During periods of very rapid sediment accumulation (glacials), this upper zone could become intensely reducing and may be the source of the significant pyrite formation seen lower in the section. Downhole, alkalinity and ammonium increase as a result of degradation of a more refractory organic fraction with very low phosphate content. This low-phosphate organic fraction is likely opal-intrinsic, implying that it would only become available for oxidation upon the slow dissolution of the opal.

The presence of dissolved Mn^{+2} and Fe^{+2} concurrent with dissolved H_2S is curious and not altogether consistent with the scenario of more intensely reducing conditions during glacial periods (because reactive Mn and Fe would have been removed from the surface sediments if such conditions existed). One possible explanation for this problem is that mildly reducing conditions at depth could have worked slowly on the mud-rich sediments sampled at the bottom of the section (and presumably present deeper below the sampled interval) to reduce relic Mn and Fe. Downhole, sulfate reduction rates are slow and insufficient to precipitate all of the dissolved Fe^{+2}. The scent of H_2S was faint in many samples, and was not detected at all in Cores 177-1090A-32H and 33H. Furthermore, the increases in Mn^{+2} and Fe^{+2} below 200 mbsf (Fig. F20) are consistent with the hypothesis that the deeper mud-rich sediments are at least part of the source of the Mn^{+2} and Fe^{+2} observed higher in the section.

Solid Phase Analysis

The shipboard solid phase analysis at Site 1091 consisted of measurements of inorganic carbon, total carbon, total nitrogen (TN), and TS (for methods see "Geochemistry," p. 18, in the Explanatory Notes" chapter). The results of Hole 1091A are presented in Table T14 and Figure F21. $CaCO_3$ contents in Hole 1091A range from 0.2 to 58.9 wt%, with an average value of 5.7 wt%. With our coarse sampling resolution, the percentage of $CaCO_3$ appears to be very low (nearly zero) in the upper Pleistocene sedimentary sequence from 12 to 78 mbsf. TOC contents vary between 0.17 and 0.91 wt%, with an average value of 0.60 wt%. TOC contents at Site 1091 are slightly higher than those of Sites 1089 and 1090, which are located between the Subtropical Convergence and the Subantarctic Front. TN contents are generally low (0.07–0.15 wt%). Although the TS content of most samples is less than 0.5 wt%, one high value (1.33 wt%) was observed in Sample 177-1091A-28H-2, 69–70 cm (256 mbsf). TOC/TN values vary between 1.7 and 7.9, indicating a predominance of marine organic material (Fig. F22). Pyrolysis analyses were not performed because of the low organic carbon in these sediments.

T14. Analytical results of IC, CaCO3, TC, TOC, TN, TS, and TOC/TN at Site 1091, p. 79.

F22. TOC vs. TN at Hole 1091A, p. 45.

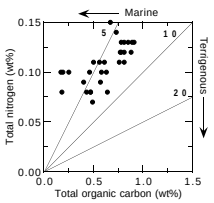

PHYSICAL PROPERTIES

GRA bulk density, magnetic susceptibility, natural gamma-ray (NGR) emission, and *P*-wave velocity were measured with the MST on whole-core sections recovered from Site 1091. Color reflectance and resistivity

were measured on the working half of all split APC cores using the OSU-SCAT (see **"Lithostratigraphy,"** p. 5, in the "Explanatory Notes" chapter). Color reflectance was also measured with the Minolta CM-2002 spectrophotometer on cores from Holes 1091D and 1091E. Other physical properties measurements conducted on discrete core samples included moisture, density, and *P*-wave velocity. Measured parameters were initial wet bulk mass (M_b), dry mass (M_d), and dry volume (V_d). Velocity was measured on split-core sections using the *P*-wave velocity sensor 3 (PWS3). Table **T15,** and Figures **F23** and **F24,** summarize the physical properties measurements performed at Site 1091.

T15. Physical properties measurements conducted at Site 1091, **p. 81.**

Multisensor Track and Density

There is good agreement between discrete-sample densities (determined using the moisture and density [MAD] method) and GRA bulk densities (Figs. **F23, F25**). Densities range between 1.1 and 1.4 gcm^3 and show a gradual increase downhole, but the median density is low (1.2 g/cm^3), reflecting the dominance of diatom-rich sediments at this site (see **"Lithostratigraphy,"** p. 4). In the upper 270 mcd, densities >~1.3 g/cm^3 are associated with carbonate oozes. Below 270 mcd, average bulk density increases as a result of lower porosities, which may, in turn, be a result of an increase in mud content and lower sedimentation rates in the lower part of the core (see **"Lithostratigraphy,"** p. 4; **"Chronostratigraphy,"** p. 6).

Reflectance generally covaries with density, resistivity, magnetic susceptibility, and NGR (Fig. **F23**). Notable exceptions occur when mud becomes a significant component of the sediment (e.g., below 270 mcd, and also in discrete intervals indicated on Fig. **F24** at 32 and 41 mcd). In such cases, resistivity, magnetic susceptibility, and NGR increase, but reflectance shows little or no response.

F23. Site 1091 porosity, resistivity, *P*-wave velocity, bulk density, magnetic susceptibility, and NGR, **p. 46.**

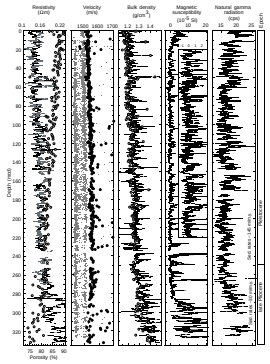

F24. Variations of resistivity, NGR, magnetic susceptibility, density, and reflectance in the upper 100 mcd, **p. 47.**

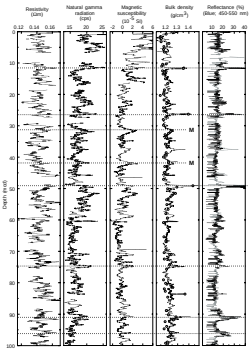

P-wave Velocity

P-wave velocities measured with the PWS3 velocimeter increased gradually and steadily downhole from values of 1510 m/s at the top to values of 1550 m/s at the bottom (Fig. **F23**), reflecting the gradual increase in bulk density. As with all previous Leg 177 sites, *P*-wave logger (PWL) velocities obtained from the MST were problematic in that values were considerably lower than those of the PWS3 and showed a clear bimodal distribution with mode averages of ~1450 and 1500 m/s (Fig. **F23**). The reason for this was a defective threshold adjustment knob, which was corrected while the first few cores were being logged at Site 1093.

F25. Relationship between GRA and MAD bulk density at Site 1091, **p. 48.**

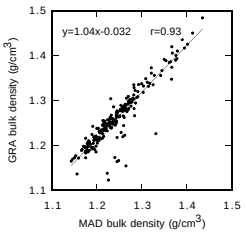

Resistivity and Porosity

The high water content of the diatom-rich sediments results in very high porosities at Site 1091 (Fig. **F23**). Porosity determined gravimetrically on discrete samples (MAD method) ranged from 74% to 90%, and resistivity showed the expected inverse relationship with porosity (values range from 0.1 to 0.2 Ωm). There is an overall gradual decrease in porosity (increase in resistivity) downhole as a result of compaction. Deviations from this trend in the upper 270 mcd are associated with intervals of high carbonate content, in which porosities are much lower. Below

270 mcd, porosity decreases in response to increasing mud content in the sediments.

Reflectance

The downhole reflectance pattern for sediments at Site 1091 is substantially different from those observed at previous sites drilled during Leg 177. This, presumably, is a result of the intermittent but generally low carbonate content of the sediments (see "Geochemistry," p. 13). The lack of carbonate can be inferred from the generally low blue reflectance values between 0 and 80 mcd, which average ~16% and are punctuated by brief reflectance peaks (Fig. F26). These brief events, some of which exceed 30% reflectance, correspond to spikes of higher GRA density (Fig. F24). These bright, dense layers correlate with carbonate-rich intervals (see "Lithostratigraphy," p. 4), although shipboard carbonate measurements (see "Geochemistry," p. 13) are too sparse to resolve these small-scale features.

Between 80 and 235 mcd, reflectance values exhibit rhythmic variability that may be related to alternation between dark diatom mats (see "Lithostratigraphy," p. 4) and brighter carbonate layers. Indication of these alternations can be seen not only as simple changes in sediment brightness (Fig. F26), but also as changes in the character of the reflectance spectra (Fig. F27). Intervals rich in carbonate exhibit bright reflectance with little divergence between the blue, red, or near-infrared bands. In contrast, intervals that are rich in diatoms exhibit a greater contrast between blue and red reflectance.

Cores from Holes 1091A and 1091B were scanned for reflectance with the OSU-SCAT system, whereas cores from Holes 1091D and 1091E holes were measured using the handheld Minolta CM-2002 spectrophotometer to increase the rate of core processing. The measurements produced by these two systems were similar enough to be of assistance during shipboard hole-to-hole correlation (see "Chronostratigraphy," p. 6). There was, however, a difference in the amplitude of the signals generated by the two instruments in intervals where sediments are diatom-rich relative to the good agreement observed between the two instruments in the carbonate-rich sediments of Site 1089 (Fig. F26). The Minolta CM-2002 signal appears somewhat muted relative to that of the OSU-SCAT. This could arise from the more accurate 4-point reflectance calibration of the OSU-SCAT as opposed to the 2-point calibration used by the CM-2002. In addition, measuring cores through Glad plastic wrap with the CM-2002 contributes to slight changes in the spectral response of the instrument (Balsam et al., 1997).

Thermal Conductivity

A total of 150 thermal conductivity measurements were made on cores from three holes at Site 1091 (Table T16, also in ASCII format in the TABLES directory; Fig. F28). The measured values range from 0.63 to 0.76 W/(mÞK), which is the lowest and narrowest range at Sites 1088–1091. The distribution of measured values is unimodal, with a mean of 0.68 W/(m·K) (Fig. F28A). The linear correlation between thermal conductivity and bulk density measurements is poor at this site (Fig. F28B), even though a correlation appears to exist visually (Fig. F28C). The low correlation coefficient is the result of low-resolution signals for both thermal conductivity and bulk density, as a result of the monotonous composition and water content of these diatom oozes.

F26. Site 1091 variations in OSU-SCAT and Minolta spectral reflectance measurements, p. 49.

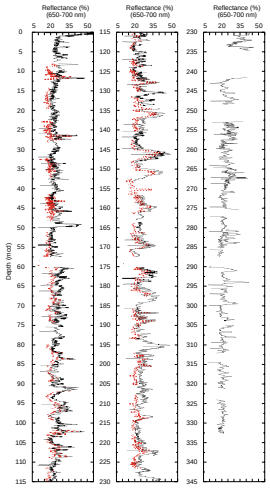

F27. Comparison of blue and red reflectance measurements from Site 1091, p. 50.

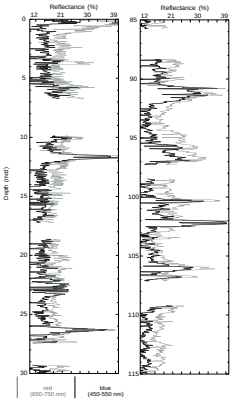

T16. Thermal conductivity measurements at Site 1091, p. 82.

F28. Thermal conductivity measurements at Site 1091, p. 51.

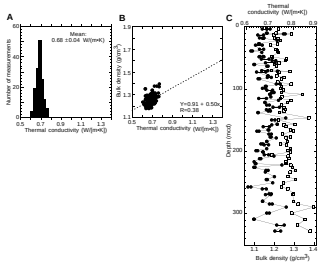

REFERENCES

Balsam, W.L., Damuth, J.E., and Schneider, R.R., 1997. Comparison of shipboard vs. shore-based spectral data from Amazon-fan cores: implications for interpreting sediment composition. *In* Flood, R.D., Piper, D.J.W., Klause, A., Peterson, L.C. (Eds.), *Proc. ODP, Sci. Results*, 155: College Station, TX (Ocean Drilling Program), 193–215.

Diekmann, B., Kuhn, G., MacKensen, A., Petschick, R., Fütterer, D.K., Gersonde, R., Rühlemann, C., and Niebler, H.-S., in press. Kaolinite and chlorite as tracers of modern and late Quaternary deep water circulation in the South Atlantic and the adjoining Southern Ocean. *In* Fischer, G., and Wefer, G. (Eds.), *Proxies in Paleoceanography: Examples from the South Atlantic:* Heidelberg (Springer).

Frank, M., Gersonde, R., and Mangini, A., in press. Sediment redistribution, $^{230}Th_{ex}$-normalization and its implications for the reconstruction of particle flux and export paleoproductivity. *In* Fischer, G., and Wefer, G., *Proxies in Paleoceanography: Examples from the South Atlantic:* Heidelberg (Springer).

Gersonde, R., and Bárcena, M.A., 1998. Revision of the late Pliocene-Pleistocene diatom biostratigraphy for the northern belt of the Southern Ocean. *Micropaleontology*, 44:1–15.

Harwood, D.M., and Maruyama, T., 1992. Middle Eocene to Pleistocene diatom biostratigraphy of Southern Ocean sediments from the Kerguelen Plateau, Leg 120. *In* Wise, S.W., Jr., Schlich, R., et al., *Proc. ODP, Sci. Results,* 120: College Station, TX (Ocean Drilling Program), 683–733.

Hodell, D.A., 1993. Late Pleistocene paleoceanography of the South Atlantic sector of the Southern Ocean: Ocean Drilling Program Hole 704A. *Paleoceanography,* 8:47–67.

Hodell, D.A., and Venz, K., 1992. Toward a high-resolution stable isotopic record of the Southern Ocean during the Pliocene-Pleistocene (4.8 to 0.8 Ma). *In* Kennett, J.P., Warnke, D.A. (Eds.), *The Antarctic Paleoenvironment: A Perspective on Global Change* (Pt. 1). Am. Geophys. Union, Antarct. Res. Ser., 56:265–310.

Kumar, K., Anderson, R.F., Mortlock, R.A., Froelich, P.N., Kubik, P., Dittrich-Hannen, B., and Suter, M., 1995. Increased biological productivity and export production in the glacial Southern Ocean. *Nature*, 378:675–680.

Lazarus, D., 1992. Antarctic Neogene radiolarians from the Kerguelen Plateau, Legs 119 and 120. *In* Wise, S.W., Jr., Schlich, R., et al., *Proc. ODP, Sci. Results,* 120: College Station, TX (Ocean Drilling Program), 785–809.

Martini, E., 1971. Standard Tertiary and Quaternary calcareous nannoplankton zonation. *In* Farinacci, A. (Ed.), *Proc. 2nd Int. Conf. Planktonic Microfossils Roma:* Rome (Ed. Tecnosci.), 2:739–785.

Okada, H., and Bukry, D., 1980. Supplementary modification and introduction of code numbers to the low-latitude coccolith biostratigraphic zonation (Bukry, 1973; 1975). *Mar. Micropaleontol.,* 5:321–325.

Raffi, I., Backman, J., Rio, D., and Shackleton, N.J., 1993. Plio-Pleistocene nannofossil biostratigraphy and calibration to oxygen isotopes stratigraphies from Deep Sea Drilling Project Site 607 and Ocean Drilling Program Site 677. *Paleoceanography,* 8:387–408.

Rio, D., Raffi, I., and Villa, G., 1990. Pliocene-Pleistocene calcareous nannofossil distribution patterns in the Western Mediterranean. *In* Kastens, K.A., Mascle, J., et al., *Proc. ODP, Sci. Results,* 107: College Station, TX (Ocean Drilling Program), 513–533.

Wei, W., 1993. Calibration of Upper Pliocene-Lower Pleistocene nannofossil events with oxygen isotope stratigraphy. *Paleoceanography,* 8:85–99.

Figure F1. Track line and shotpoints for the site survey of Site 1091 conducted during *Thompson* Cruise TTN057. The bold portion of the track line corresponds to the segment of the seismic profile displayed in Figure F2, p. 20.

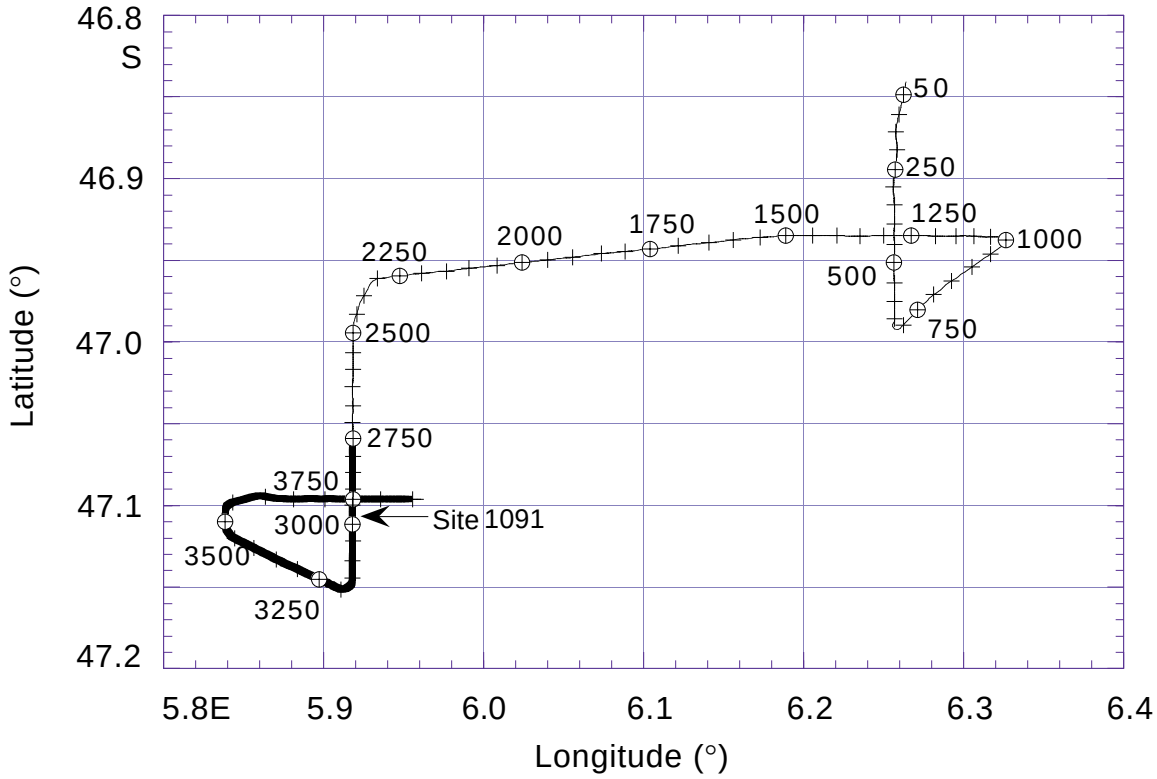

Figure F2. Single-channel seismic profile collected during site-survey *Thompson* Cruise TTN057 showing the location and penetration depth of Site 1091. SP = shotpoint.

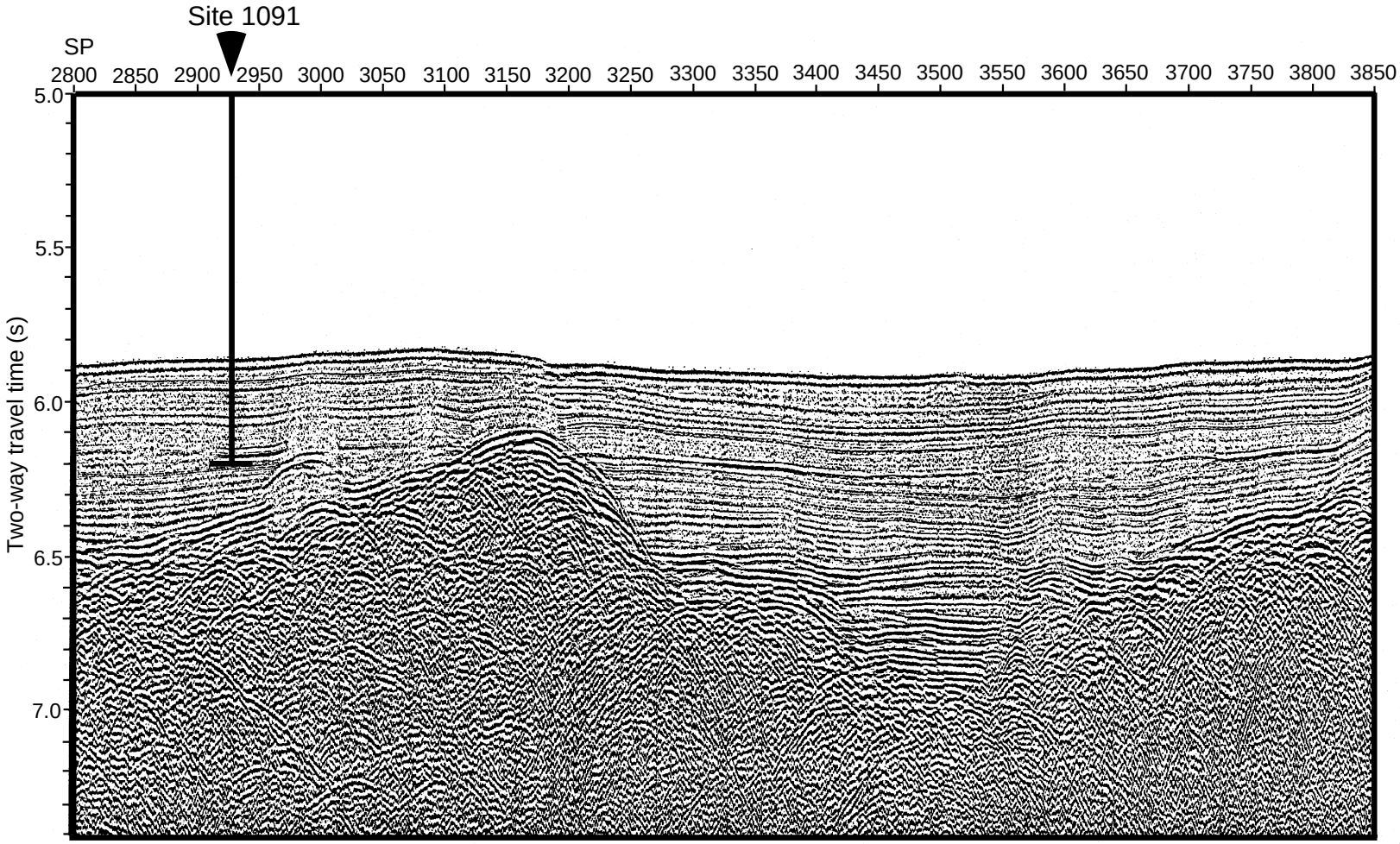

Figure F3. Lithologic summary showing core recovery, lithologic unit, graphic lithology, calcareous intervals, diatom mats, and beds tentatively interpreted as turbidites in the four holes drilled at Site 1091. Calcareous intervals, diatom mats, and turbidites are only schematically represented (their true thicknesses are smaller than shown), with true thicknesses and locations in each core accurately represented in the Site 1091 core correlation diagram (Fig. F6, p. 25). Numbers above turbidite beds correspond to designations in the core correlation diagram (Fig. F6). T.D. = total depth. (Continued on next page.)

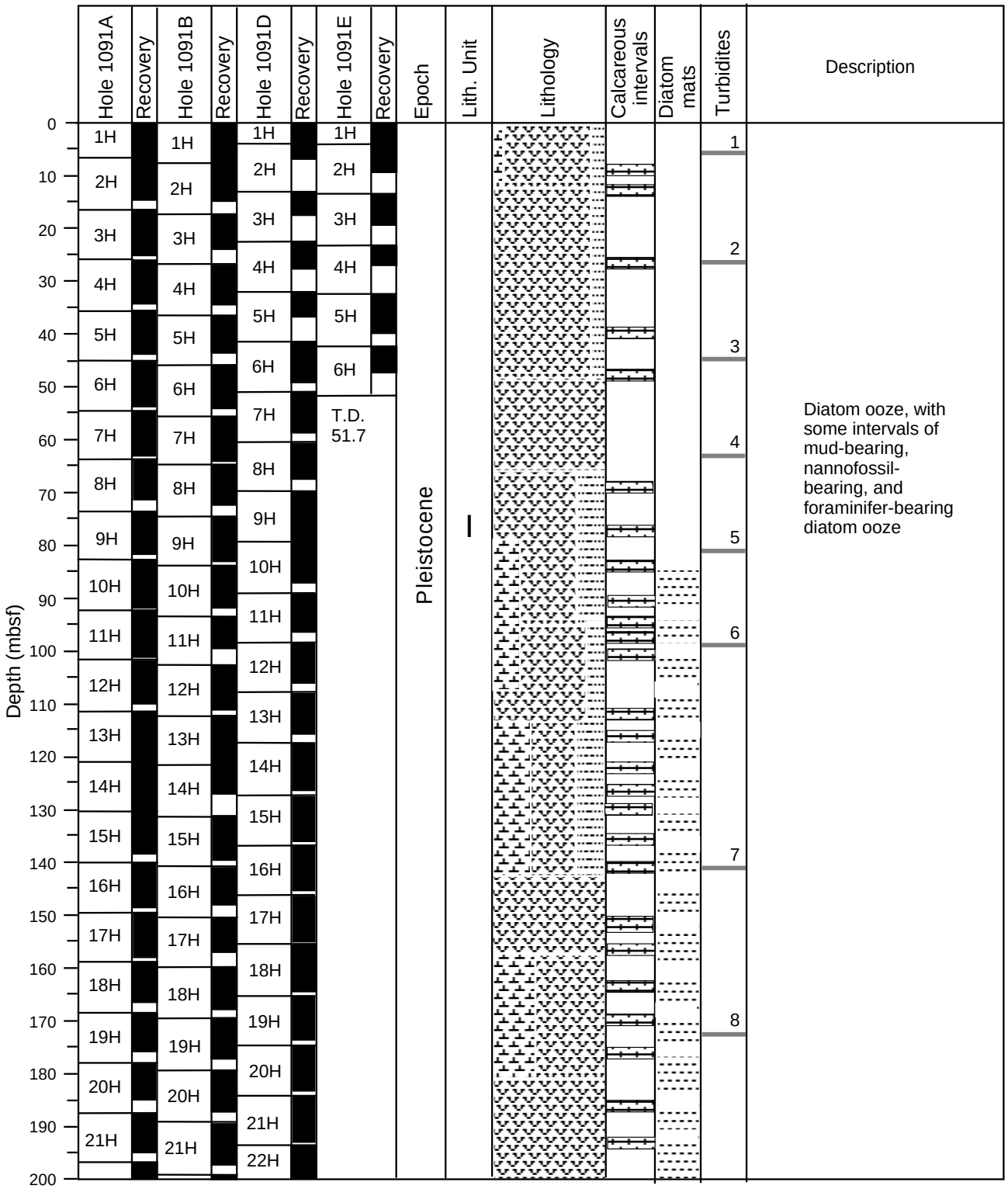

Figure F3 (continued).

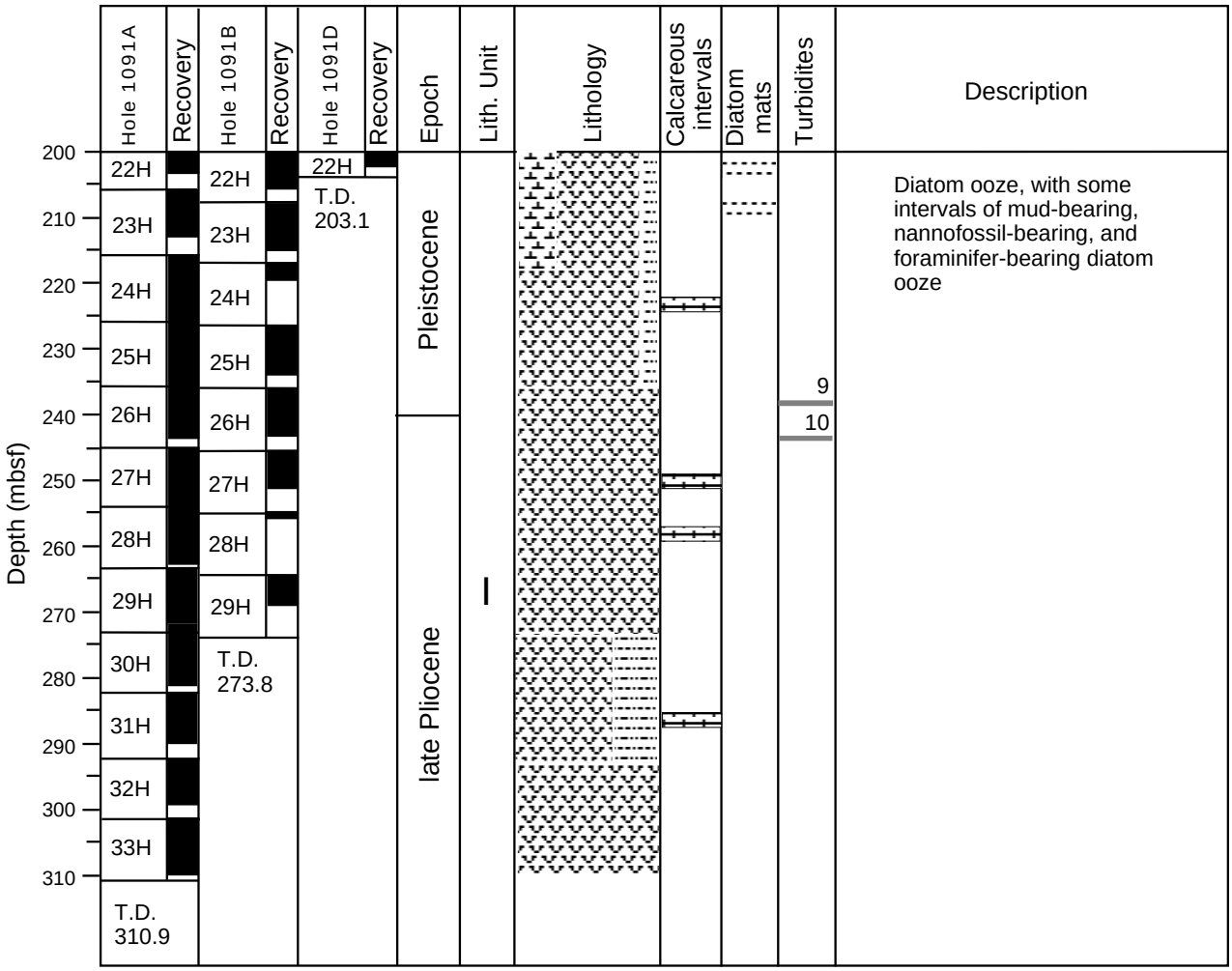

Figure F4. Lithologic composition summary of carbonate (nannofossils plus foraminifers), diatom, and mud contents determined by smear-slide (percent area), coulometry, and XRD analyses at Site 1091.

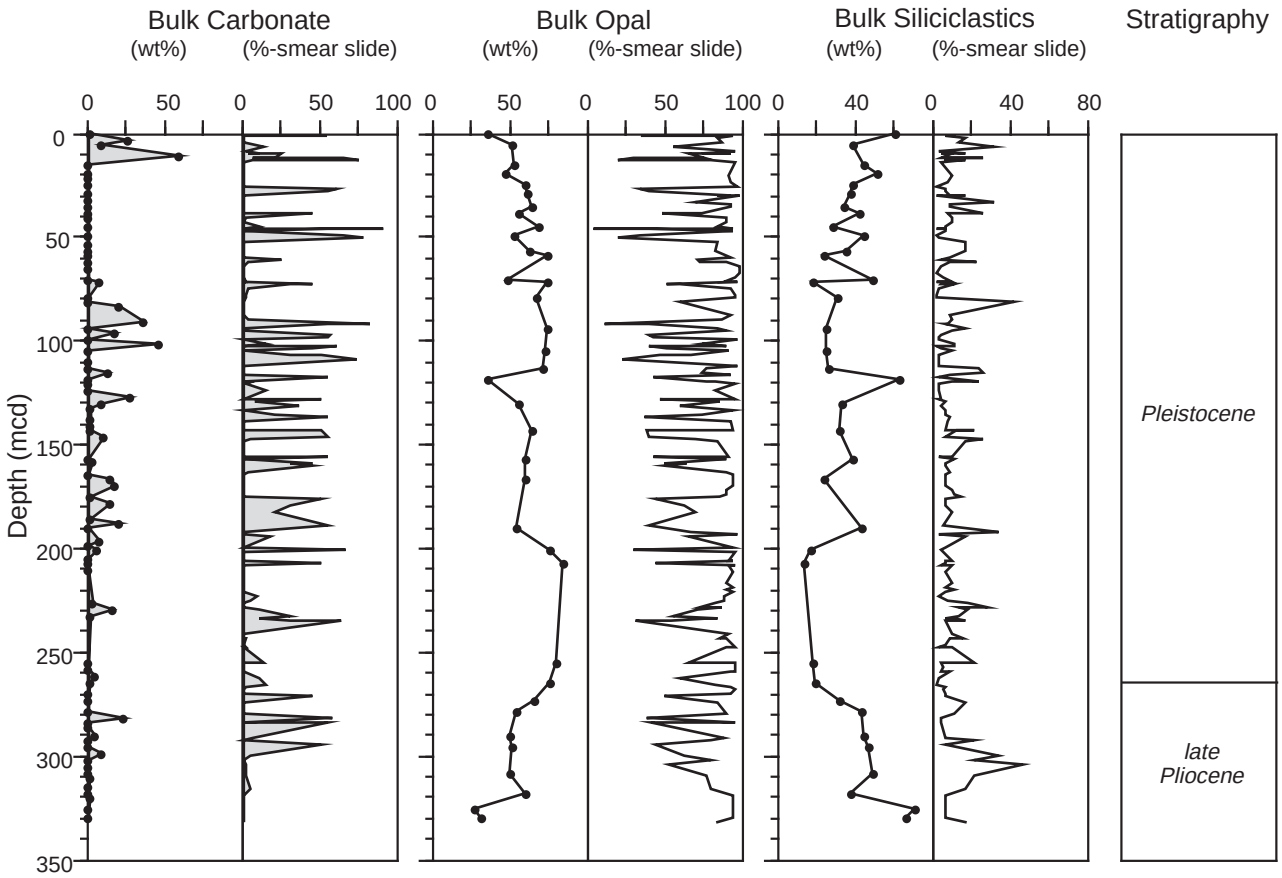

Figure F5. Diatom mats with diagnostic rough spongy surface texture observed after scraping (interval 177-1091D-14H-2, 30–70 cm).

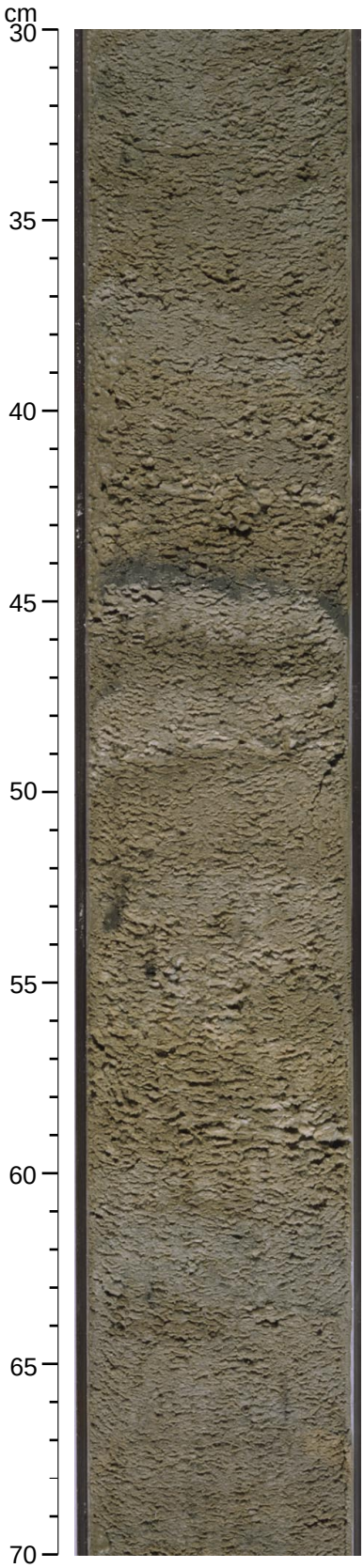

Figure F6. Core correlation diagram for Site 1091. (Continued on next four pages.)

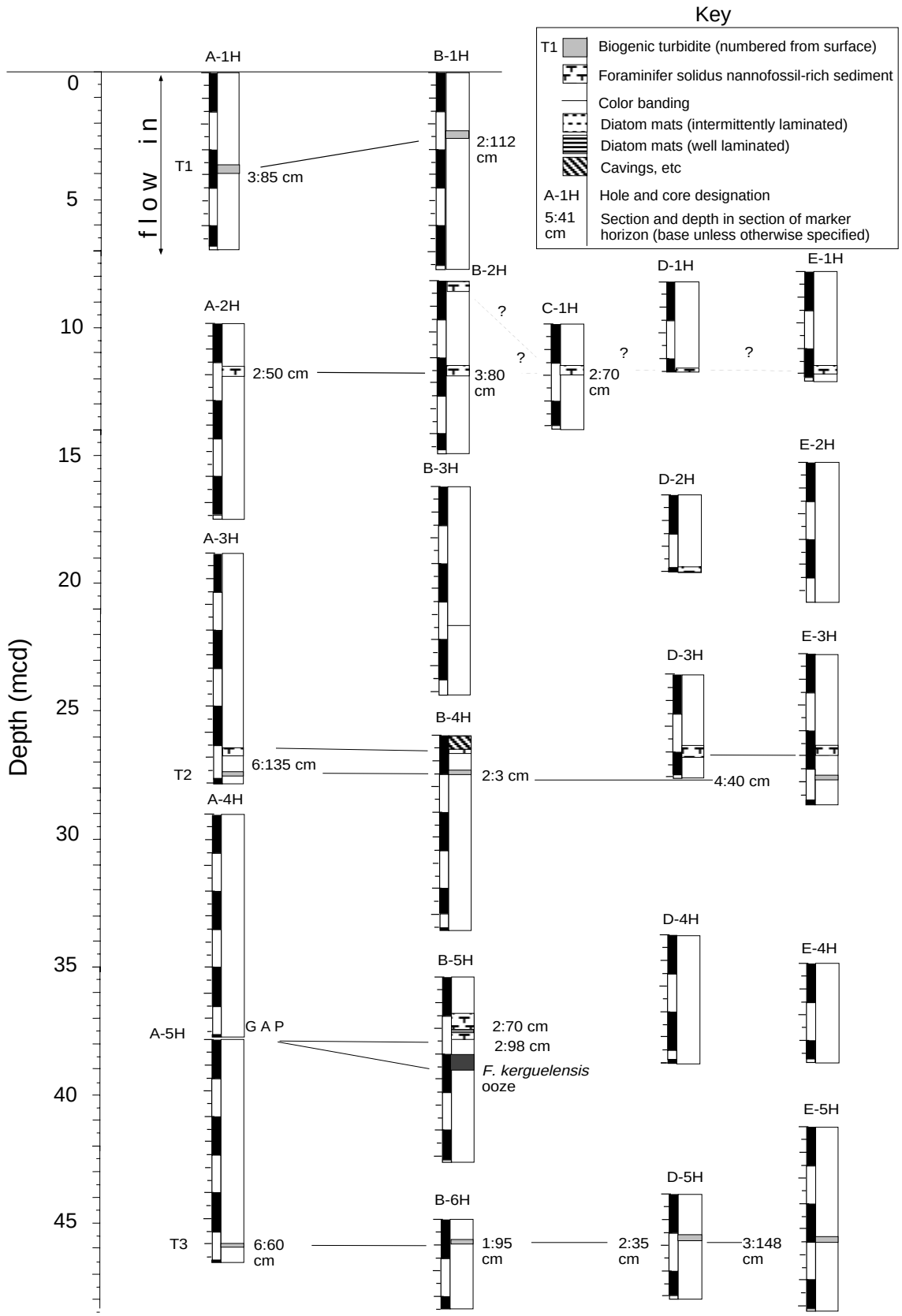

Figure F6 (continued).

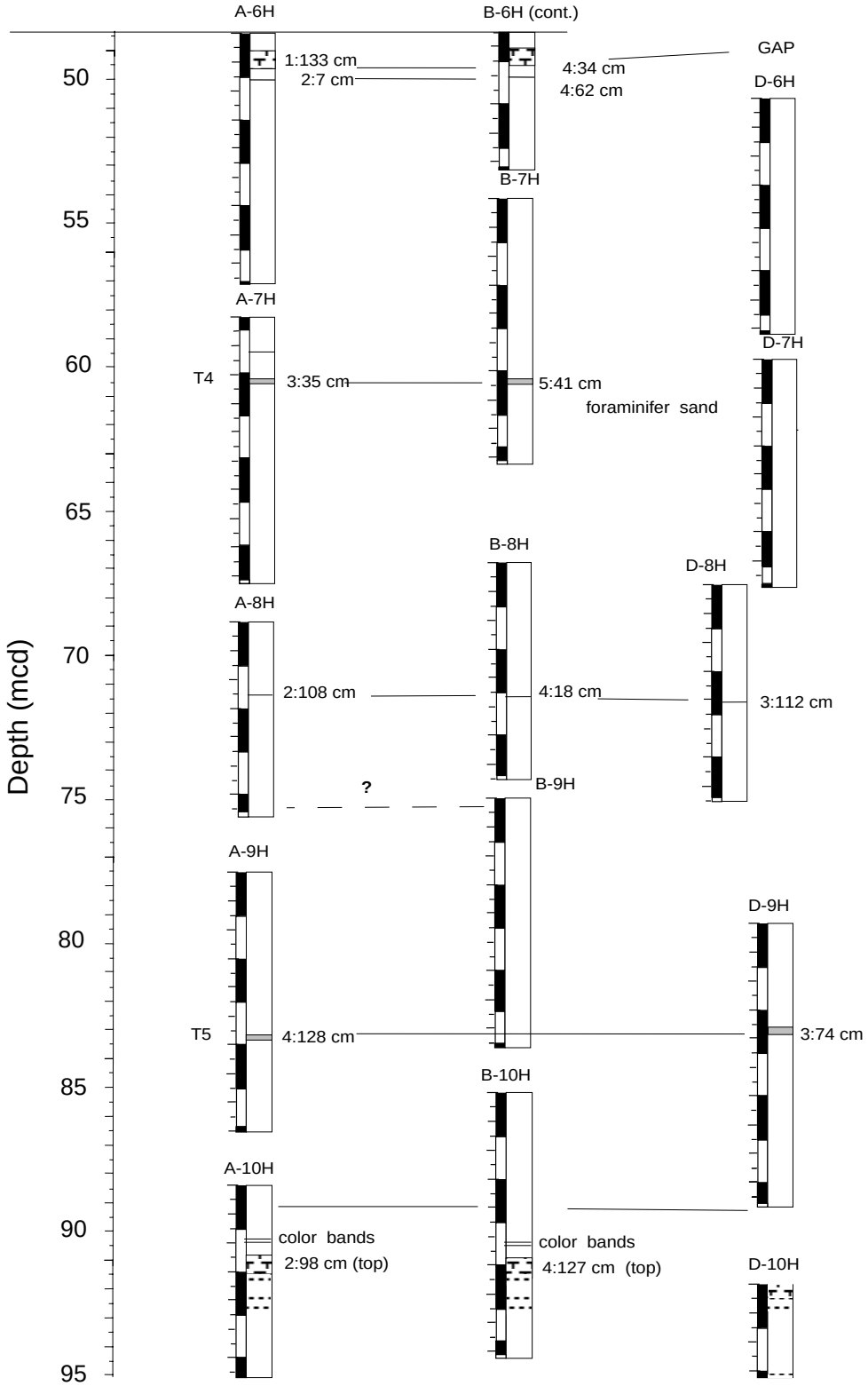

Figure F6 (continued).

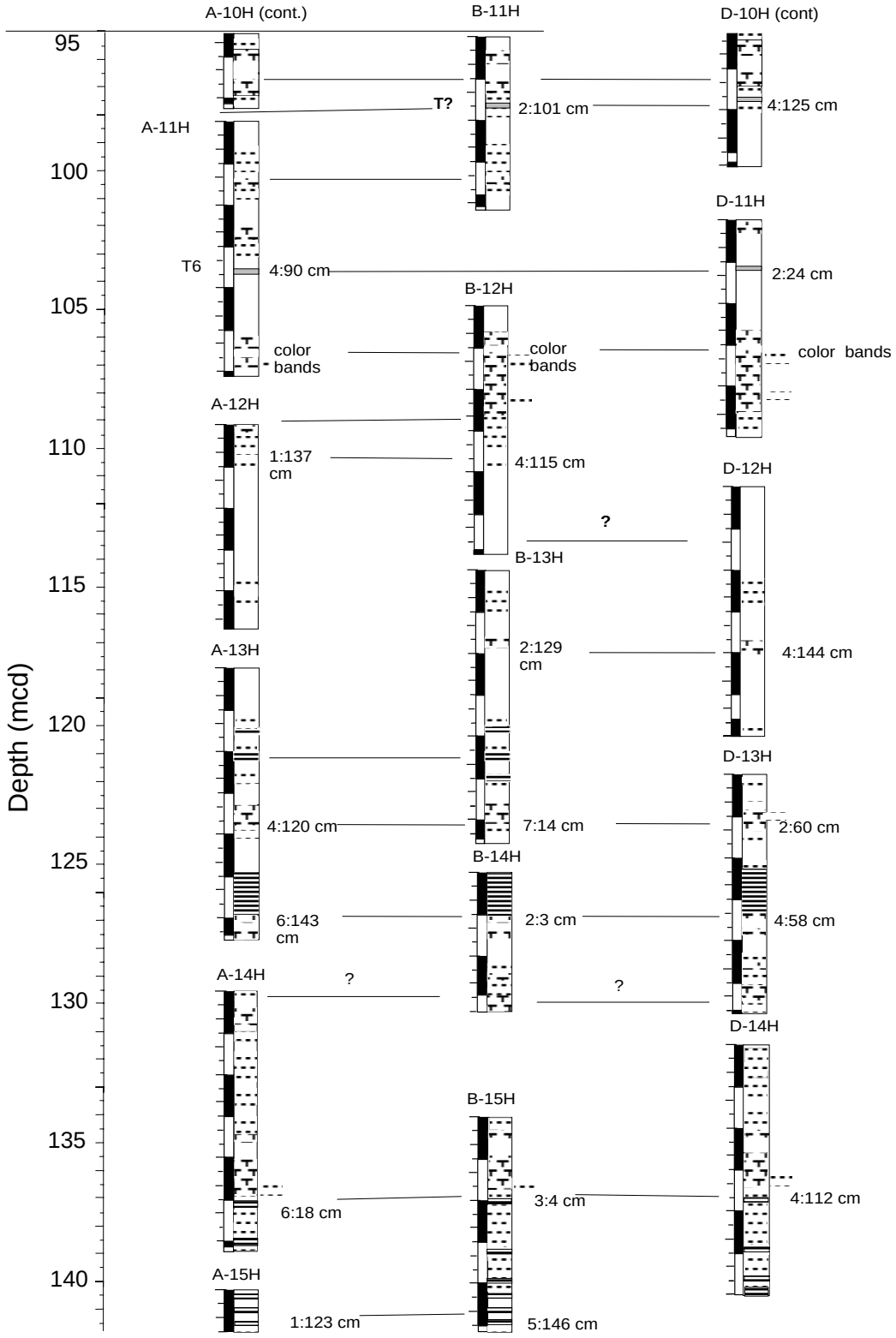

Figure F6 (continued).

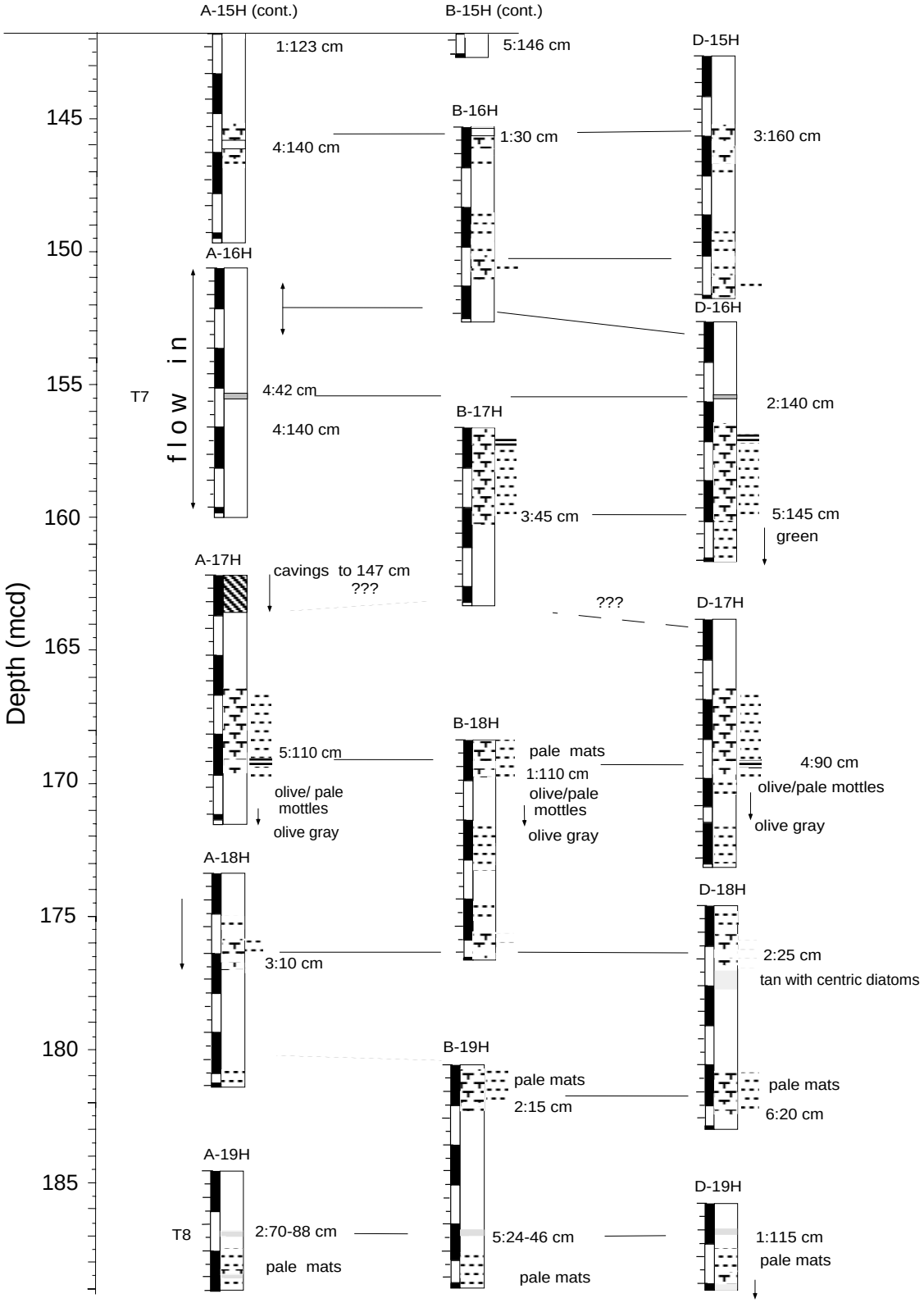

Figure F6 (continued).

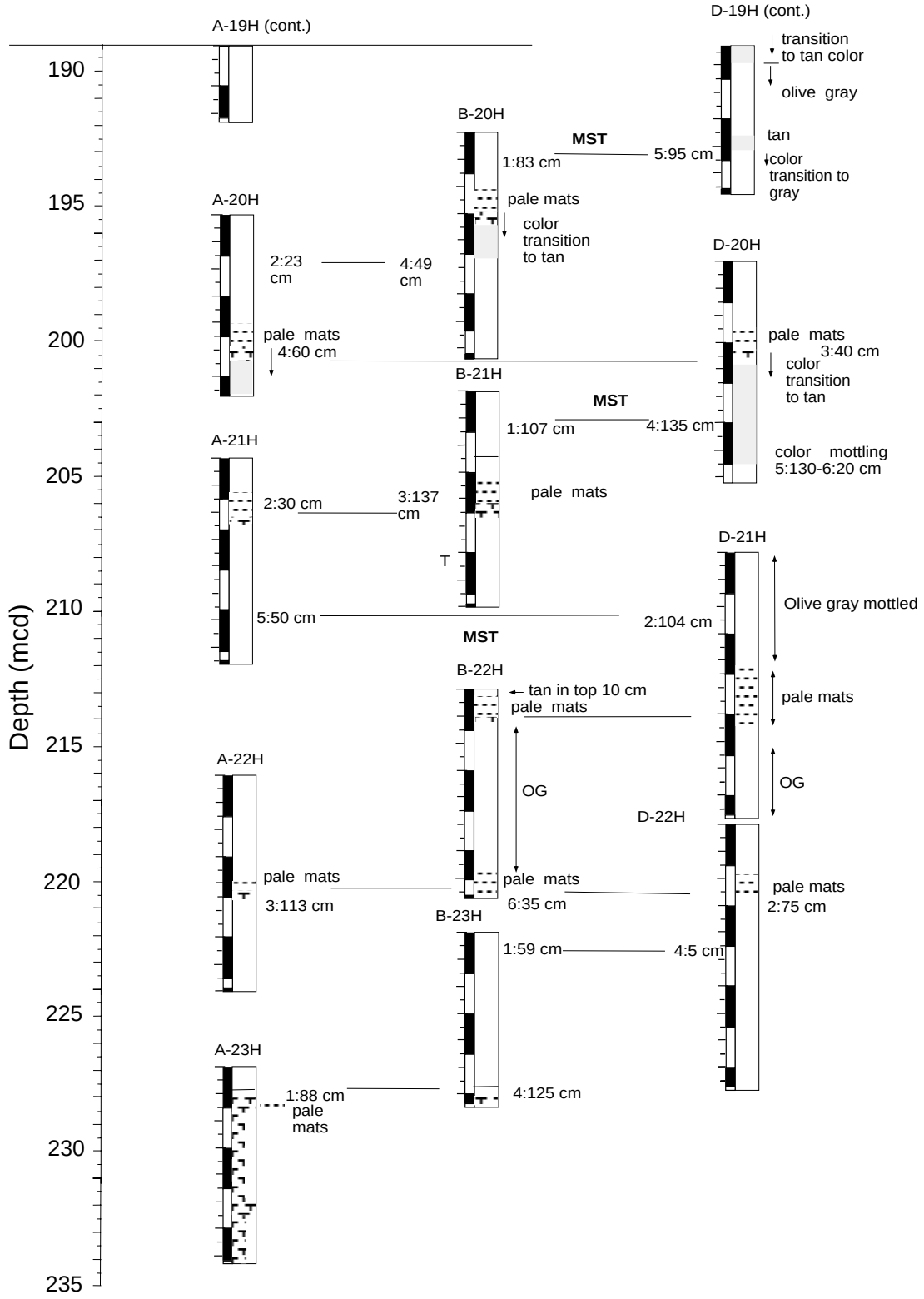

Figure F7. Laminated bedding, marked by purple and black laminae and textural differences between laminae, is common above diatom-mat layers (interval 177-1091A-6H-1, 68–88 cm).

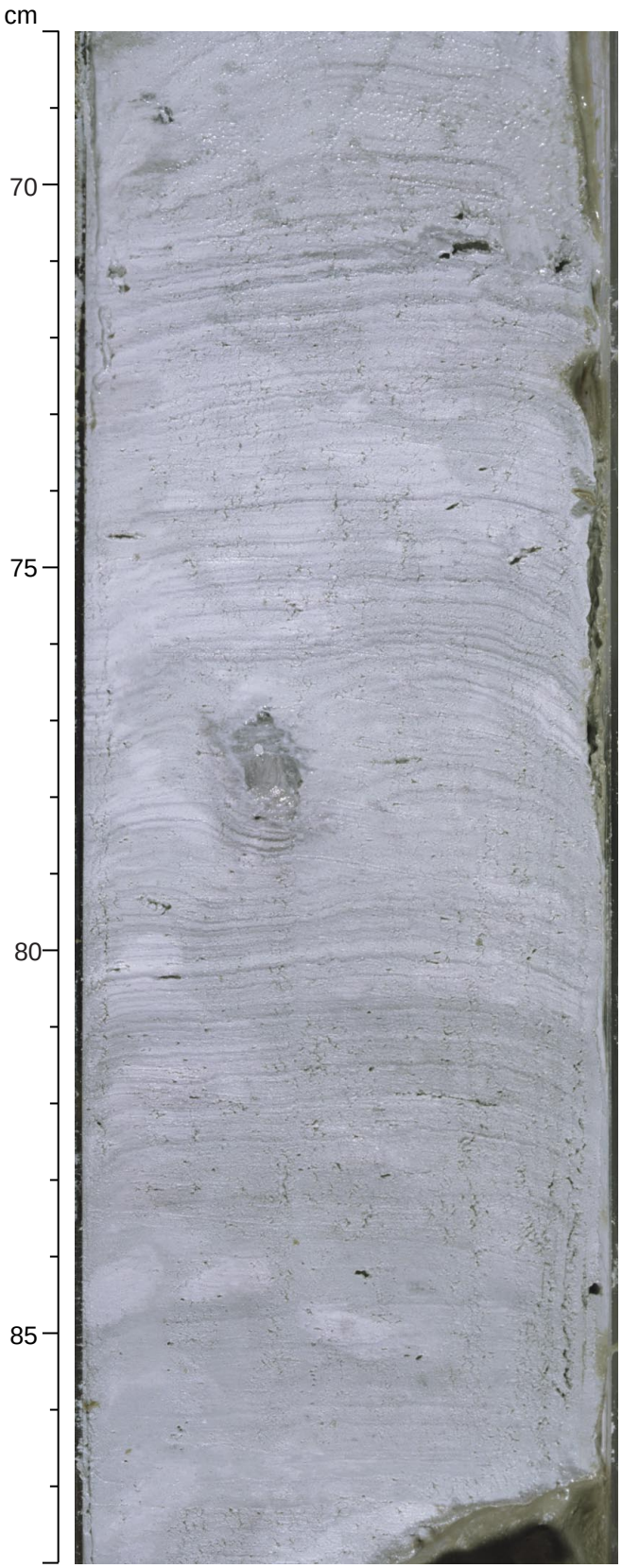

Figure F8. Large diorite dropstone (interval 177-1091A-13H-1, 75–105 cm).

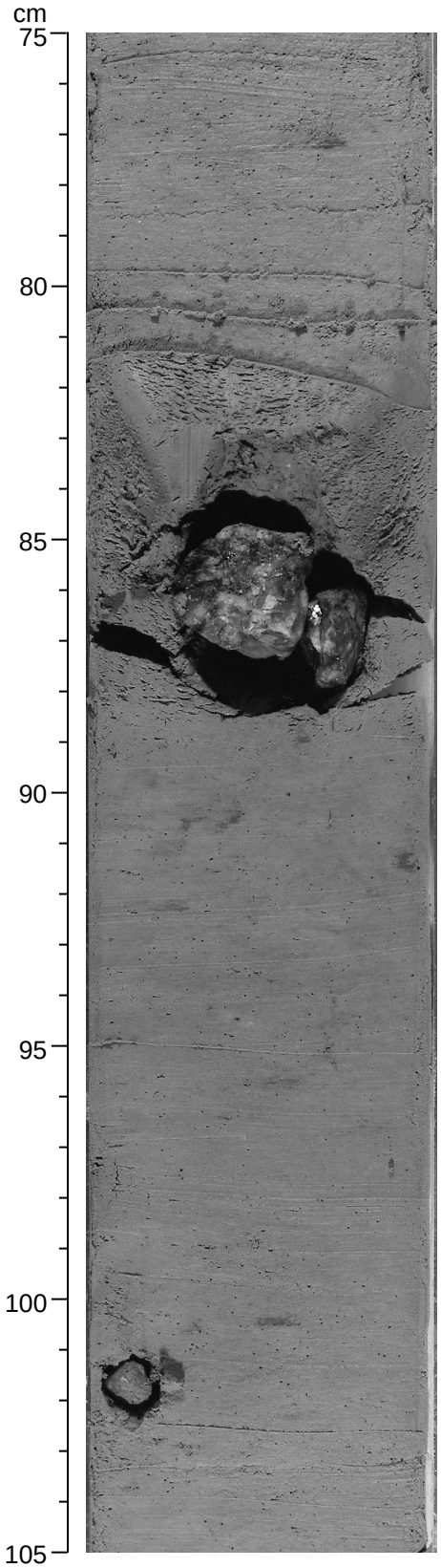

Figure F9. Thin marker bed with scoured base. The progression from cross stratification to planar lamination to indistinct bedding is characteristic of Bouma Layers C–E in a distal turbidite sequence. This particular bed is very carbonate rich, with some grading at the base (interval 177-1091B-27H-2, 140 cm, to 27H-3, 10 cm).

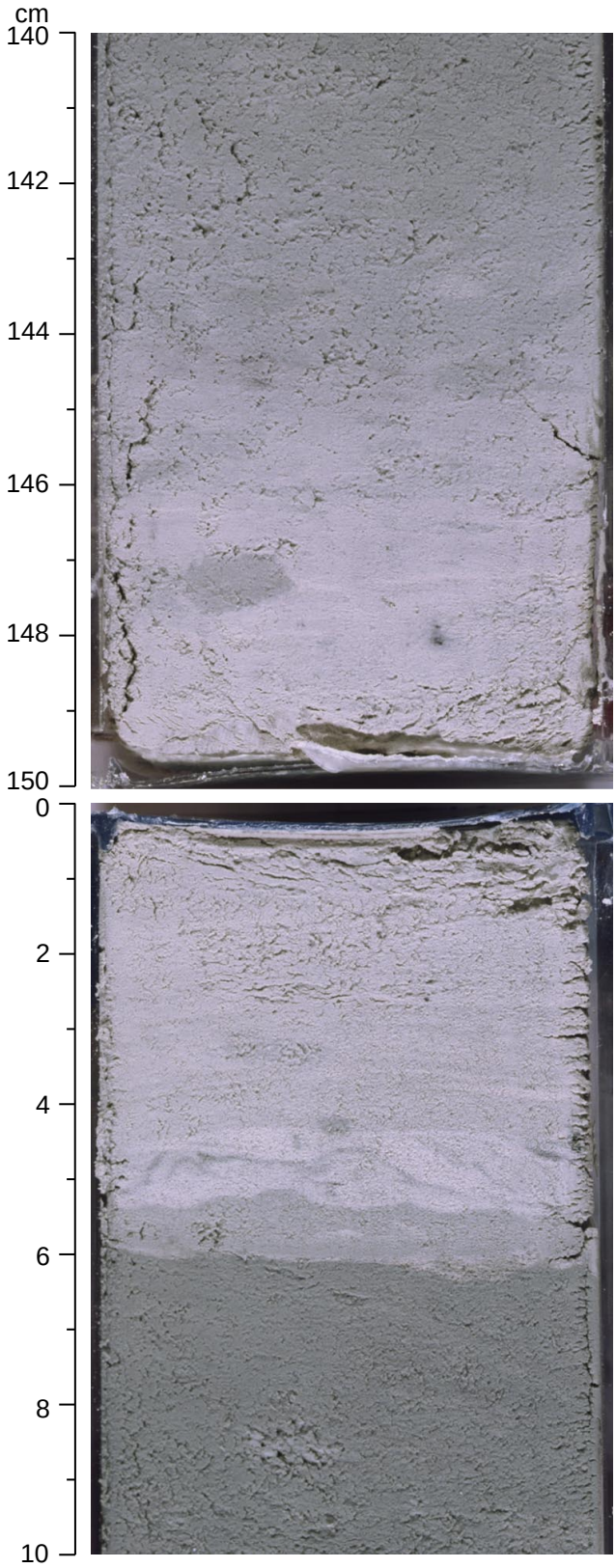

Figure F10. Thick marker bed, with color contrast to sediments above and below, and relatively structureless interior (interval 177-1091D-16H-2, 100–145 cm).

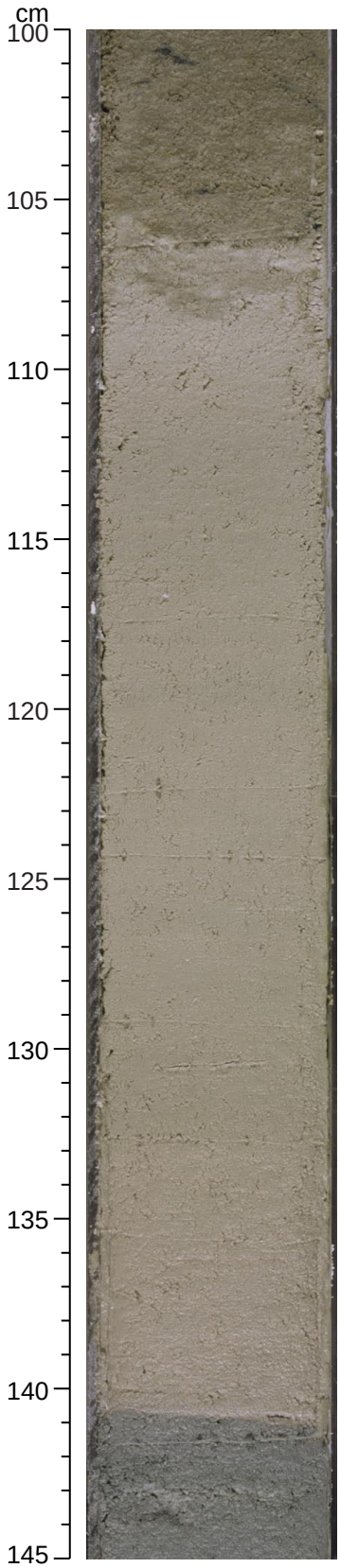

Figure F11. Smoothed (5-point average) magnetic susceptibility data (converted from instrument units to SI units) from Site 1091. Holes 1091A (left curve), 1091B (second from left curve), 1091C (middle curve), and 1091D (second from right curve), and 1091E (right curve) are horizontally offset from each other by a constant (3×10^{-5} SI units).

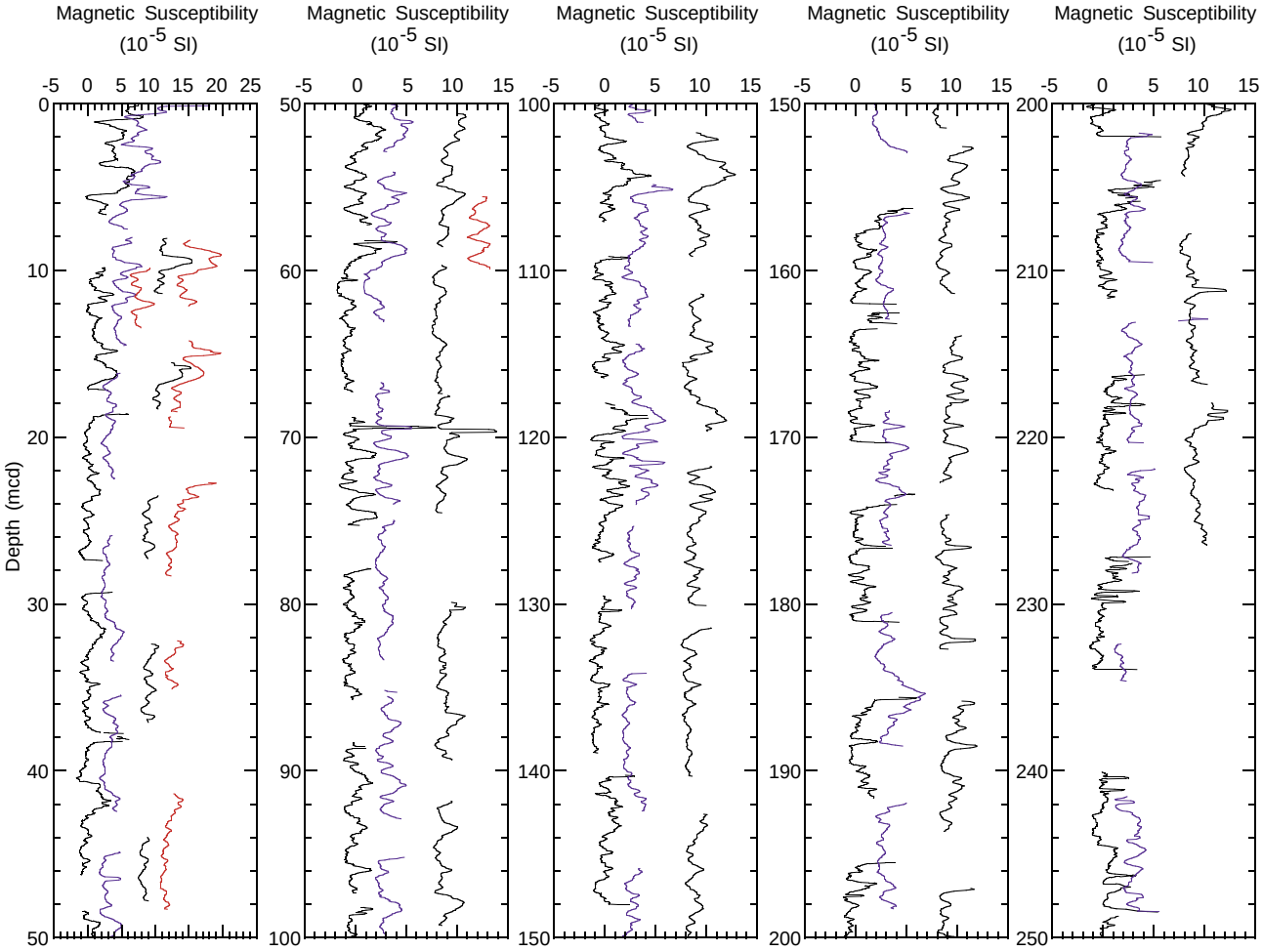

Figure F12. Smoothed (5-point average) color reflectance data (650–750 nm) from Site 1091. Holes 1091A (left curve) and 1091B (second from left curve) are OSU-SCAT data; Holes 1091C (middle), 1091D (second from right curve), and 1091E (right curve) are Minolta data. Note that the color reflectance data from the Minolta instrument are offset from the OSU-SCAT. These two records will be intercalibrated postcruise and should not be used together at this point. All holes are horizontally offset from each other by a constant (10%). Data from the top 20 cm of each core have been removed.

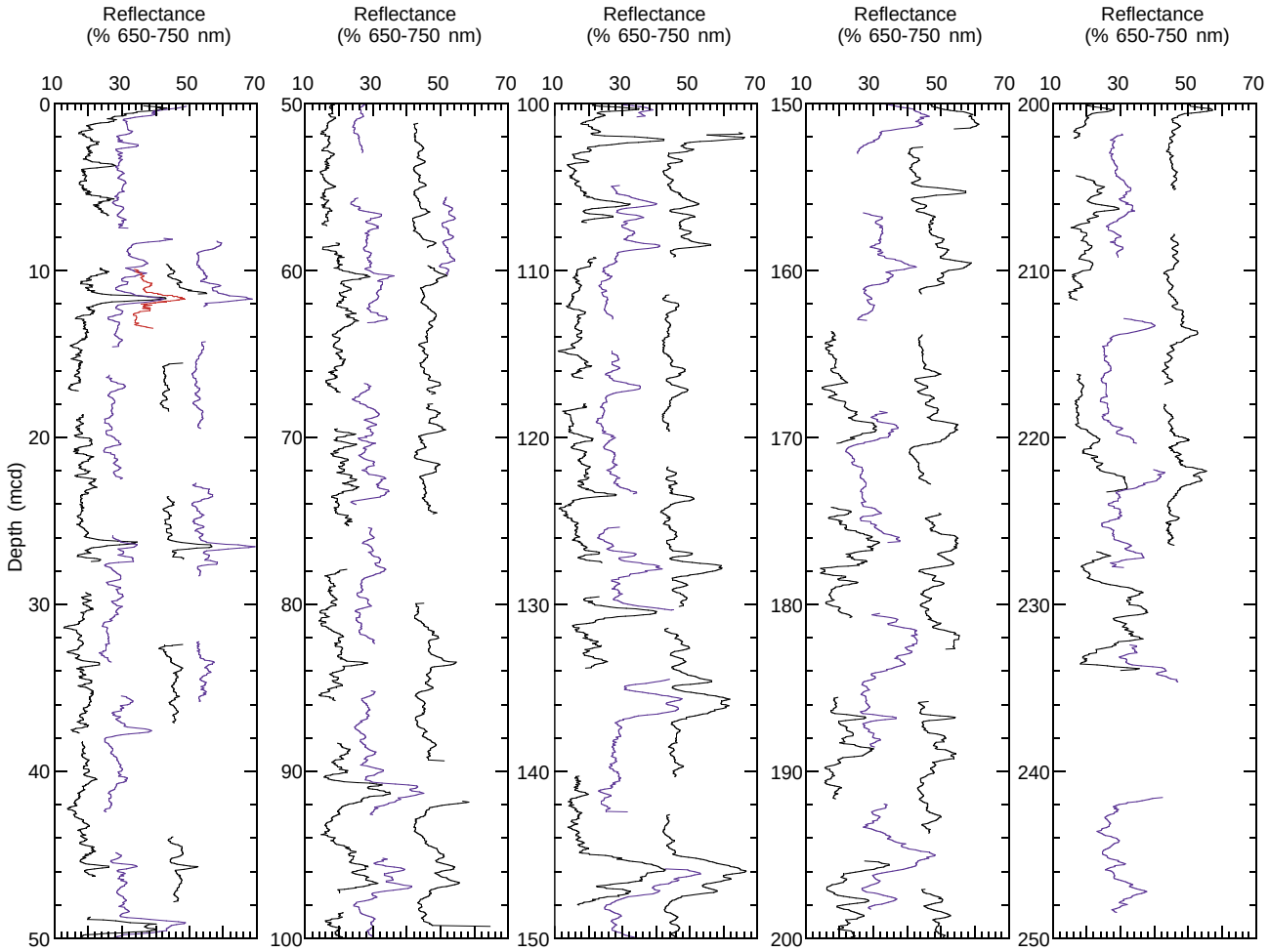

Figure F13. Smoothed (5-point average) GRA bulk density data from Site 1091. Holes 1091A (left curve), 1091B (second from left curve), 1091C (middle curve), 1091D (second from right curve), and 1091E (right curve) are horizontally offset from each other by a constant (0.15 g/cm³).

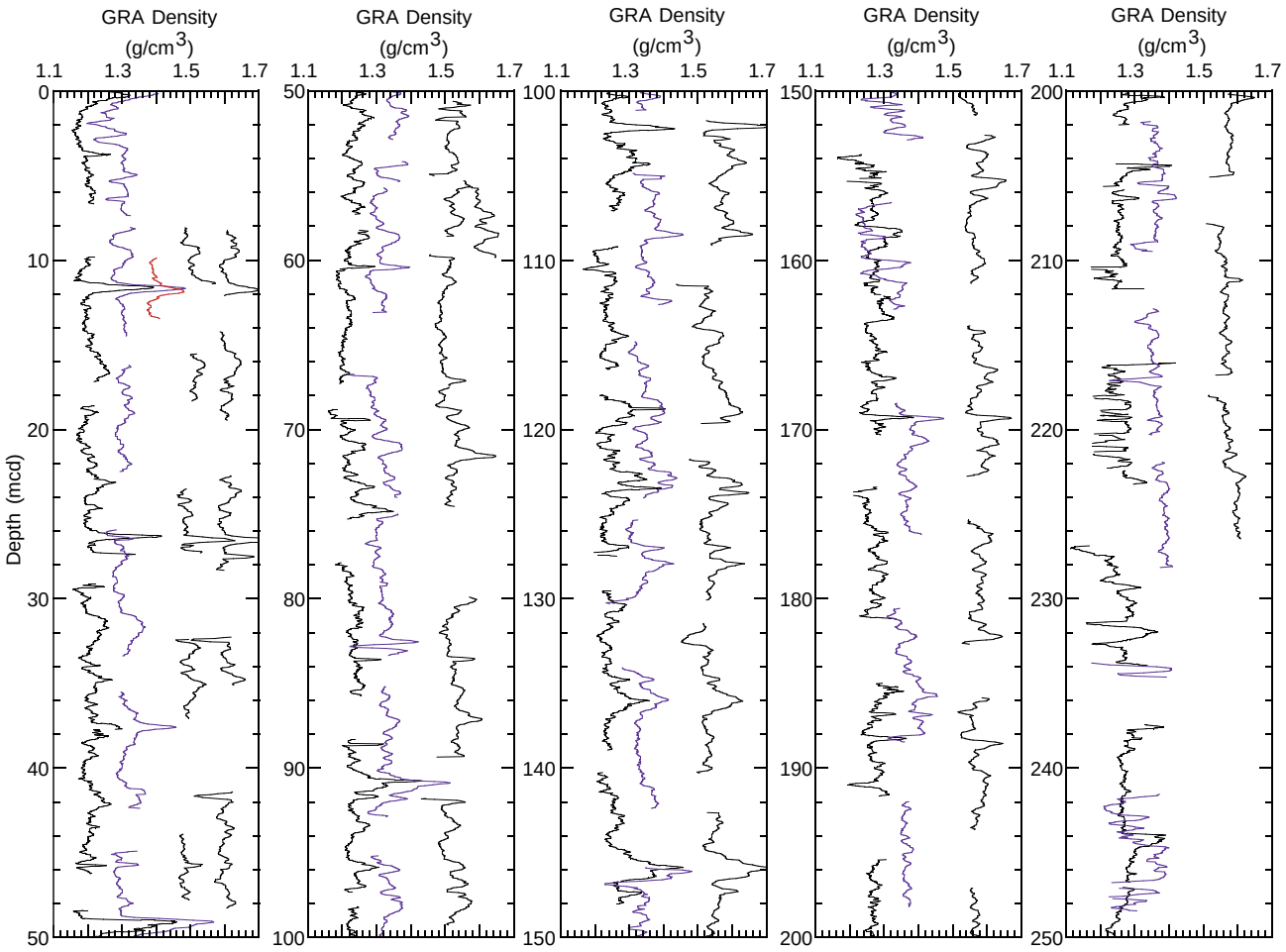

Figure F14. Spliced records of magnetic susceptibility, GRA bulk density, and color reflectance data for the upper 234 mcd of Site 1091. Only OSU-SCAT data are included in the spliced data record resulting in a number of gaps in the reflectance splice (right panel). All data sets are smoothed with a 5-point running mean. The horizontal lines in each plot identify the splice tie points.

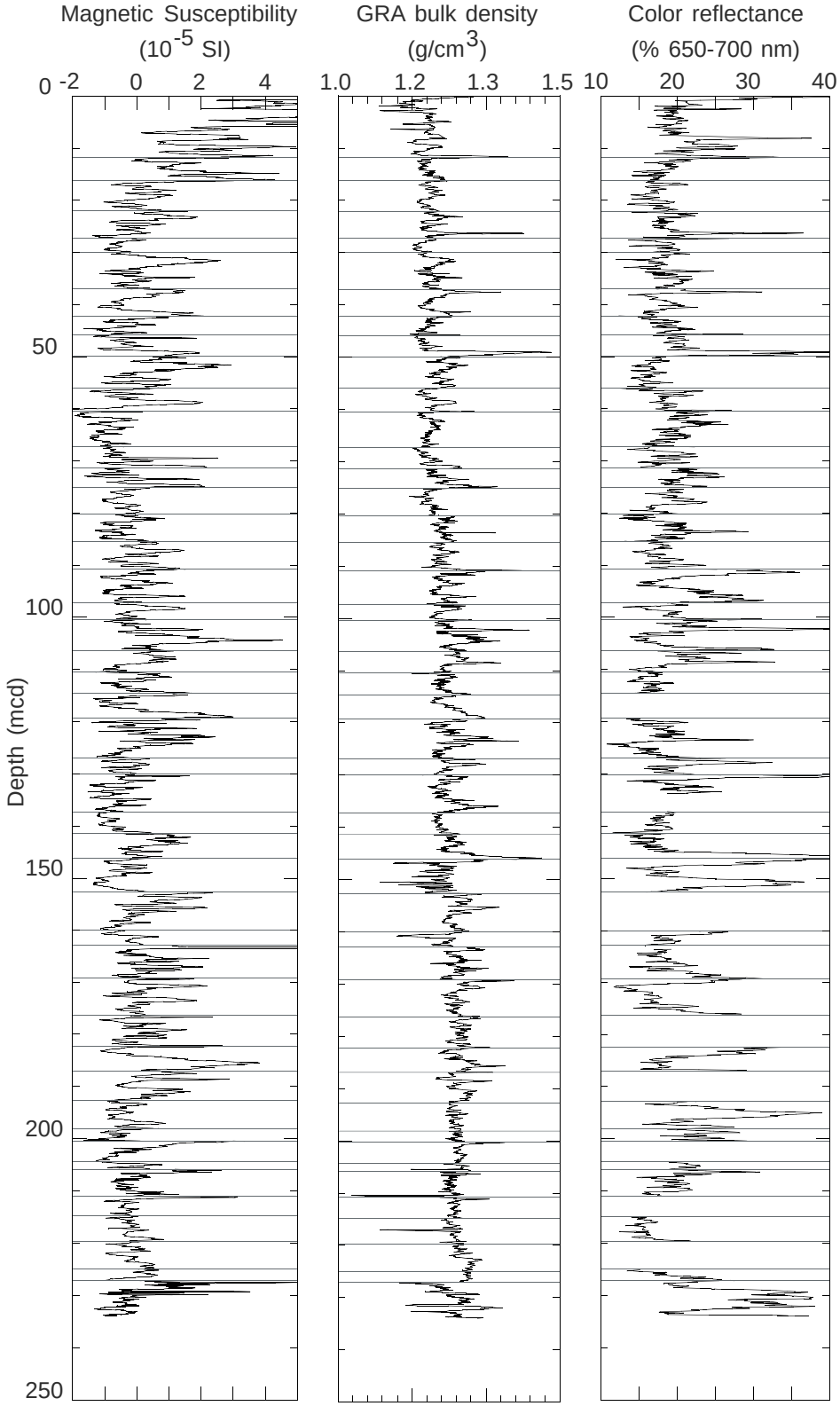

Figure F15. Biostratigraphic and magnetostratigraphic correlation chart for Site 1091, and selected absolute age designations.

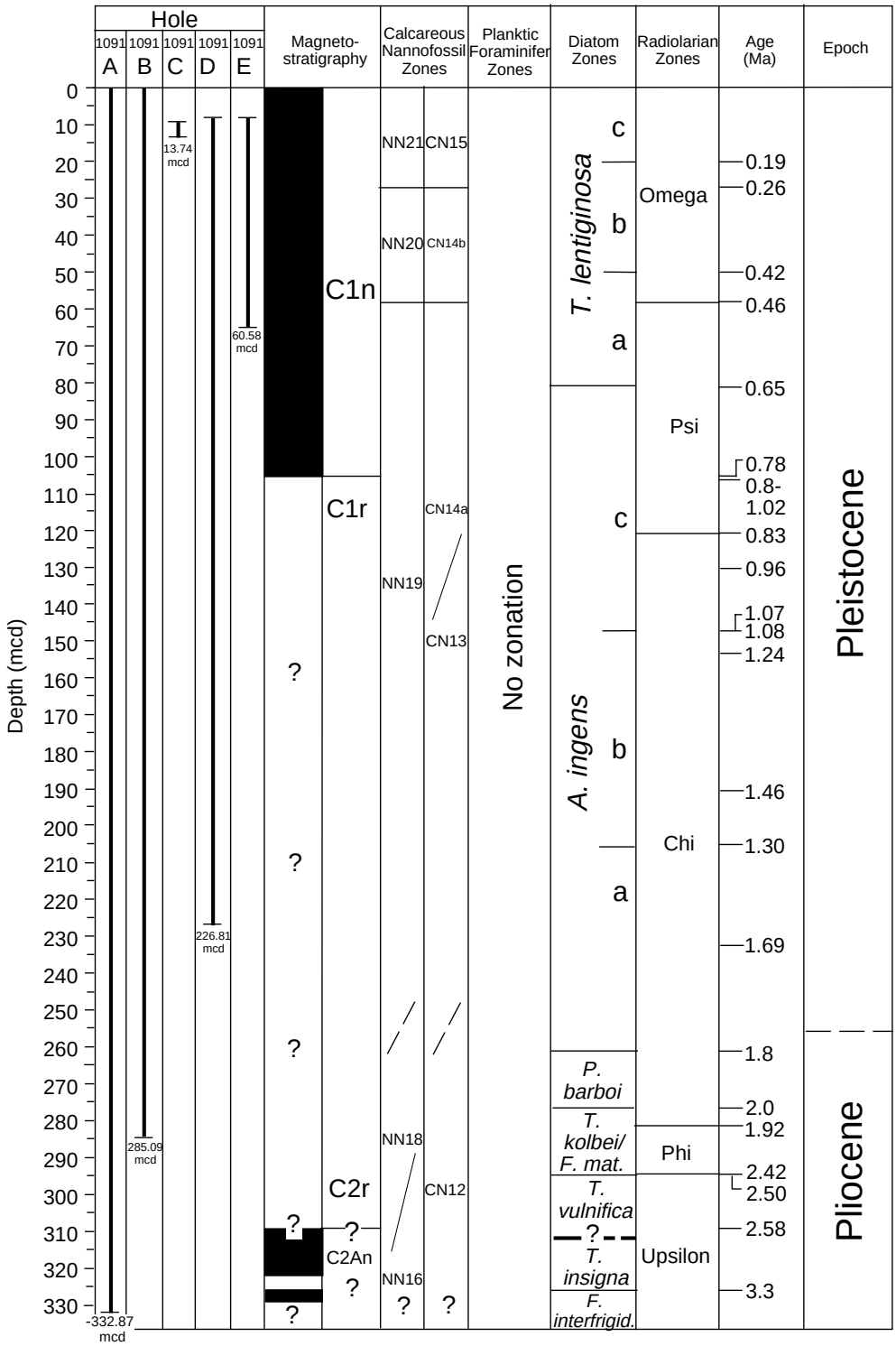

Figure F16. Diatom abundance and preservation pattern of selected biostratigraphic and paleoenvironmentally significant diatom taxa at Site 1091, correlated with the diatom biostratigraphic record. Abundance abbreviations: D = dominant, A = abundant, C = common, F = few, R = rare, T = trace. Preservation abbreviations: G = good, M = moderate, P = poor.

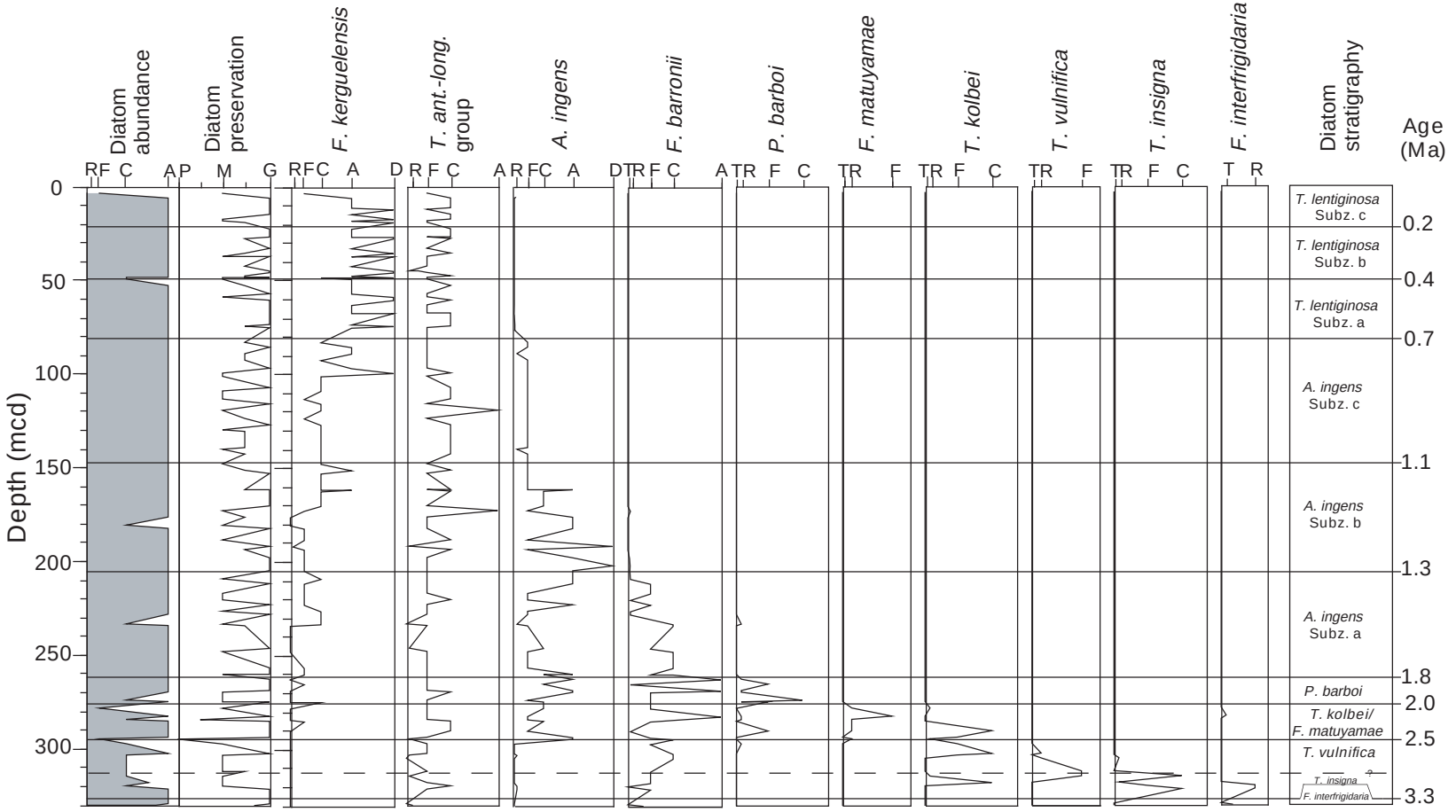

Figure F17. Inclination of the remanent magnetization after alternating-field demagnetization at peak fields of 25 or 30 mT for Holes 1091A, 1091B, and 1091D. The Brunhes, Matuyama, and Gauss Chrons are identified. Magnetic polarity shading: black = normal, white = reversed.

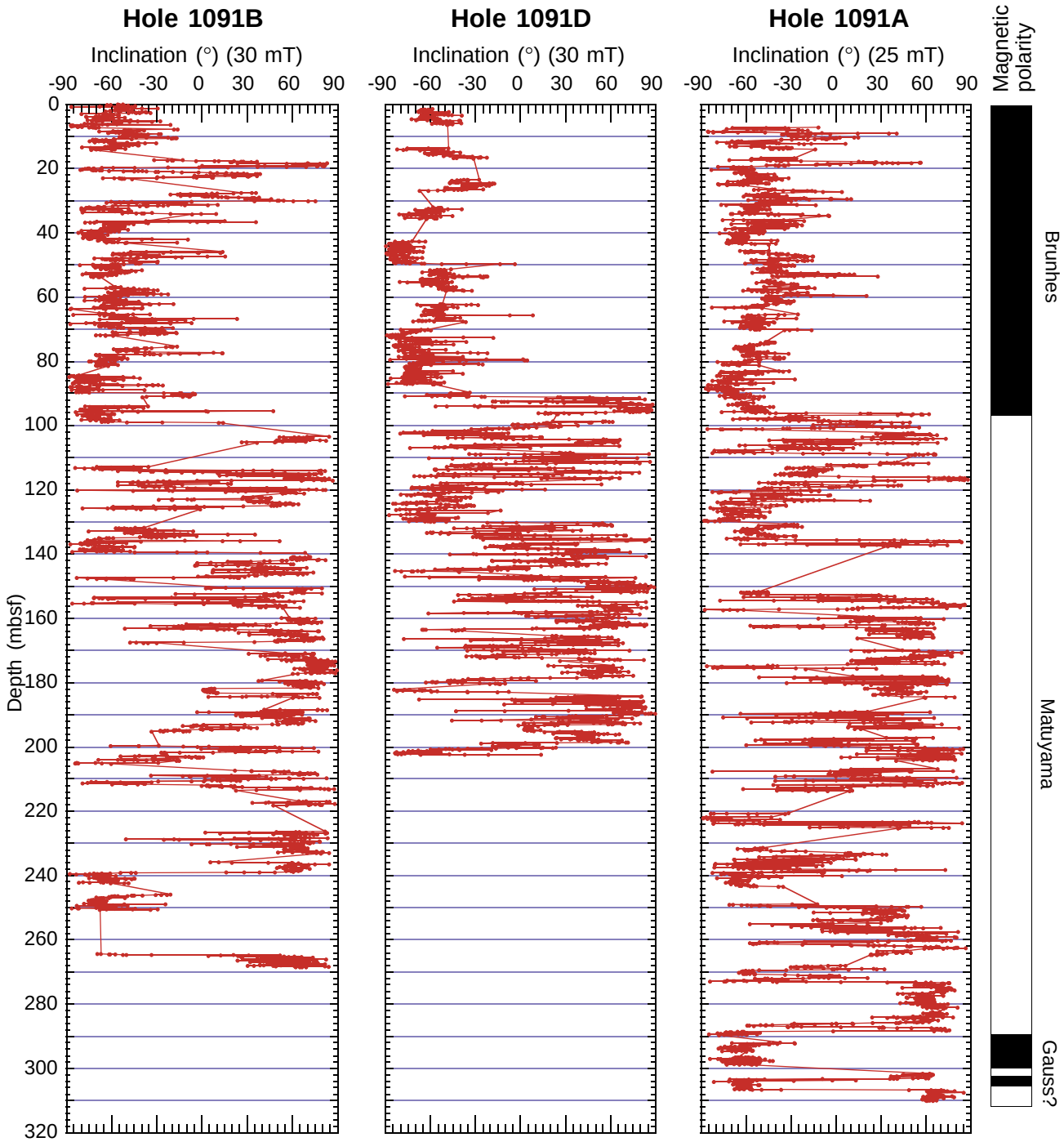

Figure F18. Age-depth plot of biostratigraphic and paleomagnetic events at Site 1091. The solid lines indicate a visual best fit through the age-depth control points. Corresponding sedimentation rate averages are given in parentheses. The dashed line indicates a possible hiatus at 315 mcd.

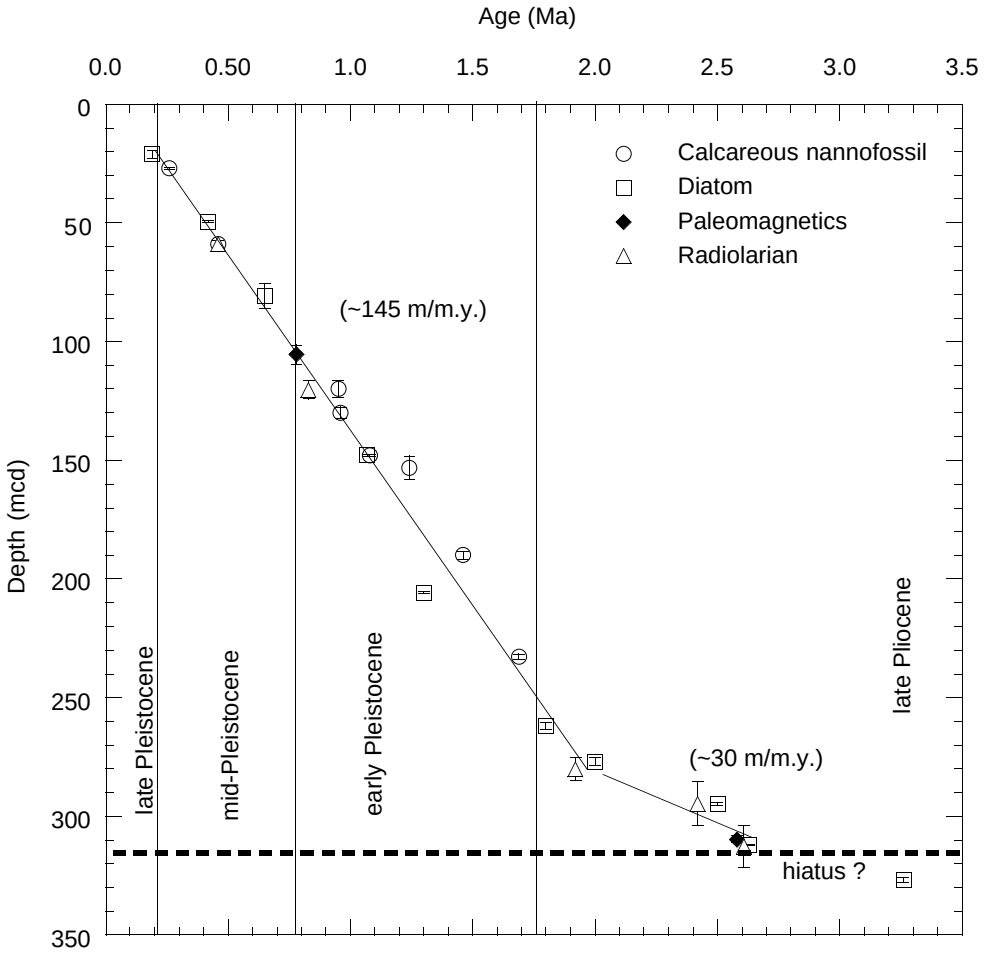

Figure F19. Concentration of methane vs. depth at Site 1091; the data are reported in Table T12, p. 76.

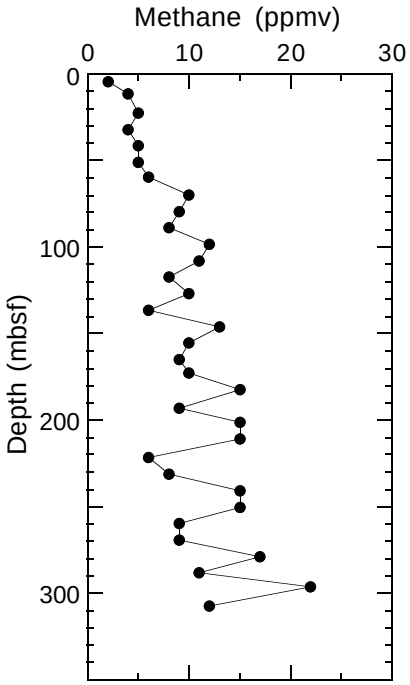

Figure F20. Interstitial water chemistry profiles vs. depth for chlorinity, alkalinity, pH, sodium, sulfate, calcium, magnesium, potassium, strontium, lithium, ammonium, phosphate, silica, manganese, and iron at Site 1091; the data are reported in Table T13, p. 77.

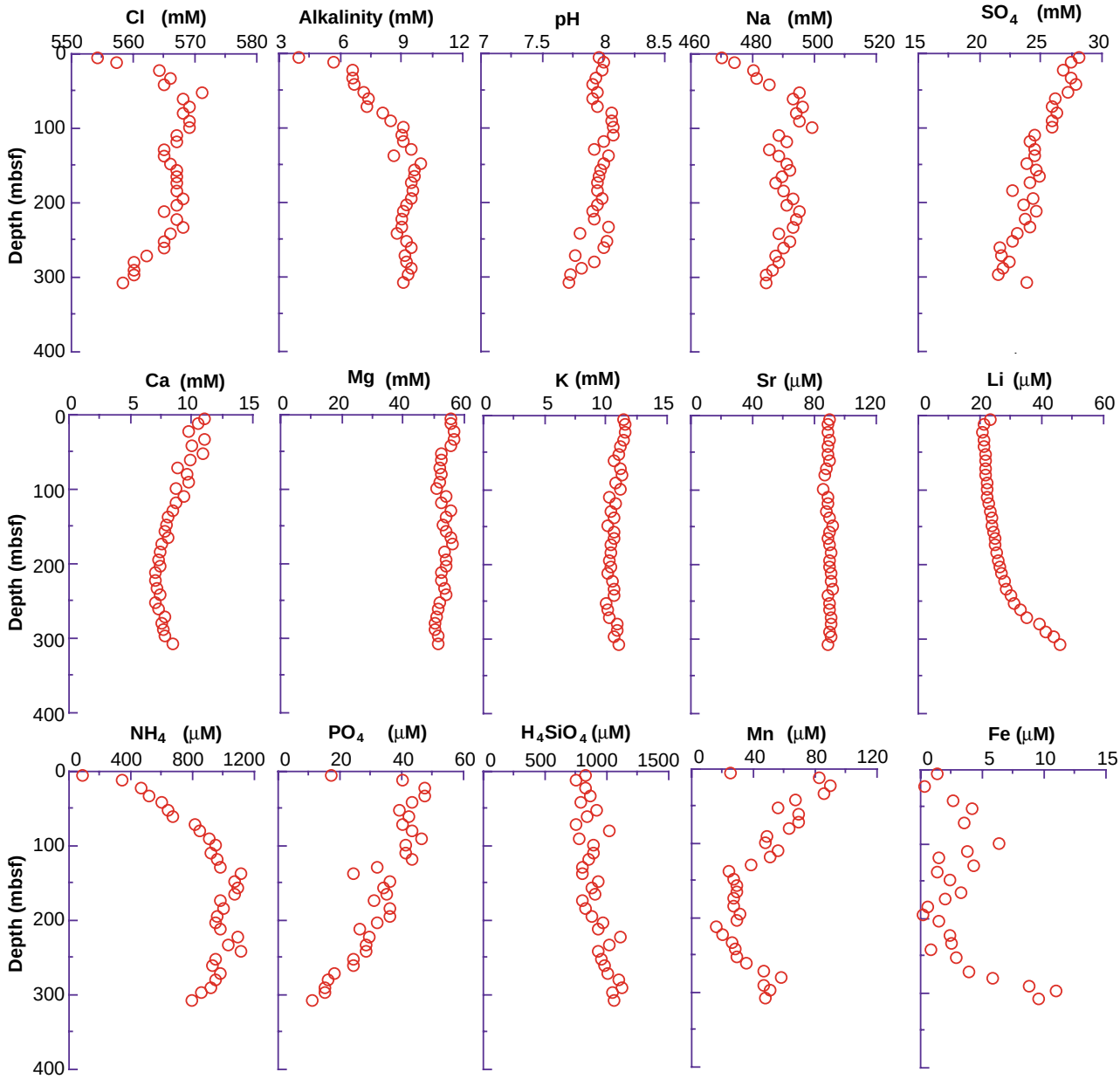

Figure F21. Concentration of calcium carbonate ($CaCO_3$), total organic carbon (TOC), total nitrogen (TN), total sulfur (TS), and TOC/TN vs. depth at Hole 1091A; the data are reported in Table **T14,** p. 79.

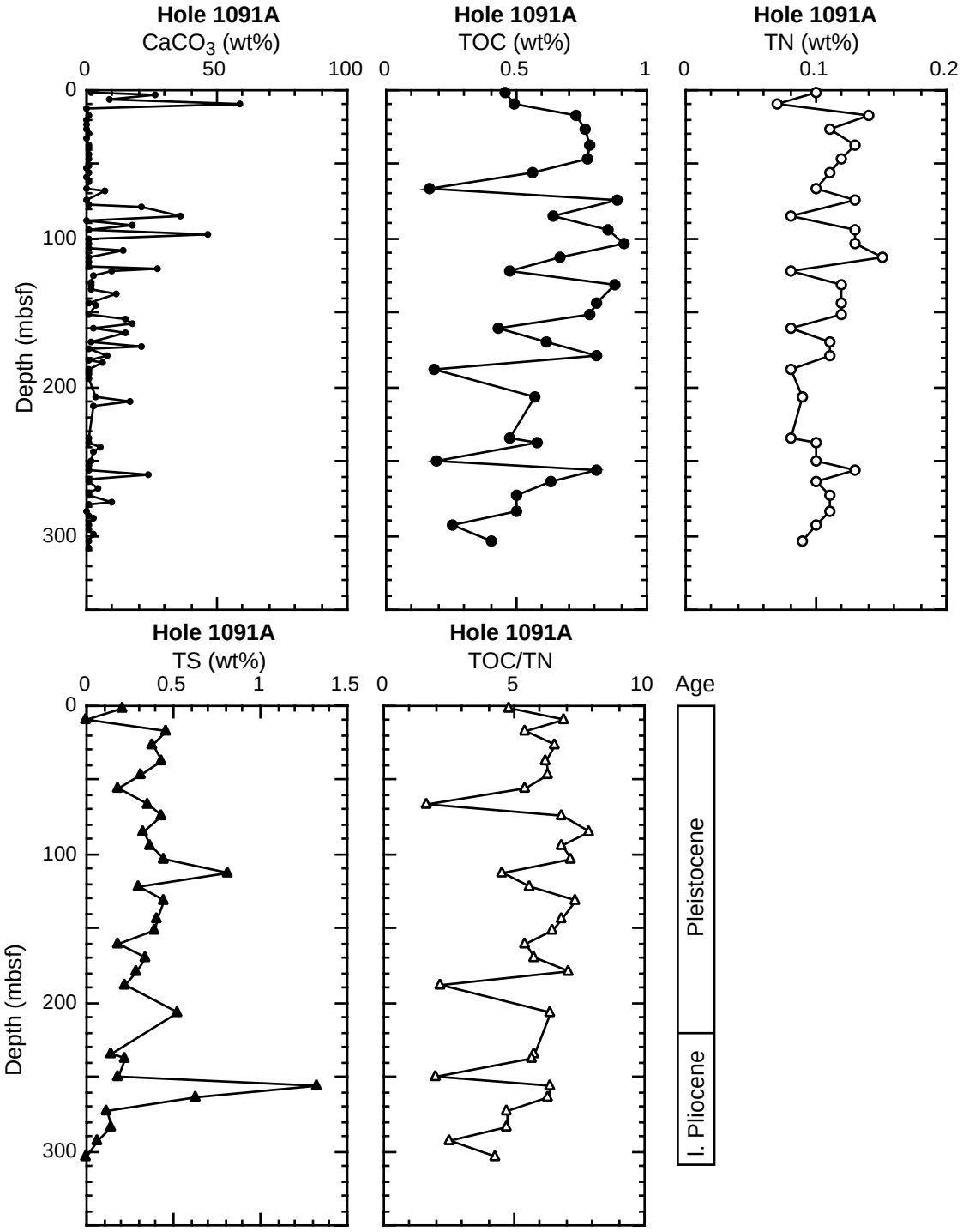

Figure F22. Diagram of total organic carbon (TOC) vs. total nitrogen (TN) at Hole 1091A. Lines show TOC/TN values of 5, 10, and 20.

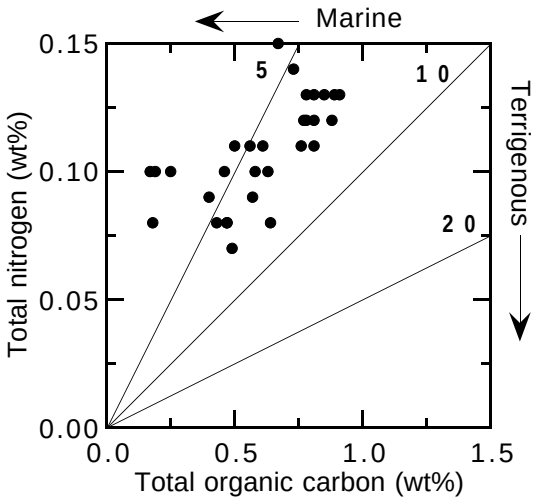

Figure F23. Site 1091 downhole variations in porosity (open circles = MAD method) and OSU-SCAT resistivity (solid line), *P*-wave velocities (small dots = PWL, solid circles = PWS3), GRA bulk density (line = smoothed data) and MAD bulk density (open circles), volume-specific magnetic susceptibility (enclosed box shows expanded scale to enhance the weak signal in this depth interval), and NGR (smoothed data).

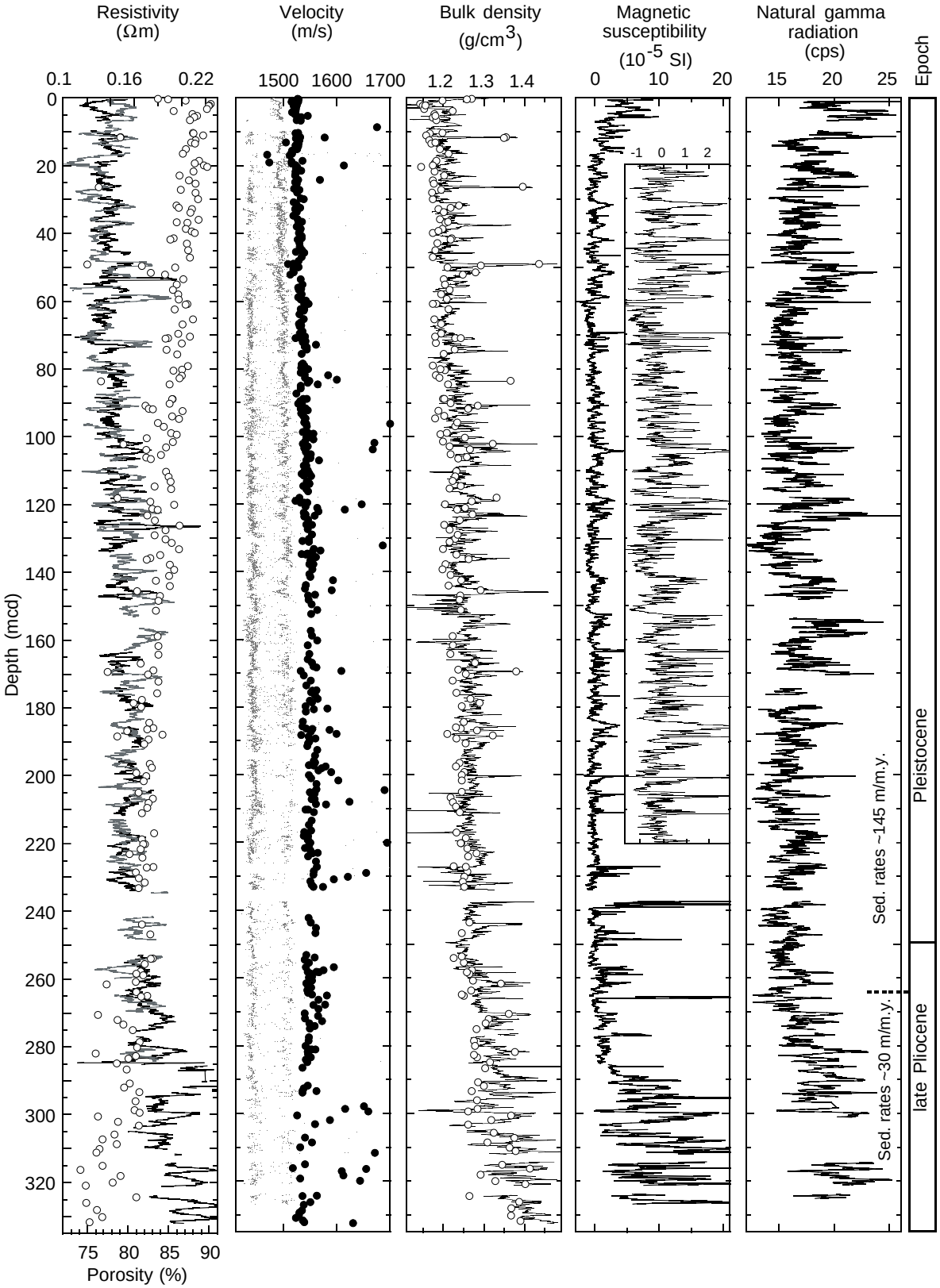

Figure F24. Downhole variations of resistivity, NGR, magnetic susceptibility, GRA density (solid line) and MAD density (open circles), and reflectance in the upper 100 mcd at Site 1091. Dashed lines = carbonate-rich layers, M = intervals where mud becomes a significant component of the sediment.

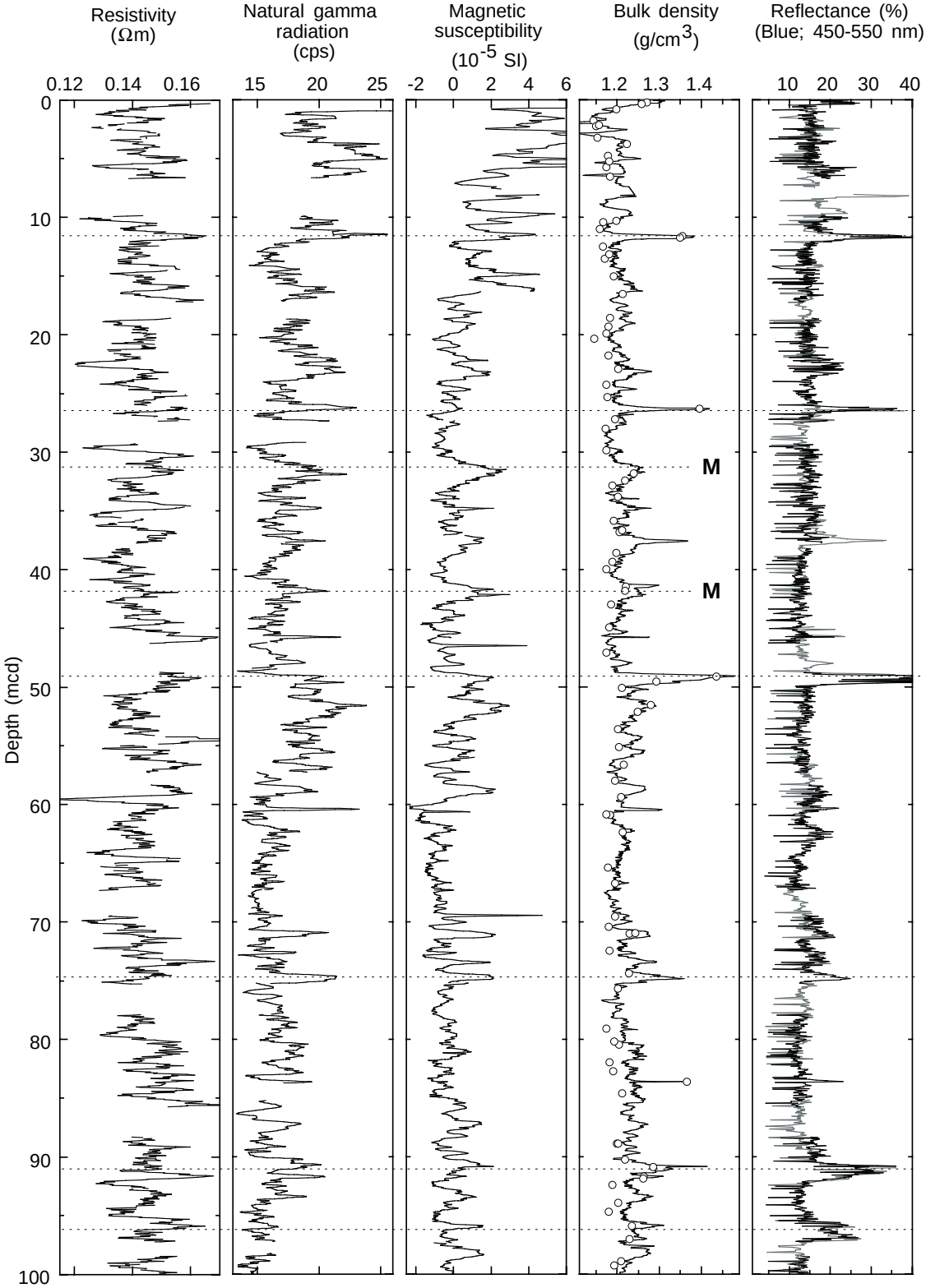

Figure F25. Relationship between GRA bulk density and gravimetric (MAD) bulk density at Site 1091.

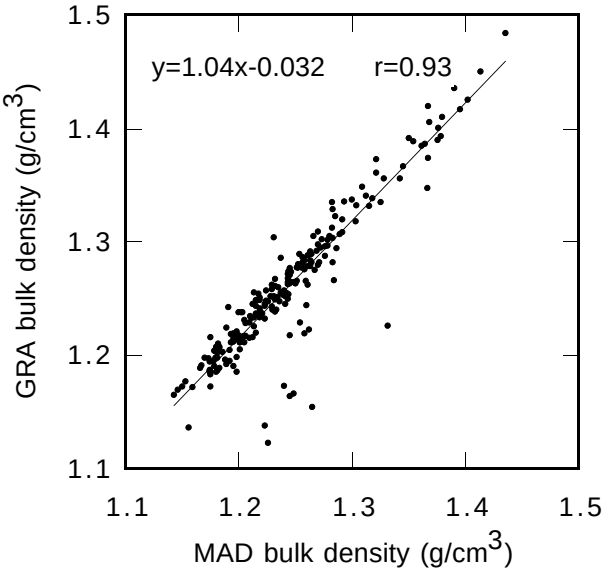

Figure F26. Site 1091 variations in spectral reflectance measurements obtained with the OSU-SCAT (solid line) and Minolta CM-2002 (dashed line) instruments.

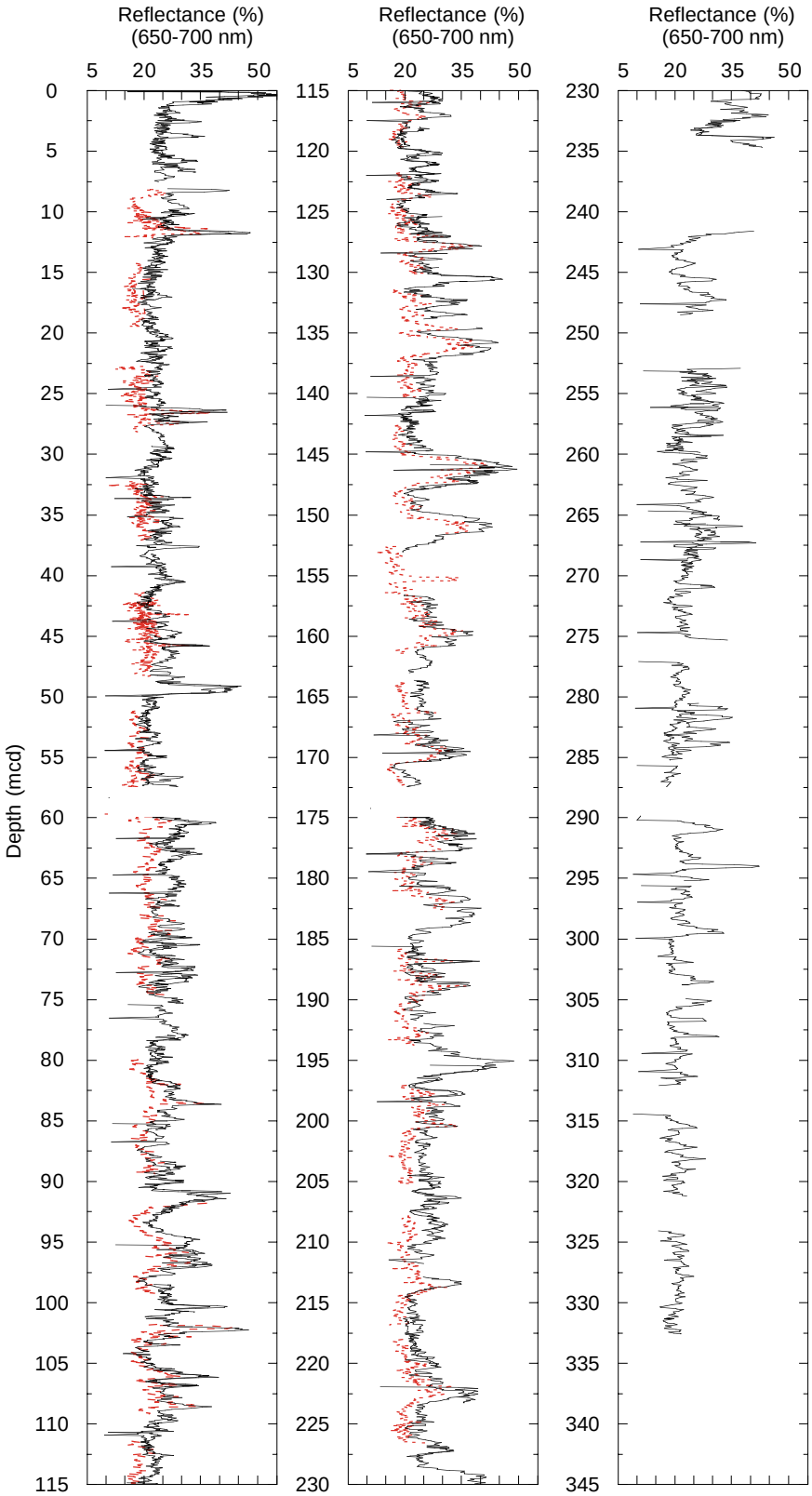

Figure F27. Comparison of blue (450–550 nm) and red (650–750 nm) OSU-SCAT reflectance measurements from Site 1091.

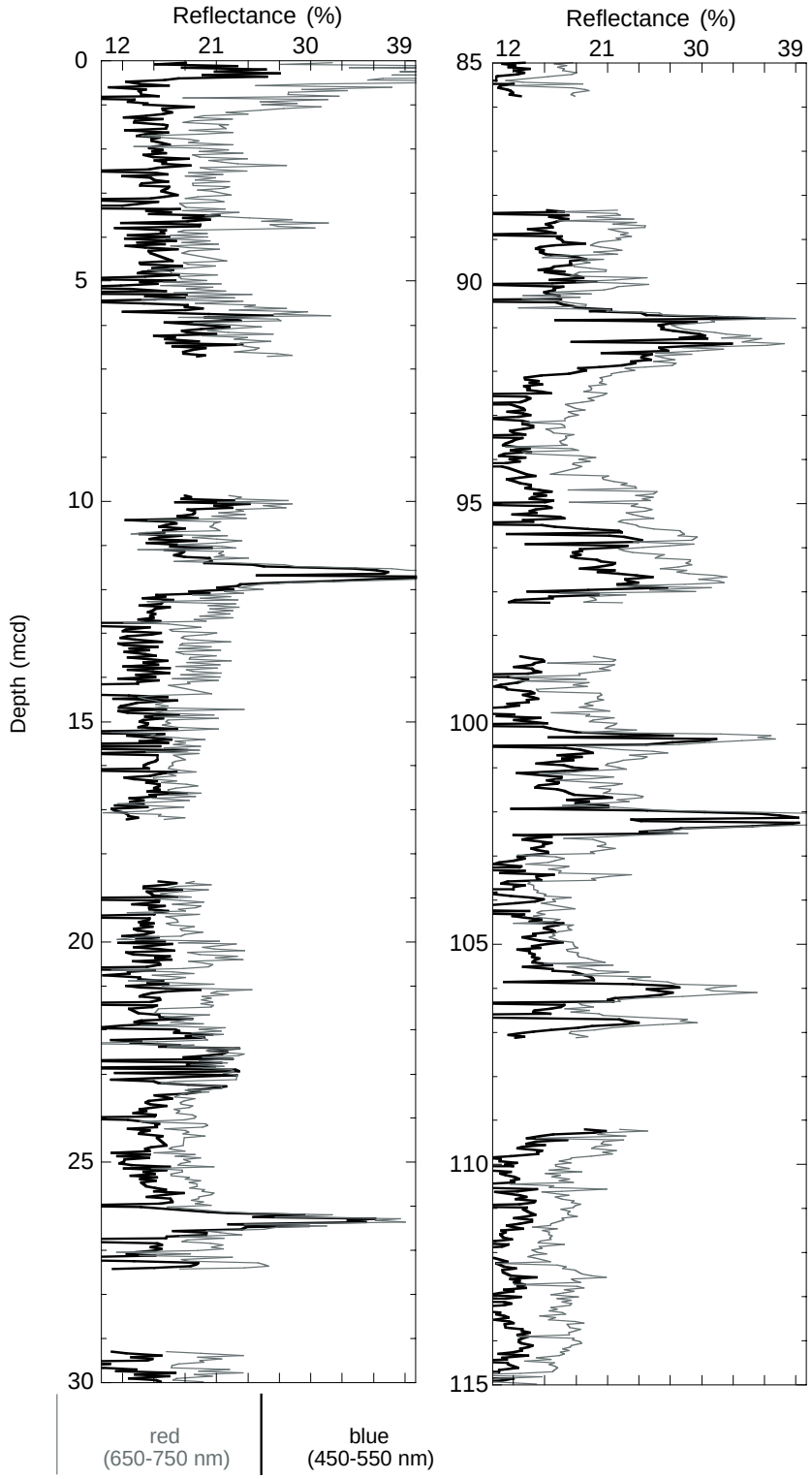

Figure F28. Thermal conductivity measurements of sediment cores at Site 1091. **A.** Frequency distribution of measured values. **B.** Correlation of measured values with interpolated GRA bulk density values. **C.** Thermal conductivity (solid circles) compared to interpolated GRA bulk density (open squares).

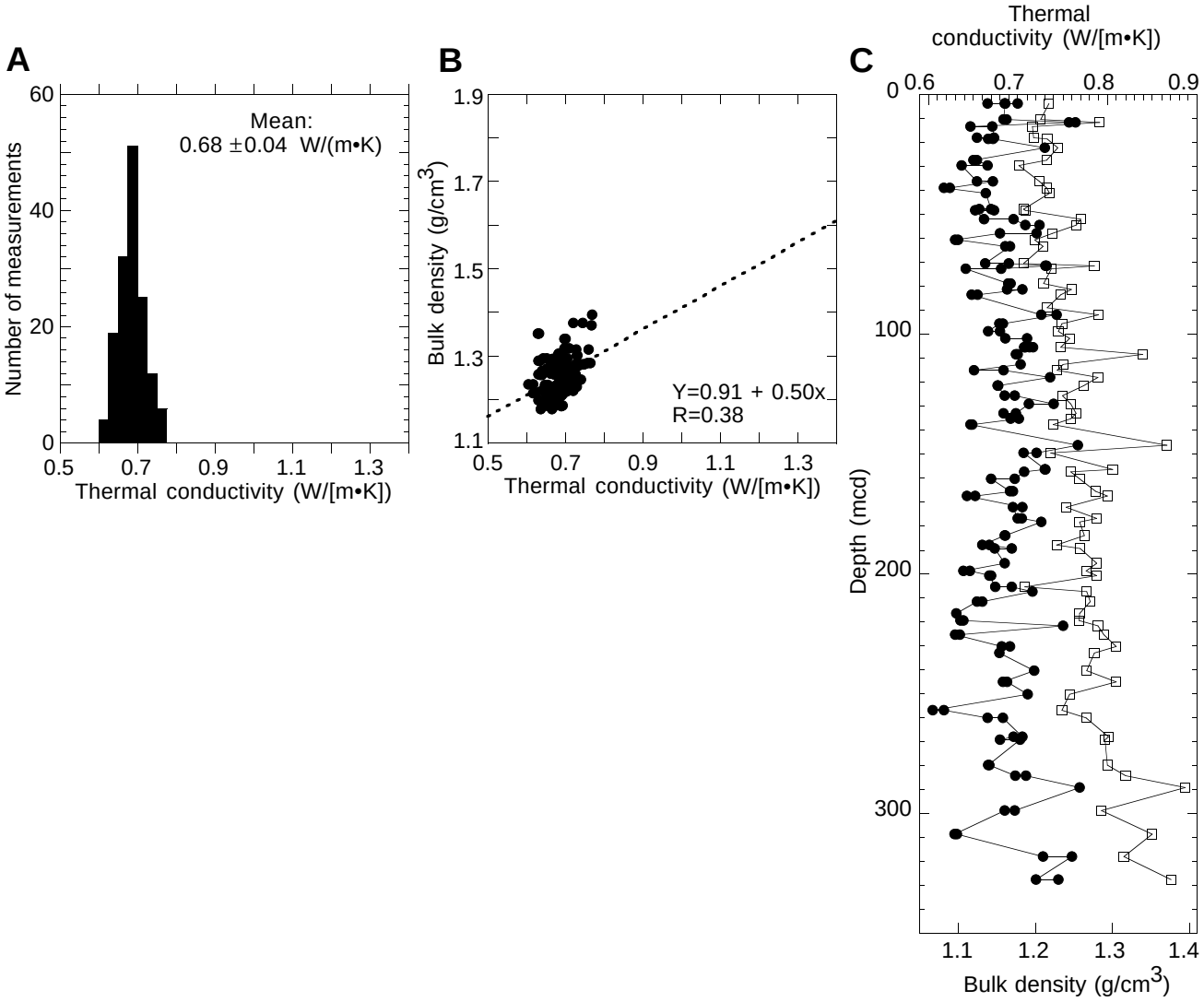

Table T1. X-ray diffraction data for Site 1091.

Core, section, interval (cm)	Depth (mbsf)	Depth (mcd)	Bulk carbonate (wt%; coulometry)	Bulk opal (wt%; XRD peak intensity)	Siliciclastics (wt%)
177-1091A-					
1H-1, 84-85	0.85	0.85	1.8	37.1	61.1
1H-4, 120-121	5.71	5.71	8.6	52.0	39.4
2H-4, 70-71	12.11	15.03	0.4	54.0	45.6
3H-1, 69-70	17.1	19.28	0.6	47.5	51.9
3H-5, 73-74	23.14	25.32	0.2	60.4	39.4
4H-1, 73-74	26.64	29.84	0.02	61.9	38.0
4H-5, 73-74	32.64	35.84	0.3	64.4	35.3
5H-1, 87-88	36.28	38.59	0.5	56.5	43.0
5H-5, 119-120	42.6	44.91	0.6	69.9	29.5
6H-2, 18-19	46.59	50.06	1.1	54.0	44.9
6H-6, 72-73	53.13	56.6	0.4	63.9	35.7
7H-2, 73-74	55.58	59.39	0.6	74.3	25.1
8H-2, 69-70	66.1	70.99	0.4	49.5	50.1
8H-3, 66-67	67.57	72.46	7.4	74.3	18.3
9H-1, 125-126	74.66	79.11	0.4	67.9	31.7
10H-4, 113-115	88.54	93.93	0.2	74.3	25.5
11H-5, 116-117	99.57	105.33	0.6	73.4	26.0
12H-3, 105-107	105.96	113.22	0.7	71.9	27.4
13H-1, 118-119	112.59	119.13	0.5	36.6	62.9
14H-1, 73-74	121.64	130.25	9.9	56.0	34.1
15H-3, 74-75	134.15	143.99	2.1	64.9	33.0
16H-3, 71-72	143.62	157.48	0.7	60.0	39.3
17H-4, 22-23	154.13	166.84	14.8	60.9	24.3
19H-5, 21-22	174.62	190.75	0.6	55.5	43.9
20H-5, 28-29	184.19	201.63	6.4	76.3	17.3
21H-3, 109-111	191.03	207.92	0.8	84.8	14.4
25H-6, 112-113	234.03	255.5	0.8	80.8	18.4
26H-6, 115-116	243.56	265.25	2.7	76.8	20.5
27H-6, 32-33	252.23	273.48	0.6	66.9	32.5
28H-2, 75-76	256.16	278.63	0.7	55.5	43.8
29H-4, 72-73	268.63	290.84	4.4	51.0	44.6
30H-1, 74-75	273.65	296.12	0.6	52.5	46.9
31H-3, 75-76	286.16	308.63	0.6	50.0	49.4
32H-3, 73-74	295.64	318.11	0.5	61.4	38.1
33H-2, 75-76	303.66	326.13	0.5	28.2	71.3
33H-5, 31-32	307.72	330.19	0.6	32.7	66.7

Notes: XRD = X-ray diffraction. This table is also available in ASCII format in the **TABLES** directory.

Table T2. Locations, descriptions, and characteristics of marker beds.

Bed	Core	Top depth (mbsf)	Top depth (mcd)	Thickness (cm)	General description from barrel sheet	Additional data, including nannofossil reworking
	177-					
1	1091A-1H-3	3.5	3.5	3.2	Pale olive graded bed, 5-mm pale basal layer	
	1091B-1H-2	2.4	2.4	1.8	Graded bed with sharp lower contact	
2	1091A-3H-6	25.1	27.3	10(?)	Sharp lower contact	
	1091B-4H-1	28.2	27.3	1.2	Pale brown layer with ~3-mm graded coarse lamina at base	
	1091E-3H-4	18.5	27.5	1.2		
3	1091A-5H-6	43.4	45.7	1.0	Pale green gray	Contains reworked early Pleistocene, early Pliocene, and Oligocene to Eocene nannofossils (1091A)
	1091B-6H-1	46.6	45.7	1.2	Graded bed	
	1091D-5H-2	33.9	45.7	1.2	Pale yellowish tan, sharp contact with thin black layer, overlain by thin foraminifer layer	
	1091E-5H-3	36.0	44.6	1.2		
4	1091A-7H-3	56.5	60.4	1.5	Contains reworked nannofossils (1091A)	
	1091B-7H-5	61.6	60.4	1.6		
	1091D-7H-1	52.4	61.0	25(?)		
5	1091A-9H-4	79.1	83.6	0.7	Light yellow	20.7% $CaCO_3$
	1091D-9H-3	73.8	83.6	1.1	Pale olive, coarser grained, sharp basal contact	
6	1091A-11H-4	97.7	103.4	1.3	Pale olive, with sharp lower contact	Contains reworked early Miocene–Oligocene nannofossils (1091A)
	1091D-11H-2	90.7	103.4	1.1	Pale olive	
7	1091A-16H-3	144.1	158.0	5.9	Tan, sharp contacts	
	1091D-16H-2	139.2	155.1	3.4	Pale brownish gray, turbidite layer (?)	
8	1091A-19H-2	170.6	186.7	1.3	Pinkish tan interval	
	1091B-19H-5	175.5	186.7	1.9	Green brown	
	1091D-19H-1	166.0	186.7	1.9	Pale olive with sharp basal contact	
9	1091A-26H-2	236.7	258.4	0.9	Tan	
	1091B-26H-4	241.2	258.4	0.7	Laminations at bottom	
10	1091A-26H-4	240.4	262.1	0.5	Laminations at bottom	
	1091B-27H-2	248.2	267.2	1.2	Gray interval with scoured base, cross-stratified above and planar laminated above this	

Table T3. Composite depths for Site 1091. (See table note. Continued on next page.)

Core	Depth (mbsf)	Offset (mbsf)	Depth (mcd)
177-1091A-			
1H	0.00	0	0.00
2H	6.90	2.92	9.82
3H	16.40	2.18	18.58
4H	25.90	3.2	29.10
5H	35.40	3.05	38.45
6H	44.90	4.21	49.11
7H	54.40	4.55	58.95
8H	63.90	5.63	69.53
9H	73.40	5.19	78.59
10H	82.90	6.13	89.03
11H	92.40	6.5	98.90
12H	101.90	8	109.90
13H	111.40	7.28	118.68
14H	120.90	9.35	130.25
15H	130.40	10.58	140.98
16H	139.90	14.6	154.50
17H	149.40	13.45	162.85
18H	158.90	15.23	174.13
19H	168.40	16.87	185.27
20H	177.90	18.18	196.08
21H	187.40	17.63	205.03
22H	196.90	19.88	216.78
23H	206.40	21.14	227.54
24H	215.90	22.21	238.11
25H	225.40	22.21	247.61
26H	234.90	22.43	257.33
27H	244.40	21.99	266.39
28H	253.90	23.21	277.11
29H	263.40	22.95	286.35
30H	272.90	23.21	296.11
31H	282.40	23.21	305.61
32H	291.90	23.21	315.11
33H	301.40	23.21	324.61
177-1091B-			
1H	0.00	0	0.00
2H	7.80	0.22	8.02
3H	17.30	-1.14	16.16
4H	26.80	-0.92	25.88
5H	36.30	-0.12	36.18
6H	45.80	-0.23	45.57
7H	55.30	-0.45	54.85
8H	64.80	2.65	67.45
9H	74.30	1.41	75.71
10H	83.80	2.09	85.89
11H	93.30	2.6	95.90
12H	102.80	2.79	105.59
13H	112.30	2.85	115.15
14H	121.80	4.26	126.06
15H	131.30	3.45	134.75
16H	140.80	5.75	146.55
17H	150.30	6.96	157.26
18H	159.80	9.34	169.14
19H	169.30	11.95	181.25
20H	178.80	13.86	192.66
21H	188.30	14.21	202.51
22H	197.80	15.76	213.56
23H	207.30	15.32	222.62
24H	216.80	16.32	233.12
25H	226.30	15.97	242.27
26H	235.80	18.01	253.81
27H	245.30	19.71	265.01
28H	254.80	20.57	275.37
29H	264.30	16.91	281.21
177-1091C-			
1H	0.00	9.79	9.79

Table T3 (continued).

Core	Depth (mbsf)	Offset (mbsf)	Depth (mcd)
177-1091D-			
1H	0.00	7.99	7.99
2H	3.60	11.92	15.52
3H	13.10	10.41	23.51
4H	22.60	9.78	32.38
5H	32.10	12.53	44.63
6H	41.60	9.74	51.34
7H	51.10	9.32	60.42
8H	60.60	7.64	68.24
9H	70.10	10.53	80.63
10H	79.60	12.9	92.50
11H	89.10	13.39	102.49
12H	98.60	13.55	112.15
13H	108.10	14.39	122.49
14H	117.60	14.54	132.14
15H	127.10	16.21	143.31
16H	136.60	16.71	153.31
17H	146.10	18.46	164.56
18H	155.60	19.65	175.25
19H	165.10	21.43	186.53
20H	174.60	23.17	197.77
21H	184.10	24.44	208.54
22H	193.60	25.07	218.67
177-1091E-			
1H	0.00	8.12	8.12
2H	4.20	10.02	14.22
3H	13.70	9.01	22.71
4H	23.20	9	32.20
5H	32.70	9.39	42.09
6H	42.20	14.1	56.30

Note: This table is also available in ASCII format in the **TABLES** directory.

Table T4. Site 1091 splice tie points.

Core, section, interval (cm)	Depth (mbsf)	Depth (mcd)		Core, section, interval (cm)	Depth (mbsf)	Depth (mcd)
177-				177-		
1091B-1H-6, 8	7.58	7.58	Append	1091B-2H-1, 0	7.8	8.02
1091B-2H-3, 80	11.60	11.82	Tie to	1091A-2H-2, 50	8.9	11.82
1091A-2H-5, 50	13.40	16.32	Tie to	1091B-3H-1, 16	17.46	16.32
1091B-3H-5, 132	23.23	22.09	Tie to	1091A-3H-3, 50.5	19.91	22.09
1091A-3H-6, 120	25.10	27.28	Tie to	1091B-4H-1, 140	28.2	27.28
1091B-4H-3, 108	30.88	29.96	Tie to	1091A-4H-1, 86	26.76	29.96
1091A-4H-6, 50	33.90	37.10	Tie to	1091B-5H-1, 92	37.22	37.1
1091B-5H-5, 68	42.98	42.86	Tie to	1091A-5H-3, 141	39.81	42.86
1091A-5H-6, 60	43.50	46.55	Tie to	1091B-6H-1, 97	46.78	46.55
1091B-6H-4, 60	50.90	50.67	Tie to	1091A-6H-2, 6	46.46	50.67
1091A-6H-6, 10	52.50	56.71	Tie to	1091B-7H-2, 36	57.16	56.71
1091B-7H-5, 40	61.70	61.25	Tie to	1091A-7H-3, 36	56.7	61.25
1091A-7H-7, 116	63.50	68.05	Tie to	1091B-8H-1, 60	65.4	68.05
1091B-8H-4, 16	69.46	72.11	Tie to	1091A-8H-2, 108	66.48	72.11
1091A-8H-5, 38	70.28	75.91	Tie to	1091B-9H-1, 20	74.5	75.91
1091B-9H-4, 84	79.64	81.05	Tie to	1091A-9H-2, 96	75.86	81.05
1091A-9H-6, 16	81.06	86.25	Tie to	1091B-10H-1, 36	84.16	86.25
1091B-10H-4, 120	89.50	91.59	Tie to	1091A-10H-2, 106	85.46	91.59
1091A-10H-7, 4	91.94	98.07	Tie to	1091B-11H-2, 66.5	95.47	98.07
1091B-11H-4, 80	98.60	101.20	Tie to	1091A-11H-2, 80	94.7	101.2
1091A-11H-6, 74	100.64	107.14	Tie to	1091B-12H-2, 3.5	104.4	107.1
1091B-12H-4, 144	108.74	111.53	Tie to	1091A-12H-2, 12.5	103.5	111.5
1091A-12H-4, 94	107.34	115.34	Tie to	1091D-12H-3, 18.5	101.8	115.3
1091D-12H-6, 40	106.50	120.05	Tie to	1091A-13H-1, 137	112.8	120
1091A-13H-6, 142	120.32	127.60	Tie to	1091B-14H-2, 4	123.3	127.6
1091B-14H-4, 24	126.54	130.80	Tie to	1091A-14H-1, 54.5	121.5	130.8
1091A-14H-6, 24	128.64	137.99	Tie to	1091B-15H-3, 22	134.5	138
1091B-15H-6, 40	139.20	142.65	Tie to	1091A-15H-2, 16.5	132.1	142.6
1091A-15H-6, 4	137.94	148.52	Tie to	1091B-16H-2, 46.5	142.8	148.5
1091B-16H-5, 84	147.64	153.39	Tie to	1091D-16H-1, 8	136.7	153.4
1091D-16H-6, 100	145.10	161.81	Tie to	1091B-17H-4, 3.5	154.8	161.8
1091B-17H-5, 36	156.66	163.62	Tie to	1091A-17H-1, 76.5	150.2	163.6
1091A-17H-5, 110	156.50	169.95	Tie to	1091B-18H-1, 79.5	160.6	170
1091B-18H-6, 36	167.66	177.00	Tie to	1091D-18H-2, 23.5	157.4	177
1091D-18H-6, 20	163.30	182.95	Tie to	1091B-19H-2, 20	171	183
1091B-19H-5, 44	175.74	187.69	Tie to	1091D-19H-1, 116	166.3	187.7
1091D-19H-5, 95	172.05	193.48	Tie to	1091B-20H-1, 80	179.6	193.5
1091B-20H-5, 17	184.98	198.84	Tie to	1091A-20H-2, 125	180.7	198.8
1091A-20H-4, 53	182.94	201.12	Tie to	1091D-20H-3, 35	178	201.1
1091D-20H-5, 130	181.90	205.07	Tie to	1091B-21H-2, 104	190.9	205.1
1091B-21H-3, 107	192.38	206.59	Tie to	1091A-21H-2, 5	189	206.6
1091A-21H-5, 100	194.03	211.66	Tie to	1091D-21H-3, 12	187.2	211.7
1091D-21H-5, 100	191.10	215.54	Tie to	1091B-22H-2, 48	199.8	215.5
1091B-22H-5, 89	204.70	220.46	Tie to	1091D-22H-2, 28.5	195.4	220.5
1091D-22H-5, 115	200.75	225.82	Tie to	1091B-23H-3, 17	210.5	225.8
1091B-23H-4, 77	212.58	227.90	Tie to	1091A-23H-1, 32	206.8	227.9
1091A-23H-5, 117	213.58	234.72				

Note: This table is also available in ASCII format in the **TABLES** directory.

Table T5. Distribution of main calcareous nannofossil species in Hole 1091A. (**See table note.** Continued on next two pages.)

Core, section, interval (cm)	Depth (mbsf)	Depth (mcd)	Abundance	Preservation	*Dictyococcites antarcticus*	*Reticulofenestra minutula*	*Reticulofenestra minuta*	*Coccolithus pelagicus*	*Pseudoemiliania lacunosa*	*Calcidiscus leptoporus*	*Calcidiscus macintyrei*	*Helicosphaera carteri*	*Gephyrocapsa* small	*Gephyrocapsa caribbeanica*	*Gephyrocapsa* medium (4-5.5 µm)	*Gephyrocapsa* large (>5.5 µm)	*Gephyrocapsa* sp. 3	*Reticulofenestra asanoi*	*Emiliania huxleyi*	Comment
177-1091A-																				
1H-1, 30-30	0.30	0.30	A	M			C	F		A		A	A		A		F		A	
1H-1, 76-76	0.76	0.76	A	M						A		A	A		A		A		F	
1H-3, 83-83	3.83	3.83	A	P			F	F					C		F				A	
2H-1, 30-30	7.20	10.12	R	P				R		R			F				R		R	
2H-2, 28-28	8.68	11.60	A	M				A		D		F	A		A		F		C	
2H-2, 40-40	8.80	11.72	A	M				C		D		A	D		A		A		C	
2H-3, 120-120	11.10	14.02	R	P									R				R		R	
2H-CC, 9-14	14.43	17.35	B																	
3H-6, 26-26	24.16	26.34	A	M				R		C		C		D	F		C		R	
3H-CC, 12-17	25.40	27.58	R	P				C		A			A							
4H-CC, 9-14	34.65	37.85	R	M				R		C			A							
5H-6, 10-10	43.00	45.31	R	M									D		C					Almost barren
5H-6, 51-51	43.41	45.72	C	M				C		C			D	C				R		Reworking
5H-6, 57-57	43.47	45.78	A	M				A		C			D	C				R		Reworking
5H-6, 58-58	43.48	45.79	A	M				A		F			D	C				R		Reworking
5H-CC, 9-15	44.09	46.40	B																	
6H-1, 66-66	45.56	49.03	A	M				R		R		R	D	F	F					
6H-1, 80-80	45.70	49.17	A	M				R		R		R	D	F	C					
6H-1, 120-120	46.10	49.57	C	M				R		R		R	D	C	F					
6H-1, 135-135	46.25	49.72	C	M				R		R		R	D	C	F					
6H-CC, 7-17	53.97	57.44	B																	
7H-3, 26-26	56.60	60.41	R	M				C	R	R			C	F	C			R		Reworking
7H-3, 28-28	56.62	60.43	C	M				C	R	R			C	F	C					Reworking
7H-CC, 15-20	63.71	67.52	B																	
8H-5, 10-10	70.00	74.89	C	M		C			C	F		F	R				R	F		
8H-CC, 15-20	70.62	75.51	R	P				R	R	R										
9H-4, 127-127	79.17	83.62	C	M				A	F	R			F		F			R		High Eocene-Oligocene reworking
9H-4, 128-128	79.18	83.63	C	M									C		F			R		
9H-CC, 11-16	81.48	85.93	R	P				R	R	R			R		R					
10H-2, 99-99	85.39	90.78	A	G		C	A	C	C	A		C	D		C		C			
10H-2, 130-130	85.70	91.09	A	M			A	A	A	A		C	A				A	R		
10H-3, 3-3	85.93	91.32	A	M				A	A	A		R	A				C			
10H-5, 145-145	90.35	95.74	C	P		F	F	C	A	C		F	C				C			
10H-6, 120-120	91.60	96.99	C	P		A	A	R	A	A			A				F	R		
10H-CC, 11-21	92.13	97.52	R	P				R	R	R			R				R			
11H-2, 65-65	94.55	100.31	A	P		C	A	D	A	C		R	A				R			
11H-3, 100-100	96.40	102.16	A	M		F	A	R	C	A			D				F			
11H-6, 45-45	100.35	106.11	A	P		A	A	F	C	A			A				F			Reworking, terrigenous input
11H-6, 110-110	101.00	106.76	F	P		C	C	R	C	F			A				F			
11H-CC, 17-22	101.70	107.46	R	P				R	R	R			R				R			
12H-1, 13-13	102.03	109.29	C	P		F	C		C	C			C				F			
12H-CC, 0-10	109.25	116.51	B																	
13H-4, 104-104	116.94	123.48	A	M		A	A	C	A	D		F			F		C	C		Reworking, terrigenous input
13H-6, 146-146	120.36	126.90	C	P				C	A	F								R		
13H-7, 5-5	120.45	126.99	A	P		A	A	C	A	C		R	C					R		
13H-7, 58-58	120.98	127.52	A	P		C	C	A	A				C				R	F		
13H-CC, 6-16	121.08	127.62	A	M		C	A	D	C	A							R	R		
14H-2, 136-136	123.76	132.37	F	P		F	A	C	C	C			A							
14H-4, 67-67	126.07	134.68	A	P		F	C	C	C	F										
14H-4, 130-130	126.70	135.31	F	P			A	A	C	C			C					R		
14H-5, 30-30	127.20	135.81	A	M			C	D	C	C			F					F		
14H-5, 108-108	127.98	136.59	A	P		C	A	A	C	C			F					R		

Table T5 (continued).

Core, section, interval (cm)	Depth (mbsf)	Depth (mcd)	Abundance	Preservation	*Dictyococcites antarcticus*	*Reticulofenestra minutula*	*Reticulofenestra minuta*	*Coccolithus pelagicus*	*Pseudoemiliania lacunosa*	*Calcidiscus leptoporus*	*Calcidiscus macintyrei*	*Helicosphaera carteri*	*Gephyrocapsa* small	*Gephyrocapsa caribbeanica*	*Gephyrocapsa* medium (4-5.5 µm)	*Gephyrocapsa* large (>5.5 µm)	*Gephyrocapsa* sp. 3	*Reticulofenestra asanoi*	*Emiliania huxleyi*	Comment
14H-CC, 11-21	130.49	139.10	B																	
15H-4, 60-60	135.50	145.34	F	M		F	C	D	A									C		
15H-4, 100-100	135.90	145.74	C	M		F	C	A	C	C		F						F		
15H-4, 135-135	136.25	146.09	C	M		F	C	D	C	C		F						F		
15H-5, 10-10	136.50	146.34	C	M		C	C	D	C	C								R		
15H-5, 35-35	136.75	146.59	C	M		F	C	D	C	C		R								
15H-5, 85-85	137.25	147.09	F	M		C	A		C	A		R						R		
15H-5, 110-110	137.50	147.34	C	M		F	C		F	F								R		
15H-5, 136-136	137.76	147.60	F	M			C		C	C								F		
15H-CC, 11-21	138.37	148.21	B																	
16H-3, 130-130	144.20	158.06	C	M			C	A	F	C		F			C	F				
16H-4, 20-20	144.60	158.46	F	M		F	F	D	F	C		R	F		F	F				
16H-CC, 7-16	148.30	162.16	R	M		A	C			A										
17H-5, 105-105	156.45	169.16	F	P		F	F	F	C	A			F		F	A				Dissolution
17H-5, 121-121	156.61	169.32	C	M		C	C	C	C	C			F		C	A				
17H-5, 140-140	156.80	169.51	F	M		F	C	C	F	F			F		F	A				
17H-5, 145-145	156.85	169.56	C	M		C	C	D	C	F		F	C		F	C				
17H-CC, 11-14	157.79	170.50	R	M		D														Almost barren
18H-3, 4-4	161.94	176.43	F	M		F	F	D	C	F			A		F	C				
18H-3, 40-40	162.30	176.79	F	M		F	F	A	C	F			C		F	C				
18H-4, 77-77	164.17	178.66	F	P		R	F	D	F	F			C		F	A				
18H-6, 36-36	166.76	181.25	F	P		R	C	A	F	F			C		A	A				
18H-CC, 9-16	166.87	181.36	C	M				C	R						F	A				
19H-2, 30-30	170.20	186.33	R	M		F		D	R	F						F				
19H-2, 70-70	170.60	186.73	F	M			A	A	R	A			F		C	F				
19H-3, 70-70	172.10	188.23	C	M		R	R	F	R	F			C		A	F				
19H-3, 102-102	172.42	188.55	C	M		R	F	D	F	F			F		F	F				
19H-3, 130-130	172.70	188.83	F	M		A	F	A	C	R			R		A	R				
19H-CC, 8-14	175.69	191.82	B																	
20H-1, 90-90	178.80	196.24	C	P				C	F	R			R		C					
20H-2, 90-90	180.30	197.74	F	P		C	F	C	C						C					
20H-3, 90-90	181.80	199.24	R	P			C	C					R							
20H-4, 43-43	182.83	200.27	C	P		C	F		F	R					C					
20H-4, 60-60	183.00	200.44	A	M				C	F	A	R				A					
20H-CC, 8-15	184.73	202.17	B																	
21H-CC, 9-14	195.01	211.90	B																	
22H-CC, 8-13	204.24	223.38	F	M				C	R	R			F		A					
23H-1, 30-30	206.70	227.10	R	P					R				C		C					
23H-2, 110-110	209.00	229.40	C	P		A	A	A		A					C					
23H-3, 30-30	209.70	230.10	A	P		A	C	A	C	C					C					
23H-4, 30-30	211.20	231.60	C	P		A	A	C	R	C					F					
23H-5, 110-110	213.50	233.90	A	P		A	A	D	C	F										
23H-CC, 8-13	213.68	234.08	C	M				D	F	R										
24H-CC, 10-15	225.49	246.96	B																	
25H-5, 140-140	232.80	254.27	A	P		D			D											
25H-CC, 0-10	235.14	256.61	B																	
26H-2, 33-33	236.73	258.42	A	M	F	A	A	D	F	F										
26H-4, 105-105	240.45	262.14	F	M	R	C	C	D	F	F										
26H-4, 60-60	240.00	261.69	R	M		A	C	F	C	R										
26H-CC, 18-23	244.03	265.72	B																	
27H-4, 62-62	249.52	270.77	C	M		C	A	D	R	F										
27H-4, 79-79	249.69	270.94	F	P		C	A	A	C	R										
27H-4, 110-110	250.00	271.25	F	P		C	C	A	C	F	R									
27H-7, 70-70	254.10	275.35	C	P		C	D	A	F											
27H-CC, 11-16	254.23	275.48	A	P			D	F	R	R										
28H-1, 10-10	254.00	276.47	C	P		A	A	A	C	F										

Table T5 (continued).

Core, section, interval (cm)	Depth (mbsf)	Depth (mcd)	Abundance	Preservation	*Dictyococcites antarcticus*	*Reticulofenestra minutula*	*Reticulofenestra minuta*	*Coccolithus pelagicus*	*Pseudoemiliania lacunosa*	*Calcidiscus leptoporus*	*Calcidiscus macintyrei*	*Helicosphaera carteri*	*Gephyrocapsa* small	*Gephyrocapsa caribbeanica*	*Gephyrocapsa* medium (4-5.5 µm)	*Gephyrocapsa* large (>5.5 µm)	*Gephyrocapsa* sp. 3	*Reticulofenestra asanoi*	*Emiliania huxleyi*	Comment
28H-1, 96-96	254.86	277.33	C	P		A	A	A	C	C										
28H-4, 40-40	258.80	281.27	R	M		C	D	C												
28H-5, 24-24	260.14	282.61	R	M		F	A	A	F	C										
28H-6, 10-10	261.50	283.97	F	M		F	A	C	C	A										
28H-CC, 22-27	263.22	285.69	B																	
29H-4, 116-116	269.06	291.27	R	P		C	C	A	C	C										
29H-6, 14-14	271.04	293.25	F	P		C	A	A	F	R										
29H-6, 90-90	271.80	294.01	F	P		F	C	D	C	C										
29H-7, 40-40	272.80	295.01	F	P		C	A	A	C	F										
29H-CC, 13-18	273.15	295.36	B																	
30H-3, 110-110	277.00	299.47	F	P		C	A	C	C	F										
30H-3, 110-110	277.00	299.47	F	P		C	A	C	C	F										
30H-CC, 10-15	281.43	303.90	B																	
31H-1, 6-6	282.46	304.93	F	M		A	A		C	F										
31H-2, 145-145	285.35	307.82	R	M		D	F		F											
31H-CC, 13-18	289.76	312.23	B																	
32H-CC, 30-35	299.17	321.64	B																	
33H-CC, 21-26	310.35	332.82	B																	

Notes: Abundance abbreviations: D = dominant, A = abundant, C = common, F = few, R = rare, B = barren. Preservation abbreviations: G = good, M = moderate, P = poor. For more specific definitions, refer to the **"Explanatory Notes"** chapter. The distributions of the species are mainly described in stratigraphic intervals where events are identified. This table is also available in ASCII format in the **TABLES** directory.

Table T6. Summary of biostratigraphic age assignments for Site 1091. (**See table note.** Continued on next two pages.)

Core, section, interval (cm)	Depth (mbsf)	Depth (mcd)	Calcareous nannofossil zone	Calcareous nannofossil age (Ma)	Diatom zone	Diatom age (Ma)	Radiolaria zone	Radiolaria age (Ma)	Comment
177-1091A-									
1H-3, 83-83	3.83	3.83			*T. lentiginosa* Subzone c	0-0.18			
1H-CC, 9-14	6.84	6.84	NN21	<0.26	*T. lentiginosa* Subzone c	0-0.18	Omega	0-0.46	
2H-CC, 9-14	14.43	17.35			*T. lentiginosa* Subzone c	0-0.18	Omega	0-0.46	
3H-CC, 12-17	25.40	27.58			*T. lentiginosa* Subzone b	0.18-0.42	Omega	0-0.46	
4H-CC, 9-14	34.65	37.85			*T. lentiginosa* Subzone b	0.18-0.42			
5H-2, 140-140	38.30	40.61			*T. lentiginosa* Subzone b	0.18-0.42			
5H-5, 130-130	42.70	45.01			*T. lentiginosa* Subzone b	0.18-0.42			
5H-6, 55-55	43.45	45.76			*T. lentiginosa* Subzone b	0.18-0.42			
5H-CC, 9-15	44.09	46.40			*T. lentiginosa* Subzone b	0.18-0.42			
6H-1, 75-75	45.65	49.12			*T. lentiginosa* Subzone b	0.18-0.42			
6H-1, 80.5-80.5	45.71	49.18							
6H-1, 85-85	45.75	49.22			*T. lentiginosa* Subzone b	0.18-0.42			
6H-1, 135-135	46.25	49.72			*T. lentiginosa* Subzone a	0.42-0.65			
6H-CC, 7-17	53.97	57.44	NN20	<0.46	*T. lentiginosa* Subzone a	0.42-0.65	Omega	0-0.46	*A. ingens* reworked
7H-3, 26-26	56.60	60.41	NN19	0.46-0.96					
7H-CC, 15-20	63.71	67.52			*T. lentiginosa* Subzone a	0.42-0.65			
8H-5, 10-10	70.00	74.89	NN19	0.46-0.88					CN: reworking
8H-CC, 15-20	70.62	75.51			*T. lentiginosa* Subzone a	0.42-0.65	Psi	0.46-0.83	*A. ingens* reworked
9H-4, 127-127	79.17	83.62	NN19	0.46-0.88					CN: high Oligocene-Eocene reworking
9H-CC, 11-16	81.48	85.93	NN19	0.46-1.69	*A. ingens* Subzone c	0.65-1.07			
10H-CC, 11-21	92.13	97.52	NN19	0.46-0.96?	*A. ingens* Subzone c	0.65-1.07	Psi	0.46-0.83	
11H-6, 45-45	100.35	106.11	NN19	0.46-0.88					
11H-CC, 17-22	101.70	107.46			*A. ingens* Subzone c	0.65-1.07			
12H-1, 13-13	102.03	109.29	NN19	0.46-0.88					
12H-CC, 0-10	109.25	116.51			*A. ingens* Subzone c	0.65-1.07	Psi	0.46-0.83	
13H-4, 104-104	116.94	123.48	NN19	0.88-0.96					
13H-7, 5-5	120.45	126.99	NN19	>0.88					
13H-7, 88-88	121.28	127.82	NN19	0.88-0.96					
13H-CC, 6-16	121.08	127.62	NN19	0.88-0.96	*A. ingens* Subzone c	0.65-1.07			
14H-4, 130-130	126.70	135.31	NN19	0.96-1.08					
14H-5, 30-30	127.20	135.81	NN19	0.96-1.08					
14H-CC, 16-21	130.54	139.15			*A. ingens* Subzone c	0.65-1.07	Chi	0.83-1.92	
15H-4, 60-60	135.50	145.34	NN19	0.96-1.08					
15H-5, 10-10	136.50	146.34	NN19	0.96-1.08					
15H-5, 136-136	137.76	147.60	NN19	0.96-1.08					
15H-CC, 11-21	138.37	148.21			*A. ingens* Subzone b	1.07-1.3			
16H-3, 130-130	144.20	158.06	NN19	1.24-1.46			Chi	0.83-1.92	
16H-4, 20-20	144.60	158.46	NN19	1.24-1.46					
16H-CC, 11-16	148.34	162.20			*A. ingens* Subzone b	1.07-1.3			
17H-5, 121-121	156.61	169.32	NN19	1.24-1.46					
17H-5, 145-145	156.85	169.56	NN19	1.24-1.46					
17H-CC, 7-14	157.75	170.46			*A. ingens* Subzone b	1.07-1.3			
18H-3, 4-4	161.94	176.43	NN19	1.24-1.46					
18H-4, 77-77	164.17	178.66	NN19	1.24-1.46					
18H-6, 36-36	166.76	181.25	NN19	1.24-1.46					
18H-CC, 11-16	166.89	181.38	NN19	1.24-1.46	*A. ingens* Subzone b	1.07-1.3	Chi	0.83-1.92	
19H-2, 30-30	170.20	186.33	NN19	1.24-1.46					
19H-2, 70-70	170.60	186.73	NN19	1.24-1.46					
19H-3, 70-70	172.10	188.23	NN19	1.24-1.46					
19H-3, 130-130	172.70	188.83	NN19	1.24-1.46					
19H-CC, 9-14	175.70	191.83			*A. ingens* Subzone b	1.07-1.3			CN: barren
20H-1, 90-90	178.80	196.24	NN19	>1.46					
20H-4, 60-60	183.00	200.44	NN19	1.46-1.69					
20H-CC, 8-15	184.73	202.17			*A. ingens* Subzone b	1.07-1.3	Chi	0.83-1.92	CN: barren
21H-2, 53-53	189.43	206.32	NN19	1.46-1.69					
21H-CC, 9-14	195.01	211.90			*A. ingens* Subzone a	1.3-1.8			CN: barren
22H-5, 120-120	204.10	223.24	NN19	1.46-1.69					
22H-CC, 8-13	204.24	223.38	NN19	1.46-1.69	*A. ingens* Subzone a	1.3-1.8	Chi	0.83-1.92	
23H-4, 30-30	211.20	231.60		1.46-1.69					
23H-5, 110-110	213.50	233.90	NN19	>1.69					

Table T6 (continued).

Core, section, interval (cm)	Depth (mbsf)	Depth (mcd)	Calcareous nannofossil zone	Calcareous nannofossil age (Ma)	Diatom zone	Diatom age (Ma)	Radiolaria zone	Radiolaria age (Ma)	Comment
23H-CC, 8-13	213.68	234.08	NN19	>1.69	*A. ingens* Subzone a	?ca. 1.5			
24H-CC, 10-15	225.49	246.96			*A. ingens* Subzone a	1.3-1.8	Chi	0.83-1.92	CN: barren
25H-CC, 0-10	235.14	256.61			*A. ingens* Subzone a	1.3-1.8			CN: barren
26H-2, 33-33	236.73	258.42		>1.69					CN: no zonation
26H-3, 70-70	238.60	260.29			*A. ingens* Subzone a	1.3-1.8			
26H-4, 105-105	240.45	262.14		>1.69					CN: no zonation
26H-5, 70-70	241.60	263.29			*P. barboi*	1.8-2.0			
26H-CC, 18-23	244.03	265.72			*P. barboi*	1.8-2.0	Chi	0.83-1.92	CN: barren
27H-3, 70-70	248.10	269.35			*P. barboi*	1.8-2.0			
27H-4, 62-62	249.52	270.77		>1.69					
27H-6, 70-70	252.60	273.85			*P. barboi*	1.8-2.0			
27H-7, 70-70	254.10	275.35		>1.69					
27H-CC, 11-16	254.23	275.48		>1.69	*P. barboi*	1.8-2.0			
28H-2, 70-70	256.10	278.57			*T. kolbei/F. matuyamae*	2.0-2.5			
28H-5, 70-70	260.60	283.07			*T. kolbei/F. matuyamae*	2.0-2.5			
28H-CC, 22-27	263.22	285.69			*T. kolbei/F. matuyamae*	2.0-2.5	Phi	1.92-2.42	CN: barren
29H-4, 90-90	268.80	291.01			*T. kolbei/F. matuyamae*	2.0-2.5			
29H-6, 120-120	272.10	294.31			*T. kolbei/F. matuyamae*	2.0-2.5			
29H-CC, 13-18	273.15	295.36			*T. vulnifica*	2.5-2.63			CN: barren
30H-2, 45-45	274.85	297.32			*T. vulnifica*	2.5-2.63			
30H-6, 8-8	280.48	302.95			*T. vulnifica*	2.5-2.63			
30H-CC, 10-15	281.43	303.90			*T. vulnifica*	2.5-2.63	Upsilon	2.42-2.61	CN: barren
31H-1, 71-71	283.11	305.58			*T. vulnifica*	2.5-2.63			
31H-5, 112-112	289.52	311.99			*T. vulnifica*	2.5-2.63			
31H-CC, 13-18	289.76	312.23			lower *T. insigna*	2.63-3.3			CN: barren
32H-1, 40-40	292.30	314.77			lower *T. insigna*	2.63-3.3			
32H-3, 68-68	295.58	318.05			lower *T. insigna*	2.63-3.3			
32H-4, 130-130	297.70	320.17			lower *T. insigna*	2.63-3.3			
32H-CC, 30-35	299.17	321.64			lower *T. insigna*	2.63-3.3	Upsilon	2.61-	CN: barren
33H-1, 48-48	301.88	324.35			lower *T. insigna*	2.63-3.3			
33H-2, 30-31	303.20	325.67			lower *T. insigna*	2.63-3.3			
33H-3, 90-90	305.30	327.77			upper *F. interfigidaria*	> 3.3			
33H-4, 116-116	307.06	329.53			upper *F. interfigidaria*	> 3.3			
33H-5, 70-70	308.10	330.57			upper *F. interfigidaria*	> 3.3			
33H-6, 120-120	310.10	332.57			upper *F. interfigidaria*	> 3.3			
33H-CC, 21-26	310.35	332.82			upper *F. interfigidaria*	> 3.3	Upsilon	2.61-	CN: barren
177-1091B-									
1H-CC, 9-14	7.74	7.74			*T. lentiginosa* Subzone c	0-0.18	Omega	0-0.46	
2H-CC, 10-15	14.49	14.71			*T. lentiginosa* Subzone c	0-0.18			
3H-CC, 9-14	23.82	22.68			*T. lentiginosa* Subzone b	0.18-0.42			
4H-CC, 9-14	34.50	33.58			*T. lentiginosa* Subzone b	0.18-0.42			
5H-CC, 9-14	43.47	42.61			*T. lentiginosa* Subzone b	0.18-0.42	Omega	0-0.46	
6H-CC, 9-14	54.04	53.07			*T. lentiginosa* Subzone a	0.42-0.65			
7H-CC, 8-13	64.44	63.25			*T. lentiginosa* Subzone a	0.42-0.65			
8H-CC, 9-14	72.26	74.17			*A. ingens* Subzone c	0.65-1.07			
9H-CC, 11-16	82.88	83.55			*A. ingens* Subzone c	0.65-1.07	Psi	0.46-0.83	
10H-CC, 9-14	91.70	93.05			*A. ingens* Subzone c	0.65-1.07			
11H-CC, 15-20	99.50	101.36			*A. ingens* Subzone c	0.65-1.07			
12H-CC, 0-10	111.42	113.47			*A. ingens* Subzone c	0.65-1.07			
13H-CC, 10-15	122.09	124.20			*A. ingens* Subzone c	0.65-1.07	Chi	0.83-1.92	
14H-CC, 20-25	127.07	130.59	NN19	0.96-1.08	*A. ingens* Subzone c	0.65-1.07			
15H-CC, 11-16	139.86	142.57			*A. ingens* Subzone c	0.65-1.07			
16H-CC, 10-15	148.11	153.12			*A. ingens* Subzone b	1.07-1.3			
17H-CC, 5-10	156.85	163.07			*A. ingens* Subzone b	1.07-1.3	Chi	0.83-1.92	
18H-CC, 9-14	168.07	176.67	NN19	1.24-1.46	*A. ingens* Subzone b	1.07-1.3			
19H-CC, 0-5	177.37	188.58			*A. ingens* Subzone b	1.07-1.3			
20H-CC, 13-17	185.33	198.45			*A. ingens* Subzone b	1.07-1.3			
21H-CC, 9-16	196.21	209.68			*A. ingens* Subzone a	1.3-1.8	Chi	0.83-1.92	CN: barren
22H-CC, 13-18	205.53	220.55			*A. ingens* Subzone a	1.3-1.8			CN: barren
23H-CC, 9-16	213.72	228.30			*A. ingens* Subzone a	1.3-1.8			CN: barren
24H-CC, 0-6	219.13	234.71		>1.69	*A. ingens* Subzone a	1.3-1.8			CN: no zonation
25H-CC, 8-14	233.34	248.57			*A. ingens* Subzone a	1.3-1.8	Chi	0.83-1.92	
26H-CC, 10-15	243.08	260.35			*A. ingens* Subzone a	1.3-1.8			

Table T6 (continued).

Core, section, interval (cm)	Depth (mbsf)	Depth (mcd)	Calcareous nannofossil zone	Calcareous nannofossil age (Ma)	Diatom zone	Diatom age (Ma)	Radiolaria zone	Radiolaria age (Ma)	Comment
27H-CC, 12-17	250.88	269.85			*P. barboi*	1.8-2.0	Chi	0.83-1.92	
28H-CC, 20-25	255.60	275.43			*P. barboi*	1.8-2.0	Chi	0.83-1.92	
29H-CC, 11-16	268.87	285.04			*T.kolbei/F. matuyamae*	2.0-2.5	Phi	1.92-2.42	
177-1091C-									
1H-CC, 7-12	3.90	3.90	NN21	<0.26	*T. lentiginosa* Subzone c	0-0.18	Omega	0-0.46	
177-1091D-									
1H-CC, 0-10	3.51	11.50	NN21	<0.26	*T. lentiginosa* Subzone c	0-0.18			
2H-CC, 15-20	6.62	18.54			*T. lentiginosa* Subzone c	0-0.18			
3H-CC, 9-14	17.02	27.43			*T. lentiginosa* Subzone b	0.18-0.42	Omega	0-0.46	
4H-CC, 6-11	27.45	37.23			*T. lentiginosa* Subzone b	0.18-0.42			
5H-CC, 11-16	36.17	47.96	NN20	0.26-0.46	*T. lentiginosa* Subzone b	0.18-0.42			
6H-CC, 12-17	49.80	58.80			*T. lentiginosa* Subzone a	0.42-0.65			
7H-CC, 10-15	58.99	67.57			*A. ingens* Subzone c	0.65-1.07	Psi	0.46-0.83	
8H-CC, 10-15	67.83	74.73	NN19	>0.46	*A. ingens* Subzone c	0.65-1.07			
9H-CC, 10-15	79.74	89.53			*A. ingens* Subzone c	0.65-1.07			
10H-CC, 9-14	87.28	99.44			*A. ingens* Subzone c	0.65-1.07			
11H-CC, 25-30	96.85	109.50			*A. ingens* Subzone c	0.65-1.07			
12H-CC, 28-35	107.19	120.00			*A. ingens* Subzone c	0.65-1.07			
13H-CC, 9-16	116.62	130.27			*A. ingens* Subzone c	0.65-1.07			
14H-CC, 0-6	126.60	140.40			*A. ingens* Subzone c	0.65-1.07			
15H-CC, 7-14	136.13	151.60	NN19	1.08-1.24	*A. ingens* Subzone b	1.07-1.3	Chi	0.83-1.92	
16H-CC, 9-14	145.60	161.57			*A. ingens* Subzone b	1.07-1.3			
17H-CC, 8-15	155.24	172.96			*A. ingens* Subzone b	1.07-1.3			
18H-CC, 8-15	163.95	182.86	NN19	>1.24	*A. ingens* Subzone b	1.07-1.3			
19H-CC, 14-19	173.24	193.93			*A. ingens* Subzone b	1.07-1.3	Chi	0.83-1.92	
20H-CC, 10-17	182.89	205.32			*A. ingens* Subzone b	1.3-1.8			
21H-CC, 9-16	193.33	217.03			*A. ingens* Subzone a	1.3-1.8			
22H-CC, 12-18	202.42	226.75	NN19	>1.46	*A. ingens* Subzone a	1.3-1.8	Chi	0.83-1.92	
177-1091E-									
1H-CC, 10-15	4.19	12.31	NN21	<0.26	*T. lentiginosa* Subzone c	0-0.18			
2H-CC, 0-10	9.52	19.54			*T. lentiginosa* Subzone c	0-0.18	Omega	0-0.46	
3H-CC, 10-15	19.46	28.47	NN20?	<0.46	*T. lentiginosa* Subzone b	0.18-0.42			
4H-CC, 9-14	27.02	36.02			*T. lentiginosa* Subzone b	0.18-0.42	Omega	0-0.46	
5H-CC, 6-11	39.78	48.43			*T. lentiginosa* Subzone b	0.18-0.42			
6H-CC, 12-17	47.17	60.53			*T. lentiginosa* Subzone a	0.42-0.65	Psi	0.46-0.83	

Notes: CN = calcareous nannofossil. This table is also available in ASCII format in the **TABLES** directory.

Table T7. Distribution of major planktic foraminifer species at Site 1091. (**See table note.** Continued on next page.)

Core, section, interval (cm)	Depth (mbsf)	Depth (mcd)	Abundance	Preservation	*Globigerina bulloides*	*Globigerina quinqueloba*	*Globigerinita glutinata*	*Globigerinita uvula*	*Globorotalia inflata*	*Globorotalia puncticulata*	*Globorotalia puncticuloides*	*Globorotalia scitula*	*Globorotalia truncatulinoides*	*Neogloboquadrina pachyderma* (sinistral)	*Neogloboquadrina pachyderma* (dextral)
177-1091A-															
1H-CC, 9-14	6.84	6.84	A	M		P	P							D	
2H-CC, 9-14	14.43	17.35	R	M		P								D	
3H-CC, 12-17	25.40	27.58	R	M	F									D	
4H-CC, 9-14	34.65	37.85	R	P	D				F		R			F	R
5H-CC, 9-15	44.09	46.40	R	P	R						P			D	
6H-CC, 7-17	53.97	57.44	F	G										D	
7H-CC, 15-20	63.71	67.52	R	G			P	P						D	
8H-CC, 15-20	70.62	75.51	C	G		C		F						D	
9H-CC, 11-16	81.48	85.93	R	G		R								D	
10H-CC, 11-21	92.13	97.52	C	G				A			R			D	
11H-CC, 17-22	101.70	107.46	F	G										D	
12H-CC, 0-10	109.25	116.51	F	G										D	
13H-CC, 6-16	121.08	127.62	C	G		F					F			D	
14H-CC, 16-21	130.54	139.15	R	G		P								D	
15H-CC, 11-21	138.37	148.21	C	G		P					P			D	
16H-CC, 11-16	148.34	162.20	C	G	P	F					P			D	
17H-CC, 7-14	157.75	170.46	C	G	P	R					P			D	
18H-CC, 11-16	166.89	181.38	A	G		A				R	F			D	
19H-CC, 9-14	175.70	191.83	R	G		P					P			D	
20H-CC, 8-15	184.73	202.17	R	G		F								D	
21H-CC, 9-14	195.01	211.90	F	G	A	F								D	
22H-CC, 8-13	204.24	223.38	A	G		D					P			D	
23H-CC, 8-13	213.68	234.08	A	G	F	A				F	F			D	
24H-CC, 10-15	225.49	246.96	R	G										D	
25H-CC, 0-10	235.14	256.61	B												
26H-CC, 18-23	244.03	265.72	R	P										D	
27H-CC, 11-16	254.23	275.48	R	G	P					D				P	
28H-CC, 22-27	263.22	285.69	R	G		P								D	
29H-CC, 13-18	273.15	295.36	F	G	R	F					P			D	
30H-CC, 10-15	281.43	303.90	R	G										P	
31H-CC, 13-18	289.76	312.23	B												
32H-CC, 30-35	299.17	321.64	B												
33H-CC, 21-26	310.35	332.82	B												
177-1091B-															
1H-CC, 9-14	7.74	7.74	A	G		A								D	P
2H-CC, 10-15	14.49	14.71	R	M	D									D	
3H-CC, 9-14	23.82	22.68	R	G	P	P								D	
4H-CC, 9-14	34.50	33.58	R	G	P	P								D	
5H-CC, 9-14	43.47	42.61	R	G	P				P					D	
6H-CC, 9-14	54.04	53.07	A	G	F				P					D	
7H-CC, 8-13	64.44	63.25	F	G	P									D	
8H-CC, 9-14	72.26	74.17	F	G		F								D	
9H-CC, 11-16	82.88	83.55	A	G		F								D	
10H-CC, 9-14	91.70	93.05	R	G										D	
11H-CC, 15-20	99.50	101.36	B												
12H-CC, 0-10	111.42	113.47	R	G						P				D	
13H-CC, 10-15	122.09	124.20	R	G						P				D	
14H-CC, 20-25	127.07	130.59	A	G						F	A			D	
15H-CC, 11-16	139.86	142.57	C	G		F				P				D	

Table T7 (continued).

Core, section, interval (cm)	Depth (mbsf)	Depth (mcd)	Abundance	Preservation	*Globigerina bulloides*	*Globigerina quinqueloba*	*Globigerinita glutinata*	*Globigerinita uvula*	*Globorotalia inflata*	*Globorotalia puncticulata*	*Globorotalia puncticuloides*	*Globorotalia scitula*	*Globorotalia truncatulinoides*	*Neogloboquadrina pachyderma* (sinistral)	*Neogloboquadrina pachyderma* (dextral)
16H-CC, 10-15	148.11	153.12	R	G										D	
17H-CC, 5-10	156.85	163.07	F	G										D	
18H-CC, 9-14	168.07	176.67	F	G		R				R				D	R
19H-CC, 0-5	177.37	188.58	R	G						D				D	
20H-CC, 13-17	185.33	198.45	C	G		F								D	
21H-CC, 9-16	196.21	209.68	R	G		P			P					D	
22H-CC, 11-18	205.51	220.53	B												
23H-CC, 9-16	213.72	228.30	R	G										P	
24H-CC, 0-6	219.13	234.71	R	G		D								A	
25H-CC, 8-14	233.34	248.57	R	G		P								D	
26H-CC, 10-15	243.08	260.35	B												
27H-CC, 12-17	250.88	269.85	F	G	P									D	
28H-CC, 20-25	255.60	275.43	A	G	R	A				F	F			D	
29H-CC, 11-16	268.87	285.04	B												
177-1091C-															
1H-CC, 7-12	3.90	3.90	A	G	A									D	
177-1091D-															
1H-CC, 0-10	3.51	11.50	A	G	D				F				P	A	
2H-CC, 15-20	6.62	18.54	R	G										D	
3H-CC, 9-14	17.02	27.43	F	G	A				P					D	R
4H-CC, 6-11	27.45	37.23	R	G	P									P	
5H-CC, 11-16	36.17	47.96	R	G	D									D	
6H-CC, 12-17	49.80	58.80	R	G										P	
7H-CC, 10-15	58.99	67.57	B												
8H-CC, 10-15	67.83	74.73	C	G		A								D	
9H-CC, 10-15	79.74	89.53	R	G		D								D	
10H-CC, 9-14	87.28	99.44	C	G										D	
11H-CC, 25-30	96.85	109.50	F	G	R	F				F				D	
12H-CC, 28-35	107.19	120.00	C	G		A				R	R			D	
13H-CC, 9-16	116.32	130.27	C	G										D	
15H-CC, 7-14	136.13	151.60	A	G		F				R	F			D	
16H-CC, 9-14	145.60	161.57	A	G		A								D	
17H-CC, 8-15	155.24	172.96	A	G		A				F				D	
18H-CC, 8-15	163.95	182.86	A	G		A				F	F			D	
19H-CC, 14-19	173.24	193.93	R	G						P				D	
20H-CC, 10-17	182.89	205.32	B												
21H-CC, 9-16	193.33	217.03	F	G		F								D	
22H-CC, 12-18	202.42	226.75	C	G		F								D	P
177-1091E-															
1H-CC, 10-15	4.19	12.31	C	G	F				R					D	
2H-CC, 0-10	9.52	19.54	R	G										D	
3H-CC, 10-15	19.46	28.47	R	G	P									P	
4H-CC, 9-14	27.02	36.02	R	G										D	
5H-CC, 6-11	39.78	48.43	R	G	P									P	
6H-CC, 12-17	47.17	60.53	R	G										D	

Notes: Abundance abbreviations: C = common, F = few, R = rare, B = barren. Preservation abbreviations: G = good, M = moderate, P = poor. For more specific definitions, refer to the **"Explanatory Notes"** chapter. This table is also available in ASCII format in the **TABLES** directory.

Table T8. Distribution of benthic foraminifers at Site 1091. (See table note. Continued on next page.)

Core, section, interval (cm)	Depth (mbsf)	Depth (mcd)	Abundance	Preservation	*Alabaminella weddelensis*	*Ammodiscus* sp.	*Anomalinoides* sp.	*Bolivina* spp.	*Cassidulina obtusa*	*Chilostomella oolina*	*Cibicidoides* spp.	*Cibicidoides micrus*	*Cibicidoides mundulus*	*Cibicidoides* aff. *wuellerstorfi*	*Cribrostomoides* sp.	*Cyclammina* sp.	*Dentalina* sp.	*Eggerella bradyi*	*Epistominella exigua*	*Fissurina* spp.	*Francesita* sp.	*Globobulimina* sp.	*Gyroidinoides soldanii*	*Gyroidinoides* spp.	Indeterminates (agg.)	Indeterminates (calc.)	*Islandiella* sp.	*Karreriella bradyi*	*Lagena* spp.	*Laticarinina pauperata*	*Lenticulina* sp.	*Martinottiella* sp.	*Melonis barleeanum*	*Melonis pompilioides*	*Miliolinella* sp.	*Nodosaria* spp.	*Nonionella* sp.	*Nuttallides umbonifera*	*Oolina* spp.	*Ophthalmidium* spp.	*Oridorsalis umbonatus*	*Parafissurina* sp.	*Polymorphina* spp.	*Pullenia bulloides*	*Pullenia quinqueloba*	*Pullenia subcarinata*	*Pyrgo murrhina*	*Pyrgo* spp.	*Quinqueloculina* sp.	*Siphotextularia* sp.	*Sphaeroidina bulloides*	*Stainforthia loeblichi*	*Stainforthia* sp.	*Triloculina trigonula*	*Triloculina trihedra*	Sample sum	Number of species	Abundance (specimens/cm^3)
177-1091A-																																																										
1H-CC, 9-14	6.84	6.84	C	G							3						3			2							6		3		1			8		1				2	10	6		5	15		1		1	4	1				1	73	22	7.3
2H-CC, 9-14	14.43	17.35	F	G	21															2							3		3			1		3					1					1	8	4	1					5				53	15	2.65
3H-CC, 12-17	25.4	27.58	C	G	14						1																8		2		1			3	1		1				2				18	19	2					9	3			84	15	8.4
4H-CC, 9-14	34.65	37.85	B																																																					0		0
5H-CC, 9-15	44.09	46.4	R	M	2													1																											1	5										9	4	0.45
6H-CC, 7-17	53.97	57.44	B																																																					0		0
7H-CC, 15-20	63.71	67.52	R	M				1											2																											4										7	3	0.35
8H-CC, 15-20	70.62	75.51	C	G	39			2			7									1		1				6	3		2				5				1				3				8	5	1	1					22	1	2	110	21	11
9H-CC, 11-16	81.48	85.93	F	M																2						5			1															1		9			2				3			23	7	2.3
10H-CC, 11-21	92.13	97.52	F	M	1						1									1						19										1									2	8						1				34	8	3.4
11H-CC, 17-22	101.7	107.46	F	M	8						1		7							1				2			3	1					2						1				1	1	8								1			37	13	3.7
12H-CC, 0-10	109.25	116.51	F	G	2																																							1		6										9	3	1.8
13H-CC, 6-16	121.08	127.62	C	M							1	1		5				6	1	2									1		2			11	1									6	2	1	4		5	4	4					57	18	8.55
14H-CC, 16-21	130.54	139.15	F	P							2									1														4												1										8	4	0.4
15H-CC, 11-21	138.37	148.21	F	M							4									1														3											2	6	1									17	6	0.85
16H-CC, 11-16	148.34	162.2	F	G	1								1	6			1	4		2	2					1	2							5							2			3				2								32	14	1.6
17H-CC, 7-14	157.75	170.46	F	M									1	2				3	1	1														9							1			1		4	1									24	10	1.2
18H-CC, 11-16	166.89	181.38	C	M										14			2	8		12							3							21							3	1		6	4	2	2		5	4						87	16	4.35
19H-CC, 9-14	175.7	191.83	R	M																														3												2										5	2	0.25
20H-CC, 8-15	184.73	202.17	F	P																	1													2												6	3		2						3	17	6	0.85
21H-CC, 9-14	195.01	211.9	B																																																					0		0
22H-CC, 8-13	204.24	223.38	C	G										11				25		3	1			11					1		2			38	1						5	1		10	7	9	3		7	2					1	138	19	6.9
23H-CC, 8-13	213.68	234.08	F	M					3		3							1		1						2				1				10					1		5	2		15			1								1	46	13	2.3
24H-CC, 10-15	225.49	246.96	R	M																														2																						2	1	0.1
25H-CC, 0-10	235.14	256.61	B																																																					0		0
26H-CC, 18-23	244.03	265.72	F	P									5		1		1	1	1	2					5	1	7			4	1													1												30	12	1.5
27H-CC, 11-16	254.23	275.48	C	M			13							59			4	41		22				9		2	13	1	2		6		1	29					7	1	65			20	3	13				4						315	29	15.75
28H-CC, 22-27	263.22	285.69	R	M																1														2	1						1															5	4	0.25
29H-CC, 13-18	273.15	295.36	R	M														2		1														3							1						1		6							14	6	0.7
30H-CC, 10-15	281.43	303.9	R	P									1											1										3							1															6	4	0.3
31H-CC, 13-18	289.76	312.23	R	G																					1																															1	1	0.05
32H-CC, 30-35	299.17	321.64	R	M							1																					3																								4	2	0.2
33H-CC, 21-26	310.35	332.82	R	P																												1																								1	1	0.05
177-1091B-																																																										
1H-CC, 9-14	7.74	7.74	C	M	16		1				6						2			5				14		2	7		2					8							4	2		5	24	2			3	1		3				107	20	21.4
2H-CC, 10-15	14.49	14.71	R	M																																									2		1									3	2	0.15
3H-CC, 9-14	23.82	22.68	R	P			1									1							1			1						2									1			1												8	7	0.4

Table T8 (continued).

Core, section, interval (cm)	Depth (mbsf)	Depth (mcd)	Abundance	Preservation	*Alabaminella weddelensis*	*Ammodiscus* sp.	*Anomalinoides* sp.	*Bolivina* spp.	*Cassidulina obtusa*	*Chillostomella oolina*	*Cibicidoides* spp.	*Cibicidoides micrus*	*Cibicidoides mundulus*	*Cibicidoides* aff. *wuellerstorfi*	*Cribrostomoides* sp.	*Cyclammina* sp.	*Dentalina* sp.	*Eggerella bradyi*	*Epistominella exigua*	*Fissurina* spp.	*Francesita* sp.	*Globobulimina* sp.	*Gyroidinoides soldanii*	*Gyroidinoides* spp.	Indeterminates (agg.)	Indeterminates (calc.)	*Islandiella* sp.	*Karreriella bradyi*	*Lagena* spp.	*Laticarinina pauperata*	*Lenticulina* sp.	*Martinotiella* sp.	*Melonis barleeanum*	*Melonis pompilioides*	*Miliolinella* sp.	*Nodosaria* spp.	*Nonionella* sp.	*Nuttallides umbonifera*	*Oolina* spp.	*Ophthalmidium* spp.	*Oridorsalis umbonatus*	*Parafissurina* sp.	Polymorphinid spp.	*Pullenia bulloides*	*Pullenia quinqueloba*	*Pullenia subcarinata*	*Pyrgo murrhina*	*Pyrgo* spp.	*Quinqueloculina* sp.	*Siphotextularia* sp.	*Sphaeroidina bulloides*	*Stainforthia loeblichi*	*Stainforthia* sp.	*Triloculina trigonula*	*Triloculina trihedra*	Sample sum	Number of species	Abundance (specimens/cm^3)
4H-CC. 9-14	34.5	33.58	R	G																																									1											1	1	0.05
5H-CC. 9-14	43.47	42.61	R	M											1																														1	3										5	3	0.25
6H-CC. 9-14	54.04	53.07	F	G										3					1	2																			1		1			1	2											11	7	0.55
7H-CC. 8-13	64.44	63.25	F	M						1	3										1			1	1						1			1					1						3	3	2		1		1					20	13	1
8H-CC. 9-14	72.26	74.17	F	M			1							1		2		2		2						2						1		1							16	1				1										30	12	1.5
9H-CC. 11-16	82.88	83.55	C	G										10						6	2						1		1					15	3	1					2			6	7	23	4			2			4	1		88	16	4.4
10H-CC. 9-14	91.7	93.05	R	M																						1								1	1											4										7	4	0.35
11H-CC. 15-20	99.5	101.36	R	M																					1																					2										3	2	0.15
12H-CC. 0-10	111.42	113.47	R	M																																										1										1	1	0.05
13H-CC. 10-15	122.09	124.2	R	M																														1												1										2	2	0.1
14H-CC. 20-25	127.07	130.59	C	G										3			1	3		2				2	2				1	1				3							4			7		4	2		1	1						37	16	7.4
15H-CC. 11-16	139.86	142.57	F	P										1							1			1										1											2		1									7	6	0.35
16H-CC. 10-15	148.11	153.12	F	M														1																9												3										13	3	0.65
17H-CC. 5-10	156.85	163.07	R	P																														3																						3	1	0.15
18H-CC. 9-14	168.07	176.67	F	M														1		1					1				1					2	1						3			1	4											15	9	0.75
19H-CC. 0-5	177.37	188.58	C	M										9				27	5	5					3		9	1						12				5			20			20						6						122	14	10.16
20H-CC. 13-17	185.33	198.45	F	M										5	1			5		3	1			2			1		2					1	1				1		6			3	7		5		1	6						51	17	2.55
21H-CC. 9-16	196.21	209.68	R	M														1																2				1																		4	3	0.2
22H-CC. 11-18	205.51	220.53	R	P																										1				1									2													4	3	0.2
23H-CC. 9-16	213.72	228.3	F	P							3					1	1	1									1							1							2			8	2											20	9	1
24H-CC. 0-6	219.13	234.71	R	P														1	1				1				1		1																											5	5	0.25
25H-CC. 8-14	233.34	248.57	R	M																														3																						3	1	0.15
26H-CC. 10-15	243.08	260.35	R	M																																																	1			1	1	0.05
27H-CC. 12-17	250.88	269.85	F	M										1				3		1	1			4			1				1			4							4					1										21	10	1.05
28H-CC. 20-25	255.6	275.43	F	M		1								15				4									1							10	1						1				4	1	4									42	10	2.1
29H-CC. 11-16	268.87	285.04	B																																																					0		

Notes: Abundance abbreviations: C = common, F = few, R = rare, B = barren. Preservation abbreviations: G = good, M = moderate, P = poor. For more specific definitions, refer to the **"Explanatory Notes"** chapter. This table is also available in ASCII format in the **TABLES** directory.

Table T9. Diatom, silicoflagellate, ebridian, *Actiniscus*, sponge spicule, and phytolith occurrence in smear slides investigated from Site 1091. (**See table note.** Continued on next five pages.)

Core, section, interval (cm)	Depth (mbsf)	Depth (mcd)	Abundance	Preservation	Silicoflagellate occurrence	Ebridian occurrence	*Actiniscus* occurrence	Sponge spicule occurrence	Opaline phytolith occurrence	*Actinocyclus actinochilus*	*Actinocyclus praeactinochilus*	*Actinocyclus curvatulus*	*Actinocyclus dimorphus*	*Actinocyclus fasciculatus*	*Actinocyclus ingens*	*Actinocyclus ingens* var. *ovalis*	*Actinocyclus karstenii*	*Asteromphalus hookeri*	*Asteromphalus parvulus*	*Azpeitia tabularis*	*Chaetoceros* spp.	*Coscinodiscus marginatus*	*Ethmodiscus rex*	*Eucampia antarctica*	*Fragilariopsis angulata*	*Fragilariopsis barronii*	*Fragilariopsis curta*	*Fragilariopsis fossilis*	*Fragilariopsis interfrigidaria*	*Fragilariopsis kerguelensis*	*Fragilariopsis matuyamae*	*F. matuyamae* var. *heteropolara*	*Fragilariopsis praecurta*	*Fragilariopsis reinholdii*	*Fragilariopsis ritscheri*	*Fragilariopsis separanda*	*Fragilariopsis weaveri*	*Fragilariopsis* sp. A (Gersonde, 1991)	*Hemidiscus cuneiformis*	*Hemidiscus karstenii*	*Proboscia barboi*	*Rhizosolenia antennata* fo. *semispina*	*Rhizosolenia hebetata* fo. *semispina*	*Rhizosolenia styliformis*
177-1091A-																																										
1H-3, 83-83	3.83	3.83	F	M	B	B	B	B	B						F					F			R					F										R				
1H-CC, 9-14	6.84	6.84	A	G	B	B	B	B	B											F			F					A														
2H-CC, 9-14	14.43	17.35	A	M	B	B	B	B	B											R	F		R					D														
3H-CC, 12-17	25.40	27.58	A	G	T	B	B	B	B														R					D														
4H-CC, 9-14	34.65	37.85	A	G	T	B	B	B	B						T					R			R					D										R				
5H-5, 130-130	42.70	45.01	A	G	T	B	B	B	B											R								D														
5H-6, 55-55	43.45	45.76	A	G	T	B	B	B	B											F								D														
5H-CC, 9-15	44.09	46.40	A	G	B	B	B	B	B											R			R					D														
6H-1, 75-75	45.65	49.12	A	G	T	B	B	B	B														R					A										R				
6H-1, 80.5-80.5	45.71	49.18	C	M	T	B	B	B	B	R										R	R		R					C										R				
6H-1, 135-135	46.25	49.72	C	M	T	B	B	B	B											R			F			R		A														
6H-CC, 7-17	53.97	57.44	A	G	T	B	B	B	B	R										F			R					A							R							
7H-CC, 15-20	63.71	67.52	A	G	T	B	B	B	B	T					R		R				R		R	T				A					R	R							
8H-CC, 15-20	70.62	75.51	A	G	B	B	B	B	B						R		R				R		R	R				A													
9H-CC, 11-16	81.48	85.93	A	G	B	B	B	B	B						F													A														
10H-CC, 11-21	92.13	97.52	A	G	T	B	B	X	B						F				T		R		F	T				A						T							
11H-CC, 17-22	101.70	107.46	A	G	T	B	B	B	B						F				T		R							C						T							
12H-CC, 0-10	109.25	116.51	A	G	T	B	B	B	B						F					R								C													
13H-CC, 6-16	121.08	127.62	A	G	R	B	B	B	B						F				T	R			R	T				C						T							
14H-CC, 16-21	130.54	139.15	A	G-M	T	B	B	B	B						F						F				T			C						R							
15H-CC, 11-21	138.37	148.21	A	M	R	B	B	B	B						F		T			R	R		X	R		T		C													
16H-CC, 11-16	148.34	162.20	A	G	B	B	B	B	B						A					R								A													
17H-CC, 7-14	157.75	170.46	A	G	T	B	X	B	B						C									R				C													
18H-CC, 11-16	166.89	181.38	C	M	B	B	B	B	B						A																										
19H-CC, 9-14	175.70	191.83	A	G	B	B	B	B	B						D													R													
20H-CC, 8-15	184.73	202.17	A	G	T	B	X	B	B						D									R	F			F													
21H-CC, 9-14	195.01	211.90	A	G	R	B	B	B	B						A		T			R			X	R	F			F													
22H-CC, 8-13	204.24	223.38	A	G	T	B	B	B	B						A										F			F													
23H-CC, 8-13	213.68	234.08	C	M	T	B	B	B	B						R										C			C										R			
24H-CC, 10-15	225.49	246.96	A	G	B	B	B	B	B						C		R								F		F														
25H-CC, 0-10	235.14	256.61	A	G	B	B	B	B	B						F										C			F										T			
26H-3, 70-70	238.60	260.29	A	G	B	B	B	B	B						A		R								F			F											T		
26H-5, 70-70	241.60	263.29	A	G	R	B	B	B	B						A		R								A			T											R		
26H-CC, 18-23	244.03	265.72	A	G	R	B	B	B	B						C										R			F											F		T
27H-3, 70-70	248.10	269.35	A	G	R	B	B	B	B						A										A												R		R		
27H-6, 70-70	252.60	273.85	C	M	B	B	B	B	B					R	F								X		F												R		C		
27H-CC, 11-16	254.23	275.48	A	G	T	B	B	B	B						C										F			C											F		
28H-2, 70-70	256.10	278.57	F	M	T	B	B	B	B						C									R	F				R							F					
28H-5, 70-70	260.60	283.07	A	G	T	B	B	B	B						F										A		T		F									R			
28H-CC, 22-27	263.22	285.69	A	G	T	B	B	B	B						C								X	R	F			F	R												
29H-4, 90-90	268.80	291.01	A	G	T	B	B	B	B						F							F		R	R				R										F			
29H-6, 120-120	272.10	294.31	A	G	T	B	B	B	B			R	R		A					F		R		R	F											R					
29H-CC, 13-18	273.15	295.36	F	P	T	B	B	X	B		R		R		A					F	F			R	C				R	R										R		
30H-2, 45-45	274.85	297.32	C	M	T	B	B	B	B								F					R			F											R		R			
30H-6, 8-8	280.48	302.95	A	G	T	B	B	B	B								R					R			C											R					
30H-CC, 10-15	281.43	303.90	C	M	T	B	B	B	B					R	R		R						X		C										R				T		
31H-1, 71-71	283.11	305.58	C	M	B	B	B	B	B													R			C											F	R	R			
31H-5, 112-112	289.52	311.99	C	M	T	B	B	B	B				R				F					F			F																
31H-CC, 13-18	289.76	312.23	C	G-M	T	B	B	B	B				R		T		F					F	X	F	F							R				T		T		R		
32H-1, 40-40	292.30	314.77	C	M	T	B	B	B	B				R				F								F											R					

Table T9 (continued).

Core, section, interval (cm)	Depth (mbsf)	Depth (mcd)	Diatom abundance	Diatom preservation	Silicoflagellate occurrence	Ebridian occurrence	*Actiniscus* occurrence	Sponge spicule occurrence	Opaline phytolith occurrence	*Rouxia antarctica*	*Rouxia isopolica*	*Thalassionema nitzschioides*	*Thalassionema nitzschioides* fo. 1	*Thalassiosira complicata*	*Thalassiosira convexa*	*Thalassiosira convexa* var. *aspinosa*	*Thalassiosira eccentrica*	*Thalassiosira elliptipora*	*Thalassiosira fasciculata*	*Thalassiosira gracilis*	*Thalassiosira insigna*	*Thalassiosira inura*	Transition forms *T. insigna*/*T. inura*	*Thalassiosira kolbei*	*Thalassiosira lentiginosa*	*Thalassiosira oestrupii*	*Thalassiosira oliverana*	*Thalassiosira striata*	*Thalassiosira tetraoestrupii* var. *reimeri*	*Thalassiosira vulnifica*	*Thallassiothrix antarctica-longissima* gr.	Diatom zone	Diatom age (Ma)
177-1091A-																																
1H-3, 83-83	3.83	3.83	F	M	B	B	B	B	B																F		F			F	*T. lentiginosa* Subzone c	0-0.18
1H-CC, 9-14	6.84	6.84	A	G	B	B	B	B	B																C		R			C	*T. lentiginosa* Subzone c	0-0.18
2H-CC, 9-14	14.43	17.35	A	M	B	B	B	B	B																R		R			C	*T. lentiginosa* Subzone c	0-0.18
3H-CC, 12-17	25.40	27.58	A	G	T	B	B	B	B																F	R	R			F	*T. lentiginosa* Subzone b	0.18-0.42
4H-CC, 9-14	34.65	37.85	A	G	T	B	B	B	B			R													C		R			F	*T. lentiginosa* Subzone b	0.18-0.42
5H-5, 130-130	42.70	45.01	A	G	T	B	B	B	B																R					R	*T. lentiginosa* Subzone b	0.18-0.42
5H-6, 55-55	43.45	45.76	A	G	T	B	B	B	B																R	R				R-F	*T. lentiginosa* Subzone b	0.18-0.42
5H-CC, 9-15	44.09	46.40	A	G	B	B	B	B	B		R														F	R				F	*T. lentiginosa* Subzone b	0.18-0.42
6H-1, 75-75	45.65	49.12	A	G	T	B	B	B	B			R								R					F	R	R			F	*T. lentiginosa* Subzone b	0.18-0.42
6H-1, 80.5-80.5	45.71	49.18	C	M	T	B	B	B	B			R													F	R	R			F	*T. lentiginosa* Subzone b	0.18-0.42
6H-1, 135-135	46.25	49.72	C	M	T	B	B	B	B																C	R				F	*T. lentiginosa* Subzone a	0.42-0.65
6H-CC, 7-17	53.97	57.44	A	G	T	B	B	B	B																F					F	*T. lentiginosa* Subzone a	0.42-0.65
7H-CC, 15-20	63.71	67.52	A	G	T	B	B	B	B		T									T					F					F	*T. lentiginosa* Subzone a	0.42-0.65
8H-CC, 15-20	70.62	75.51	A	G	B	B	B	B	B																F		R			F	*T. lentiginosa* Subzone a	0.42-0.65
9H-CC, 11-16	81.48	85.93	A	G	B	B	B	B	B											R					F					F	*A. ingens* Subzone c	0.65-1.07
10H-CC, 11-21	92.13	97.52	A	G	T	B	B	X	B										T						C					F	*A. ingens* Subzone c	0.65-1.07
11H-CC, 17-22	101.70	107.46	A	G	T	B	B	B	B									F	R						F		R			C	*A. ingens* Subzone c	0.65-1.07
12H-CC, 0-10	109.25	116.51	A	G	T	B	B	B	B		F							F							F	R	R			F	*A. ingens* Subzone c	0.65-1.07
13H-CC, 6-16	121.08	127.62	A	G	R	B	B	B	B									F	R						F		R			C	*A. ingens* Subzone c	0.65-1.07
14H-CC, 16-21	130.54	139.15	A	G-M	T	B	B	B	B		T							R							F		R			C	*A. ingens* Subzone c	0.65-1.07
15H-CC, 11-21	138.37	148.21	A	M	R	B	B	B	B										R						F	R	F			F	*A. ingens* Subzone b	1.07-1.3
16H-CC, 11-16	148.34	162.20	A	G	B	B	B	B	B																F		R			F	*A. ingens* Subzone b	1.07-1.3
17H-CC, 7-14	157.75	170.46	A	G	T	B	X	B	B										R						F					F	*A. ingens* Subzone b	1.07-1.3
18H-CC, 11-16	166.89	181.38	C	M	B	B	B	B	B																					F	*A. ingens* Subzone b	1.07-1.3
19H-CC, 9-14	175.70	191.83	A	G	B	B	B	B	B																					R	*A. ingens* Subzone b	1.07-1.3
20H-CC, 8-15	184.73	202.17	A	G	T	B	X	B	B										R											F	*A. ingens* Subzone b	1.07-1.3
21H-CC, 9-14	195.01	211.90	A	G	R	B	B	B	B										T	T							R		T	F	*A. ingens* Subzone a	1.3-1.8
22H-CC, 8-13	204.24	223.38	A	G	T	B	B	B	B																F	R			R	F	*A. ingens* Subzone a	1.3-1.8
23H-CC, 8-13	213.68	234.08	C	M	T	B	B	B	B												T			T				F	T		*A. ingens* Subzone a	1.3-1.8
24H-CC, 10-15	225.49	246.96	A	G	B	B	B	B	B	R		A						T							F			R		R	*A. ingens* Subzone a	1.3-1.8
25H-CC, 0-10	235.14	256.61	A	G	B	B	B	B	B			A													R					F	*A. ingens* Subzone a	1.3-1.8
26H-3, 70-70	238.60	260.29	A	G	B	B	B	B	B																				R	F	*A. ingens* Subzone a	1.3-1.8
26H-5, 70-70	241.60	263.29	A	G	R	B	B	B	B			F													R				R	F	*P. barboi*	1.8-2.0
26H-CC, 18-23	244.03	265.72	A	G	R	B	B	B	B			C							T						F				R	F	*P. barboi*	1.8-2.0
27H-3, 70-70	248.10	269.35	A	G	R	B	B	B	B																R		R		R	F	*P. barboi*	1.8-2.0
27H-6, 70-70	252.60	273.85	C	M	B	B	B	B	B																				F	F	*P. barboi*	1.8-2.0
27H-CC, 11-16	254.23	275.48	A	G	T	B	B	B	B																F		R		F	F	*P. barboi*	1.8-2.0
28H-2, 70-70	256.10	278.57	F	M	T	B	B	B	B															R	F		R		R	F	*T. kolbei/F. matuyamae*	2.0-2.5
28H-5, 70-70	260.60	283.07	A	G	T	B	B	B	B														R		C				F	F	*T. kolbei/F. matuyamae*	2.0-2.5
28H-CC, 22-27	263.22	285.69	A	G	T	B	B	B	B			R													F		R		R	C	*T. kolbei/F. matuyamae*	2.0-2.5
29H-4, 90-90	268.80	291.01	A	G	T	B	B	B	B															C	R	R	R		R	C	*T. kolbei/F. matuyamae*	2.0-2.5
29H-6, 120-120	272.10	294.31	A	G	T	B	B	B	B			C												F	F		R			F	*T. kolbei/F. matuyamae*	2.0-2.5
29H-CC, 13-18	273.15	295.36	F	P	T	B	B	X	B	R														R	F	R	R		R	R	*T. vulnifica*	2.5-2.63
30H-2, 45-45	274.85	297.32	C	M	T	B	B	B	B			R												F			F	R	R	T	F	*T. vulnifica*	2.5-2.63
30H-6, 8-8	280.48	302.95	A	G	T	B	B	B	B														R	C	R		F		R	R	F	*T. vulnifica*	2.5-2.63
30H-CC, 10-15	281.43	303.90	C	M	T	B	B	B	B	R												R		F	R	R	R			R	*T. vulnifica*	2.5-2.63
31H-1, 71-71	283.11	305.58	C	M	B	B	B	B	B			F									R		F		R				R	R	*T. vulnifica*	2.5-2.63
31H-5, 112-112	289.52	311.99	C	M	T	B	B	B	B			C				R						R	F		R				F	F	*T. vulnifica*	2.5-2.63
31H-CC, 13-18	289.76	312.23	C	G-M	T	B	B	B	B	T		R	R		T	R						T	F		F		C		F	F	lower *T. insigna*	2.63-3.3
32H-1, 40-40	292.30	314.77	C	M	T	B	B	B	B												C	R		R	F		F			F	R	lower *T. insigna*	2.63-3.3

Table T9 (continued).

Core, section, interval (cm)	Depth (mbsf)	Depth (mcd)	Abundance	Preservation	Silicoflagellate occurrence	Ebridian occurrence	*Actiniscus* occurrence	Sponge spicule occurrence	Opaline phytolith occurrence	*Actinocyclus actinochilus*	*Actinocyclus praeactinochilus*	*Actinocyclus curvatulus*	*Actinocyclus dimorphus*	*Actinocyclus fasciculatus*	*Actinocyclus ingens*	*Actinocyclus ingens* var. *ovalis*	*Actinocyclus karstenii*	*Asteromphalus hookeri*	*Asteromphalus parvulus*	*Azpeitia tabularis*	*Chaetoceros* spp.	*Coscinodiscus marginatus*	*Ethmodiscus rex*	*Eucampia antarctica*	*Fragilariopsis angulata*	*Fragilariopsis barronii*	*Fragilariopsis curta*	*Fragilariopsis fossilis*	*Fragilariopsis interfrigidaria*	*Fragilariopsis kerguelensis*	*Fragilariopsis matuyamae*	*F. matuyamae* var. *heteropolara*	*Fragilariopsis praecurta*	*Fragilariopsis reinholdii*	*Fragilariopsis ritscherii*	*Fragilariopsis separanda*	*Fragilariopsis weaveri*	*Fragilariopsis* sp. A (Gersonde, 1991)	*Hemidiscus cuneiformis*	*Hemidiscus karstenii*	*Proboscia barboi*	*Rhizosolenia antennata* fo. *semispina*	*Rhizosolenia hebetata* fo. *semispina*	*Rhizosolenia styliformis*
32H-3, 68-68	295.58	318.05	A-C	M	T	B	B	B	B																F																
32H-4, 130-130	297.70	320.17	C	M	B	B	B	B	B						R													R								R						
32H-CC, 30-35	299.17	321.64	A	G	B	B	B	X	B						R						R		R		F		R								F		R	T			
33H-1, 48-48	301.88	324.35	A	G	T	B	B	B	B						R																				R						
33H-2, 30-31	303.20	325.67	A	G	B	B	B	B	B						F																				R						
33H-3, 90-90	305.30	327.77	A	G	B	B	B	B	B						F	F									F										F						
33H-4, 116-116	307.06	329.53	A	G	B	B	B	B	B																													C				
33H-5, 70-70	308.10	330.57	C	M	B	B	B	B	B						R																				F						
33H-6, 120-120	310.10	332.57	C	M	T	B	B	B	B						R								R		C		R					R			F						
33H-CC, 21-26	310.35	332.82	F	M	T	B	B	B	B						R						R				F		R								F						
177-1091B-																																										
1H-CC, 9-14	7.74	7.74	A	G	T	B	B	B	B	T										R	R		R							A												
2H-CC, 10-15	14.49	14.71	A	G	T	B	B	B	B											R	F		R							A												
3H-CC, 9-14	23.82	22.68	A	G	T	B	B	X	B											R	R		R							A					R				F			
4H-CC, 9-14	34.50	33.58	A	G	T	B	B	B	B											F	R		R							A									R			
5H-CC, 9-14	43.47	42.61	A	G-M	B	B	B	B	B	T										F	R		F							A					T					T	T	
6H-CC, 9-14	54.04	53.07	A	G-M	T	B	B	B	B	T										F	F									A					T							
7H-CC, 8-13	64.44	63.25	A	G	T	B	B	B	B											R	F									A					F							
8H-CC, 9-14	72.26	74.17	A	G	T	B	B	B	B						R					F			R							A					R							
9H-CC, 11-16	82.88	83.55	A	G-M	B	B	B	B	B						F															C				T	T						
10H-CC, 9-14	91.70	93.05	A	G-M	B	B	B	B	B						F					R	F	X	R							C												
11H-CC, 15-20	99.50	101.36	A	M	T	B	B	B	B						F					F		X	T							C					R							
12H-CC, 0-10	111.42	113.47	A	M	B	B	B	B	B						F						C				R					F												
13H-CC, 10-15	122.09	124.20	A	G-M	T	B	B	B	B						F						F									F				R	T						
14H-CC, 20-25	127.07	130.59	A	G-M	T	B	B	B	B						F							X								C											
15H-CC, 11-16	139.86	142.57	A	G-M	R	B	B	B	B						F				T				R							C				T							
16H-CC, 10-15	148.11	153.12	A	G	T	B	B	B	B						F			T							T					C			T						T		
17H-CC, 5-10	156.85	163.07	A	G	B	B	B	B	B						C											T				C											T
18H-CC, 9-14	168.07	176.67	A	G-M	T	B	B	B	B						A																											T
19H-CC, 0-5	177.37	188.58	A	M	T	B	X	B	B						F					R										F											
20H-CC, 13-17	185.33	198.45	A	G	B	B	B	B	B						A										R					F											
21H-CC, 9-16	196.21	209.68	A	M	B	B	B	B	B						A								R		R					C											
22H-CC, 13-18	205.53	220.55	A	M	T	B	B	B	B						F										R					F											
23H-CC, 9-16	213.72	228.30	A	G	T	B	B	B	B						F										R					C											
24H-CC, 0-6	219.13	234.71	A	G-M	R	B	B	B	B						F										C														T		T	
25H-CC, 8-14	233.34	248.57	A	M	R	B	B	B	B						F										C																	
26H-CC, 10-15	243.08	260.35	A	M	T	B	B	B	B						C							X			C					F									T			
27H-CC, 12-17	250.88	269.85	A	M	B	B	B	B	B						A								T		F														R			
28H-CC, 20-25	255.60	275.43	A	M	T	B	B	B	X						C										F														R			
29H-CC, 11-16	268.87	285.04	C	M-P	T	B	B	B	B					T	F							X	R		C						R						R		R			
177-1091C-																																										
1H-CC, 7-12	3.90	3.83																																								
177-1091D-																																										
1H-CC, 0-10	3.51	11.50	A	G	T	B	B	B	B												R		R							A												
2H-CC, 15-20	6.62	18.54	A	M	R	B	B	B	B												F		F			T				A												
3H-CC, 9-14	17.02	27.43	A	G	B	B	B	B	B												R		R							A					T				T			
4H-CC, 6-11	27.45	37.23	A	M	T	B	B	B	B											F			R							A									T			
5H-CC, 11-16	36.17	47.96	A	G-M	R	B	B	B	B										T	F										A												
6H-CC, 12-17	49.80	58.80	A	M	B	B	B	B	B									T		R			R							D												
7H-CC, 10-15	58.99	67.57	A	G	T	B	B	B	B						R					F			R							D												
8H-CC, 10-15	67.83	74.73	A	G-M	B	B	B	B	B						R				T	R										D												
9H-CC, 10-15	79.74	89.53	A	G-M	T	B	B	B	B						R		R			R			R							A												
10H-CC, 9-14	87.28	99.44	A	M	B	B	B	B	B						F							X								D												

Table T9 (continued).

Core, section, interval (cm)	Depth (mbsf)	Depth (mcd)	Diatom abundance	Diatom preservation	Silicoflagellate occurrence	Ebridian occurrence	*Actiniscus* occurrence	Sponge spicule occurrence	Opaline phytolith occurrence	*Rouxia antarctica*	*Rouxia isopolica*	*Thalassionema nitzschioides*	*Thalassionema nitzschioides* fo. 1	*Thalassiosira complicata*	*Thalassiosira convexa*	*Thalassiosira convexa* var. *aspinosa*	*Thalassiosira eccentrica*	*Thalassiosira elliptipora*	*Thalassiosira fasciculata*	*Thalassiosira gracilis*	*Thalassiosira insigna*	*Thalassiosira inura*	Transition forms *T. insigna*/*T. inura*	*Thalassiosira kolbei*	*Thalassiosira lentiginosa*	*Thalassiosira oestrupii*	*Thalassiosira oliverana*	*Thalassiosira striata*	*Thalassiosira tetraoestrupii* var. *reimeri*	*Thalassiosira vulnifica*	*Thallassiothrix antarctica-longissima* gr.	Diatom zone	Diatom age (Ma)
32H-3, 68-68	295.58	318.05	A-C	M	T	B	B	B	B						R						R		C			F			F	lower *T. insigna*	2.63-3.3
32H-4, 130-130	297.70	320.17	C	M	B	B	B	B	B			F									F	R	R	R			F			C	lower *T. insigna*	2.63-3.3
32H-CC, 30-35	299.17	321.64	A	G	B	B	B	X	B			F	T						T		C	F				F	R	C	T	F	lower *T. insigna*	2.63-3.3
33H-1, 48-48	301.88	324.35	A	G	T	B	B	B	B												R	R		R			R			C	lower *T. insigna*	2.63-3.3
33H-2, 30-31	303.20	325.67	A	G	B	B	B	B	B												R	R		R			F			A	lower *T. insigna*	2.63-3.3
33H-3, 90-90	305.30	327.77	A	G	B	B	B	B	B													R		C		R	F			C	upper *F. interfigidaria*	
33H-4, 116-116	307.06	329.53	A	G	B	B	B	B	B																		R				upper *F. interfigidaria*	> 3.3
33H-5-,70-70	308.10	330.57	C	M	B	B	B	B	B													R		R						F	upper *F. interfigidaria*	
33H-6, 120-120	310.10	332.57	C	M	T	B	B	B	B					R								R		R			C			F	upper *F. interfigidaria*	> 3.3
33H-CC, 21-26	310.35	332.82	F	M	T	B	B	B	B										R			R				F			T	F	upper *F. interfigidaria*	> 3.3
177-1091B-																																	
1H-CC, 9-14	7.74	7.74	A	G	T	B	B	B	B																	C				C	*T. lentiginosa* Subzone c	0-0.18
2H-CC, 10-15	14.49	14.71	A	G	T	B	B	B	B																	F				C	*T. lentiginosa* Subzone c	0-0.18
3H-CC, 9-14	23.82	22.68	A	G	T	B	B	X	B																	F	F			C	*T. lentiginosa* Subzone b	0.18-0.42
4H-CC, 9-14	34.50	33.58	A	G	T	B	B	B	B																	F	R	R		F	*T. lentiginosa* Subzone b	0.18-0.42
5H-CC, 9-14	43.47	42.61	A	G-M	B	B	B	B	B											R						F		T		F	*T. lentiginosa* Subzone b	0.18-0.42
6H-CC, 9-14	54.04	53.07	A	G-M	T	B	B	B	B		T										T					F	T	R		C	*T. lentiginosa* Subzone a	0.42-0.65
7H-CC, 8-13	64.44	63.25	A	G	T	B	B	B	B		F															F		R		F	*T. lentiginosa* Subzone a	0.42-0.65
8H-CC, 9-14	72.26	74.17	A	G	T	B	B	B	B		T															F				C	*A. ingens* Subzone c	0.65-1.07
9H-CC, 11-16	82.88	83.55	A	G-M	B	B	B	B	B		R										T					F		R		F	*A. ingens* Subzone c	0.65-1.07
10H-CC, 9-14	91.70	93.05	A	G-M	B	B	B	B	B																	F				F	*A. ingens* Subzone c	0.65-1.07
11H-CC, 15-20	99.50	101.36	A	M	T	B	B	B	B		F										R					C	R			F	*A. ingens* Subzone c	0.65-1.07
12H-CC, 0-10	111.42	113.47	A	M	B	B	B	B	B		R								R	R										C	*A. ingens* Subzone c	0.65-1.07
13H-CC, 10-15	122.09	124.20	A	G-M	T	B	B	B	B		R								F	R						F				F	*A. ingens* Subzone c	0.65-1.07
14H-CC, 20-25	127.07	130.59	A	G-M	T	B	B	B	B		T								F	R						F		R		C	*A. ingens* Subzone c	0.65-1.07
15H-CC, 11-16	139.86	142.57	A	G-M	R	B	B	B	B										R	T						F				C	*A. ingens* Subzone c	0.65-1.07
16H-CC, 10-15	148.11	153.12	A	G	T	B	B	B	B										R							F		R		F	*A. ingens* Subzone b	1.07-1.3
17H-CC, 5-10	156.85	163.07	A	G	B	B	B	B	B										R	T							R			C	*A. ingens* Subzone b	1.07-1.3
18H-CC, 9-14	168.07	176.67	A	G-M	T	B	B	B	B																	F		R		F	*A. ingens* Subzone b	1.07-1.3
19H-CC, 0-5	177.37	188.58	A	M	T	B	X	B	B											T						F	T			C	*A. ingens* Subzone b	1.07-1.3
20H-CC, 13-17	185.33	198.45	A	G	B	B	B	B	B			F							T							R		T		F	*A. ingens* Subzone b	1.07-1.3
21H-CC, 9-16	196.21	209.68	A	M	B	B	B	B	B																			F		F	*A. ingens* Subzone a	1.3-1.8
22H-CC, 13-18	205.53	220.55	A	M	T	B	B	B	B																	F		R	R	C	*A. ingens* Subzone a	1.3-1.8
23H-CC, 9-16	213.72	228.30	A	G	T	B	B	B	B			T														C		R	R	F	*A. ingens* Subzone a	1.3-1.8
24H-CC, 0-6	219.13	234.71	A	G-M	R	B	B	B	B			F														R	R	R	R	F	*A. ingens* Subzone a	1.3-1.8
25H-CC, 8-14	233.34	248.57	A	M	R	B	B	B	B			C	R															R		F	*A. ingens* Subzone a	1.3-1.8
26H-CC, 10-15	243.08	260.35	A	M	T	B	B	B	B			R							T							F	F		R	F	*A. ingens* Subzone a	1.3-1.8
27H-CC, 12-17	250.88	269.85	A	M	B	B	B	B	B			F														F		R	T	C	*P. barboi*	1.8-2.0
28H-CC, 20-25	255.60	275.43	A	M	T	B	B	B	X																	F			T	F	*P. barboi*	1.8-2.0
29H-CC, 11-16	268.87	285.04	C	M-P	T	B	B	B	B			R											T			F			R	F	*T. kolbei*/*F. matuyamae*	2.0-2.5
177-1091C-																																	
1H-CC, 7-12	3.90	3.83																														*T. lentiginosa* Subzone c	0-0.18
177-1091D-																																	
1H-CC, 0-10	3.51	11.50	A	G	T	B	B	B	B												R					F				C	*T. lentiginosa* Subzone c	0-0.18
2H-CC, 15-20	6.62	18.54	A	M	R	B	B	B	B																	F	T	R		F	*T. lentiginosa* Subzone c	0-0.18
3H-CC, 9-14	17.02	27.43	A	G	B	B	B	B	B												T					F				C	*T. lentiginosa* Subzone b	0.18-0.42
4H-CC, 6-11	27.45	37.23	A	M	T	B	B	B	B																	F				F	*T. lentiginosa* Subzone b	0.18-0.42
5H-CC, 11-16	36.17	47.96	A	G-M	R	B	B	B	B																	F				C	*T. lentiginosa* Subzone b	0.18-0.42
6H-CC, 12-17	49.80	58.80	A	M	B	B	B	B	B																	F		R		F	*T. lentiginosa* Subzone a	0.42-0.65
7H-CC, 10-15	58.99	67.57	A	G	T	B	B	B	B		R															C				C	*A. ingens* Subzone c	0.65-1.07
8H-CC, 10-15	67.83	74.73	A	G-M	B	B	B	B	B		R															F				C	*A. ingens* Subzone c	0.65-1.07
9H-CC, 10-15	79.74	89.53	A	G-M	T	B	B	B	B																	F				F	*A. ingens* Subzone c	0.65-1.07
10H-CC, 9-14	87.28	99.44	A	M	B	B	B	B	B																	F				C	*A. ingens* Subzone c	0.65-1.07

Table T9 (continued).

Core, section, interval (cm)	Depth (mbsf)	Depth (mcd)	Abundance	Preservation	Silicoflagellate occurrence	Ebridian occurrence	*Actiniscus* occurrence	Sponge spicule occurrence	Opaline phytolith occurrence	*Actinocyclus actinochilus*	*Actinocyclus praeactinochilus*	*Actinocyclus curvatulus*	*Actinocyclus dimorphus*	*Actinocyclus fasciculatus*	*Actinocyclus ingens*	*Actinocyclus ingens* var. *ovalis*	*Actinocyclus karstenii*	*Asteromphalus hookeri*	*Asteromphalus parvulus*	*Azpeitia tabularis*	*Chaetoceros* spp.	*Coscinodiscus marginatus*	*Ethmodiscus rex*	*Eucampia antarctica*	*Fragilariopsis angulata*	*Fragilariopsis barronii*	*Fragilariopsis curta*	*Fragilariopsis fossilis*	*Fragilariopsis interfrigidaria*	*Fragilariopsis kerguelensis*	*Fragilariopsis matuyamae*	*F. matuyamae* var. *heteropolara*	*Fragilariopsis praecurta*	*Fragilariopsis reinholdii*	*Fragilariopsis ritscherii*	*Fragilariopsis separanda*	*Fragilariopsis weaveri*	*Fragilariopsis* sp. A (Gersonde, 1991)	*Hemidiscus cuneiformis*	*Hemidiscus karstenii*	*Proboscia barboi*	*Rhizosolenia antennata* fo. *semispina*	*Rhizosolenia hebetata* fo. *semispina*	*Rhizosolenia styliformis*
11H-CC, 25-30	96.85	109.50	A	M	B	B	B	B	B	T					F														C												
12H-CC, 28-35	107.19	120.00	A	M	B	B	B	B	B						F								R						C												
13H-CC, 9-16	116.62	130.27	A	M	T	B	B	B	B						F														C												
14H-CC, 0-6	126.60	140.40	A	M	B	B	B	B	B						R						R								C											T	
15H-CC, 7-14	136.13	151.60	A	G-M	R	B	B	B	B						F				T										A												
16H-CC, 9-14	145.60	161.57	A	G-M	B	B	B	B	B						F														C												T
17H-CC, 8-15	155.24	172.96	A	M	B	B	B	B	B						F										R				F												
18H-CC, 8-15	163.95	182.86	A	G	T	B	B	B	B						A														F												
19H-CC, 14-19	173.24	193.93	A	G-M	T	B	B	B	B						F								X						F												
20H-CC, 10-17	182.89	205.32	A	G	T	B	B	B	B						A										R				F												
21H-CC, 9-16	193.33	217.03	A	M	B	B	B	B	B						F										F	R			F								R				
22H-CC, 12-18	202.42	226.75	A	M	T	B	B	B	B						F										R				C												
177-1091E-																																										
1H-CC, 10-15	4.19	12.31	A	G	R	B	B	B	B											R				R					D												
2H-CC, 0-10	9.52	19.54	A	G-M	F	B	B	B	B									T						R					D											T	
3H-CC, 10-15	19.46	28.47	A	G-M	B	B	B	B	B											R				R					D					R							
4H-CC, 9-14	27.02	36.02	A	G-M	R	B	B	B	B									T		F									D												
5H-CC, 6-11	39.78	48.43	A	G-M	R	B	B	B	B											C				R					D												
6H-CC, 12-17	47.17	60.53	A	G	R	B	B	B	B						T			T		F									D					R							

Notes: Abundance abbreviations: A = abundant, C = common, F = few, R = rare, T = trace, X = present, B = barren. Preservation abbreviations: G = good, M = moderate, P = poor. For more specific definitions, refer to the **"Explanatory Notes"** chapter. This table is also available in ASCII format in the **TABLES** directory.

Table T9 (continued).

Core, section, interval (cm)	Depth (mbsf)	Depth (mcd)	Diatom abundance	Diatom preservation	Silicoflagellate occurrence	Ebridian occurrence	*Actiniscus* occurrence	Sponge spicule occurrence	Opaline phytolith occurrence	*Rouxia antarctica*	*Rouxia isopolica*	*Thalassionema nitzschioides*	*Thalassionema nitzschioides* fo. 1	*Thalassiosira complicata*	*Thalassiosira convexa*	*Thalassiosira convexa* var. *aspinosa*	*Thalassiosira eccentrica*	*Thalassiosira elliptipora*	*Thalassiosira fasciculata*	*Thalassiosira gracilis*	*Thalassiosira insigna*	*Thalassiosira inura*	Transition forms *T. insigna*/*T. inura*	*Thalassiosira kolbei*	*Thalassiosira lentiginosa*	*Thalassiosira oestrupii*	*Thalassiosira oliverana*	*Thalassiosira striata*	*Thalassiosira tetraoestrupii* var. *reimeri*	*Thalassiosira vulnifica*	*Thallassiothrix antarctica-longissima* gr.	Diatom zone	Diatom age (Ma)
11H-CC, 25-30	96.85	109.50	A	M	B	B	B	B	B								R								F					C	*A. ingens* Subzone c	0.65-1.07
12H-CC, 28-35	107.19	120.00	A	M	B	B	B	B	B								R								F					A	*A. ingens* Subzone c	0.65-1.07
13H-CC, 9-16	116.62	130.27	A	M	T	B	B	B	B							R									F		R			C	*A. ingens* Subzone c	0.65-1.07
14H-CC, 0-6	126.60	140.40	A	M	B	B	B	B	B									T	T											C	*A. ingens* Subzone c	0.65-1.07
15H-CC, 7-14	136.13	151.60	A	G-M	R	B	B	B	B																F					C	*A. ingens* Subzone b	1.07-1.3
16H-CC, 9-14	145.60	161.57	A	G-M	B	B	B	B	B																F					C	*A. ingens* Subzone b	1.07-1.3
17H-CC, 8-15	155.24	172.96	A	M	B	B	B	B	B																F					A	*A. ingens* Subzone b	1.07-1.3
18H-CC, 8-15	163.95	182.86	A	G	T	B	B	B	B											T					F					F	*A. ingens* Subzone b	1.07-1.3
19H-CC, 14-19	173.24	193.93	A	G-M	T	B	B	B	B																F					C	*A. ingens* Subzone b	1.07-1.3
20H-CC, 10-17	182.89	205.32	A	G	T	B	B	B	B																F					F	*A. ingens* Subzone b	1.07-1.3
21H-CC, 9-16	193.33	217.03	A	M	B	B	B	B	B																		F		R	F	*A. ingens* Subzone a	1.3-1.8
22H-CC, 12-18	202.42	226.75	A	M	T	B	B	B	B																		F		R	F	*A. ingens* Subzone a	1.3-1.8
177-1091E-																																
1H-CC, 10-15	4.19	12.31	A	G	R	B	B	B	B											R					F					F	*T. lentiginosa* Subzone c	0-0.18
2H-CC, 0-10	9.52	19.54	A	G-M	F	B	B	B	B																F					F	*T. lentiginosa* Subzone c	0-0.18
3H-CC, 10-15	19.46	28.47	A	G-M	B	B	B	B	B																F		R			C	*T. lentiginosa* Subzone b	0.18-0.42
4H-CC, 9-14	27.02	36.02	A	G-M	R	B	B	B	B																F		R			C	*T. lentiginosa* Subzone b	0.18-0.42
5H-CC, 6-11	39.78	48.43	A	G-M	R	B	B	B	B																F					F	*T. lentiginosa* Subzone b	0.18-0.42
6H-CC, 12-17	47.17	60.53	A	G	R	B	B	B	B	C										R					F					C	*T. lentiginosa* Subzone a	0.42-0.65

Table T10. Control points used to calculate sedimentation rates at Site 1091.

Code	Event/Zone/Chron	Depth range of stratigraphic datums: Top Core, section, interval (cm)	Top Depth (mbsf)	Top Depth (mcd)	Base Core, section, interval (cm)	Base Depth (mbsf)	Base Depth (mcd)	Mean Depth (mbsf)	Mean Depth (mcd)	Age (Ma)	Sedimentation rate (m/m.y.)
		177-			177-						
DIAT	TOP *T. lentiginosa* Subzone b	1091E-2H-CC, 9-14	9.52	19.54	1091B-3H-CC, 12-17	23.82	22.68	16.67	21.11	0.19	
CN	FO *E. huxleyi*	1091A-3H-6, 26-26	24.16	26.34	1091A-3H-CC, 12-17	25.4	27.58	24.78	26.96	0.26	
DIAT	BOT *T. lentiginosa* Subzone b	1091A-6H-1, 85-85	45.75	49.22	1091A-6H-1, 135-135	46.25	49.72	46.00	49.47	0.42	
CN	LO *P. lacunosa*	1091A-6H-CC, 7-17	53.97	57.44	1091A-7H-3, 26-26	56.60	60.41	55.28	58.92	0.46	
RAD	TOP Psi Zone	1091A-6H-CC, 7-17	53.97	57.44	1091E-6H-CC, 12-17	47.17	60.53	50.57	58.98	0.46	
DIAT	TOP *A. ingens* Subzone c	1091B-8H-CC, 15-20	70.62	75.51	1091A-9H-CC, 11-16	81.48	85.93	76.05	80.72	0.65	
PMAG	BOT C1n (Brunhes)	1091A-11H-3, 50-50	95.50	101.26	1091A-12H-1, 50-50	102.40	109.66	98.95	105.46	0.78	
CN	LO *R. asanoi*	1091A-12H-CC, 0-10	109.25	116.51	1091A-13H-4, 104-104	116.94	123.48	113.10	120.00	0.88-1.02	
RAD	TOP Chi Zone	1091A-12H-CC, 0-10	109.25	116.51	1091B-13H-CC, 10-15	122.09	124.20	115.67	120.36	0.83	
CN	RE *Gephyrocapsa* medium (4-5.5 µm)	1091A-13H-CC, 6-16	121.08	127.62	1091A-14H-2, 136-136	123.76	132.37	122.42	130.00	0.96	~145
DIAT	TOP *A. ingens* Subzone b	1091A-15H-3, 136-136	137.76	147.60	1091A-15H-CC, 11-21	138.37	148.21	138.06	147.90	1.07	
CN	FO *R. asanoi*	1091A-15H-5, 136-136	137.76	147.60	1091A-15H-CC, 11-21	138.37	148.21	138.06	147.90	1.08	
CN	LO *Gephyrocapsa* large (>5.5 µm)	1091A-15H-CC, 11-21	138.37	148.21	1091A-16H-3, 130-130	144.20	158.06	141.28	153.14	1.24	
CN	FO *Gephyrocapsa* large (>5.5 µm)	1091A-19H-3, 130-130	172.70	188.33	1091A-19H-CC, 8-14	175.69	191.82	174.20	190.08	1.46	
DIAT	TOP *A. ingens* Subzone a	1091D-20H-CC, 8-15	182.89	205.32	1091A-21H-2, 53-53	189.43	206.32	186.16	205.82	1.30	
CN	FO *Gephyrocapsa* medium (4-5.5 µm)	1091A-23H-4, 30-30	211.20	231.60	1091A-23H-5, 110-110	213.50	233.90	212.35	232.75	1.69	
DIAT	TOP *P. barboi* Zone	1091B-26H-3, 70-70	243.08	260.35	1091A-26H-5 70-70	241.60	263.29	242.34	261.82	1.80	
RAD	TOP Phi Zone	1091B-28H-CC, 20-25	255.60	275.23	1091B-29H-CC, 11-16	268.87	285.04	262.24	280.14	1.92	
DIAT	TOP *T. kolbei-F. matuyamae* Zone	1091A-27H-CC, 11-16	254.12	275.37	1091A-28H-2, 70-70	256.10	278.57	255.11	276.97	2.00	
RAD	TOP Upsilon Zone	1091A-28H-CC, 22-27	263.22	285.69	1091A-30H-CC, 10-15	281.43	303.90	272.33	294.79	2.42	
DIAT	TOP *T. vulnifica* Zone	1091A-29H-6, 120-120	272.10	294.31	1091A-29H-CC, 13-18	273.15	295.36	272.62	294.84	2.50	
PMAG	BOT C2r (Matuyama)	1091A-31H-3, 40-40	285.80	308.27	1091A-31H-5, 30-30	288.70	311.17	287.25	309.72	2.58	~30
DIAT	TOP *T. insigna* Zone	1091A-31H-5, 112-112	289.52	311.99	1091A-31H-CC, 13-18	289.76	312.23	289.64	312.11	2.63	
RAD	FO *C. davisiana*	1091A-30H-CC, 10-15	281.43	303.90	1091A-32H-CC, 30-35	299.17	321.64	290.30	312.77	2.61	
DIAT	TOP *F. interfrigidara* Zone	1091A-33H-2, 30-31	303.20	325.67	1091A-33H-3, 90-90	305.30	327.77	304.25	326.72	3.26	

Notes: Code abbreviations: CN = calcareous nannofossil, DIAT = diatom, RAD = radiolaria, PMAG = magnetic polarity. Event abbreviations: FO = first occurrence, LO = last occurrence, RE = reentrance, TOP = top of zone, BOT = bottom of zone. This table is also available in ASCII format in the **TABLES** directory.

Table T11. Distribution of the main components of the radiolarian assemblages at Site 1091. (**See table note.** Continued on next page.)

Core, section, interval (cm)	Depth (mbsf)	Depth (mcd)	Abundance	Preservation	*Antarctissa denticulata*	*Antarctissa longa*	*Botryostrobus aquilonalis*	*Botryostrobus auritus*	*Cyladophora davisiana*	*Cycladophora pliocenica*	*Dictyophimus crisiae*	*Eucyrtidium carvertense*	*Helotholus vema*	*Lamprocyrtis heteroporos*	*Litheliu nautiloides*	*Prunopyle antarctica*	*Pseudocubus warreni*	*Pterocanium trilobum*	*Pterocorys* spp.	*Saccospyris antarctica*	*Saturnalis circularis*	*Siphocampe lineata*	*Spongodiscus osculosa*	*Spongoplegma antarcticum*	*Spongotrochus glacialis*	*Spongurus pylomaticus*	*Stylatractus universus*	*Theocorys redondoenseis*	*Triceraspyris antarctica*
177-1091A-																													
1H-CC, 9-14	6.84	6.84																											
2H-CC, 9-14	14.43	17.35																											
3H-CC, 12-17	25.4	27.58	A	E	A	A			A	R	F				F	F			F	F				F	F	F			
4H-CC, 9-14	34.65	37.85																											
5H-CC, 9-15	44.09	46.4																											
6H-CC, 7-17	53.97	57.44	A	E	A	A	F		C	F					F		F			F				C	F	F	F		F
7H-CC, 15-20	63.71	67.52																											
8H-CC, 15-20	70.62	75.51	A	E	A	A			C	R	F				F		F			F		F	F	F	F	F	R		F
9H-CC, 11-16	81.84	85.93																											
10H-CC, 11-21	92.13	97.52	A	E	A	A			C	R	F				F		F			F		F	F	F	F	F			F
11H-CC, 17-22	101.7	107.46																											
12H-CC, 0-10	109.25	116.51	A	E	A	C			C						F					F			F	F		F			
13H-CC, 6-16	121.08	127.62																											
14H-CC, 16-21	130.54	139.15	A	E	A	C			F									R		F	F			F		F	R		
15H-CC, 11-21	138.37	148.21																											
16H-CC, 11-16	148.34	162.2	A	E	A	A			C									R		F	F	F	F	F					F
17H-CC, 7-14	157.75	170.46																											
18H-CC, 11-16	166.89	181.38	A	E	A	C			C		F							F		F	F	F		F	F	F			F
19H-CC, 9-14	175.7	191.83																											
20H-CC, 8-15	184.73	202.17	C	E	A	A	F		C											F		F			F	F			
21H-CC, 9-14	195.01	211.8																											
22H-CC, 8-13	204.24	223.38	A	E	A	A			C						F					F	F	F		F		F			F
23H-CC, 8-13	213.68	234.08																											
24H-CC, 10-15	225.49	246.96	A	E	A	A			F		F				F					F		F		F					F
25H-CC, 0-10	235.14	256.61																											
26H-CC, 18-23	244.03	265.72	A	E	A	F			C	R					F					F	F	F	F	F		F			F
27H-CC, 11-16	254.23	275.48																											
28H-CC, 22-27	263.22	285.69	A	E	A	F		F	F	F	F	F			F							F							
29H-CC, 13-18	273.15	295.36																											
30H-CC, 10-15	281.43	303.9	A	E	A	F		F	F	F	F	F	R		F						F	F		F					
31H-CC, 13-18	289.76	312.23																											
32H-CC, 30-35	299.17	321.64	A	E	C	F		F		F	F	F	F	R							F						F		
33H-CC, 21-26	310.35	332.82	A	E	C	F		F		F	F	F	F								F						F		
177-1091B-																													
1H-CC, 9-14	7.74	7.74	A	E	A	A	F		C						F					F		F	F	F	F	F			F
2H-CC, 10-15	14.49	14.71																											
3H-CC, 9-14	23.82	22.68																											
4H-CC, 9-14	34.5	33.58																											
5H-CC, 9-14	43.47	42.61	A	E	A	C			C		F				F									F					
6H-CC, 9-14	54.04	53.07																											
7H-CC, 8-13	64.44	63.25																											
8H-CC, 9-14	72.26	74.17																											
9H-CC, 11-16	82.88	83.55	A	E	A	C	F	F	C	R	F	R			F		F	R		F	F			F		F	R		
10H-CC, 9-14	91.7	93.05																											
11H-CC, 15-20	99.5	101.36																											
12H-CC, 0-10	111.42	113.47																											
13H-CC, 10-15	122.09	124.2	A	E	A	C			C	R								R		F					F				F
14H-CC, 20-25	127.07	130.59																											
15H-CC, 11-16	139.86	142.57																											
16H-CC, 10-15	148.11	153.17																											
17H-CC, 5-10	156.85	163.07	A	E	A	C	F		C						F			R		F	F	F	F		F				F
18H-CC, 9-14	168.07	176.67																											
19H-CC, 0-5	177.37	188.58																											
20H-CC, 13-17	185.33	198.45																											
21H-CC, 9-16	196.21	209.68	A	E	A	C			C		F									F	F	F				F			

Table T11 (continued).

Core, section, interval (cm)	Depth (mbsf)	Depth (mcd)	Abundance	Preservation	*Antarctissa denticulata*	*Antarctissa longa*	*Botryostrobus aquilonalis*	*Botryostrobus auritus*	*Cycladophora davisiana*	*Cycladophora pliocenica*	*Dictyophimus crisiae*	*Eucyrtidium carvertense*	*Helotholus vema*	*Lamprocyrtis heteroporos*	*Lithelius nautiloides*	*Prunopyle antarctica*	*Pseudocubus warreni*	*Pterocanium trilobum*	*Pterocorys* spp.	*Saccospyris antarctica*	*Saturnalis circularis*	*Siphocampe lineata*	*Spongodiscus osculosa*	*Spongoplegma antarcticum*	*Spongotrochus glacialis*	*Spongurus pylomaticus*	*Stylatractus universus*	*Theocorys redondoenseis*	*Triceraspyris antarctica*
22H-CC, 13-18	205.53	220.55																											
23H-CC, 9-16	213.72	228.3																											
24H-CC, 0-6	219.13	234.71																											
25H-CC, 8-14	233.34	248.57	A	E	C	C			C	R					F					F	F	F		F	F				
26H-CC, 10-15	243.08	260.35																											
27H-CC, 12-17	250.88	269.85	A	E	A	C		F	C	R					F					F	F	F	F		F	F			F
28H-CC, 20-25	255.6	275.43	A	E	C	C			F	F	F		F		F									F	F	F	F		F
29H-CC, 11-16	268.87	285.04	A	E	C	F		F				F	F		F						F	F							
177-1091C-																													
1H-CC, 7-12	3.9	3.9	A	E	A	C	F		C	R					F				F	F					F				F
177-1091D-																													
1H-CC, 0-10	3.51	11.5																											
2H-CC, 15-20	6.62	18.54																											
3H-CC, 9-14	17.02	27.43	A	E	A	C		F	C											F		F		F		F			F
4H-CC, 6-11	27.45	37.23																											
5H-CC, 11-16	36.17	47.96																											
6H-CC, 12-17	49.8	58.8																											
7H-CC, 10-15	58.99	67.57	A	E	A	C			C	R					F					F				F	F	F	F		
8H-CC, 10-15	67.83	74.73																											
9H-CC, 10-15	79.74	89.53																											
10H-CC, 9-14	87.28	99.44																											
11H-CC, 25-30	96.85	109.5	A	E	A	C			C						F					F						F			F
12H-CC, 28-35	107.19	120																											
13H-CC, 9-16	116.62	130.27																											
14H-CC, 0-6	126.6	140.4																											
15H-CC, 7-14	136.13	151.6	A	E	C	F			C						F			R			F	F					R		F
16H-CC, 9-14	145.6	161.57																											
17H-CC, 8-15	155.24	172.96																											
18H-CC, 8-15	163.95	182.86																											
19H-CC, 14-19	173.24	193.93	A	E	C	C			C											F	F	F		F	F				F
20H-CC, 10-17	182.89	205.32																											
21H-CC, 9-16	193.33	217.03																											
22H-CC, 12-18	202.42	226.75	A	E	C	C			F						F			R		F	F		F		F	F			
177-1091E-																													
1H-CC, 10-15	4.19	12.31																											
2H-CC, 0-10	9.52	19.54	A	E	A	C		F	C	R									F	F		F		F					F
3H-CC, 10-15	19.46	28.47																											
4H-CC, 9-14	27.02	36.02	A	E	A	C		F	C						F				F	F		F		F		F			F
5H-CC, 6-11	39.78	48.43																											
6H-CC, 12-17	47.17	60.53	A	E	A	C			C						F				F	F	F	F		F		F	F		F

Notes: Abundance abbreviations: A = abundant, C = common, F = few, R = rare. Preservation abbreviations: E = excellent. For more specific definitions, refer to the **"Explanatory Notes"** chapter. This table is also available in ASCII format in the **TABLES** directory.

Table T12. Concentrations of methane obtained by the headspace technique at Site 1091.

Core, section, interval (cm)	Depth (mbsf)	C_1 (ppmv)
177-1091A-		
1H-4, 0-5	4.53	2
2H-4, 0-5	11.42	4
3H-5, 0-5	22.42	5
4H-5, 0-5	31.92	4
5H-5, 0-5	41.42	5
6H-5, 0-5	50.92	5
7H-5, 0-5	59.36	6
8H-5, 0-5	69.92	10
9H-5, 0-5	79.42	9
10H-5, 0-5	88.92	8
11H-5, 0-5	98.42	12
12H-5, 0-5	107.92	11
13H-5, 0-5	117.42	8
14H-5, 0-5	126.92	10
15H-5, 0-5	136.43	6
16H-5, 0-5	145.93	13
17H-5, 0-5	155.43	10
18H-5, 0-5	164.92	9
19H-4, 0-5	172.92	10
20H-4, 0-5	182.42	15
21H-5, 0-5	193.06	9
22H-4, 0-5	201.42	15
23H-4, 0-5	210.92	15
24H-5, 0-5	221.62	6
25H-5, 0-5	231.42	8
26H-5, 0-5	240.92	15
27H-5, 0-5	250.42	15
28H-5, 0-5	259.92	9
29H-5, 0-5	269.42	9
30H-5, 0-5	278.92	17
31H-5, 0-5	288.42	11
32H-4, 0-5	296.42	22
33H-5, 0-5	307.42	12

Note: C_1 = methane.

Table T13. Interstitial water chemistry from shipboard measurements at Site 1091. (Continued on next page.)

Core, section, interval (cm)	Depth (mbsf)	pH	Method	Alkalinity (mM)	Method	Salinity	Method	Cl (mM)	Method	SO_4 (mM)	Method	Na (mM)	Method	Mg (mM)	Method	Ca (mM)	Method
177-1091A-																	
1H-3, 145-150	4.48	7.96	ISE	3.933	T	34.5	R	554	T	28.06	I	470	CB	55.25	I	11.03	I
2H-3, 145-150	11.38	8.00	ISE	5.644	T	35.0	R	557	T	27.42	I	474	CB	55.27	I	10.54	I
3H-4, 145-150	22.38	7.98	ISE	6.563	T	35.5	R	564	T	26.78	I	480	CB	56.52	I	9.72	I
4H-4, 145-150	31.88	7.93	ISE	6.553	T	35.5	R	566	T	27.42	I	481	CB	56.49	I	10.94	I
5H-4, 145-150	41.38	7.91	ISE	6.614	T	35.5	R	565	T	27.86	I	485	CB	55.50	I	9.95	I
6H-4, 145-150	50.88	7.95	ISE	7.153	T	35.5	R	571	T	27.15	I	495	CB	52.50	I	10.82	I
7H-4, 145-150	59.32	7.90	ISE	7.367	T	35.5	R	568	T	26.16	I	493	CB	52.29	I	9.84	I
8H-4, 145-150	69.88	7.95	ISE	7.242	T	35.5	R	569	T	25.92	I	496	CB	51.68	I	8.75	I
9H-4, 145-150	79.38	8.06	ISE	8.054	T	35.5	R	568	T	26.26	I	494	CB	52.07	I	9.57	I
10H-4, 145-150	88.88	8.06	ISE	8.419	T	35.5	R	569	T	25.89	I	495	CB	51.98	I	9.72	I
11H-4, 145-150	98.38	8.08	ISE	9.093	T	35.5	R	569	T	25.87	I	499	CB	50.87	I	8.72	I
12H-4, 145-150	107.88	8.08	ISE	8.997	T	35.5	R	567	T	24.38	I	488	CB	53.99	I	9.29	I
13H-4, 145-150	117.38	8.00	ISE	9.038	T	35.5	R	567	T	24.00	I	491	CB	52.28	I	8.68	I
14H-4, 140-150	126.85	7.92	ISE	9.407	T	35.5	R	565	T	24.38	I	485	CB	55.35	I	8.43	I
15H-4, 140-150	136.35	8.04	ISE	8.585	T	35.5	R	565	T	24.48	I	488	CB	53.97	I	7.97	I
16H-4, 140-150	145.85	8.00	ISE	9.912	T	35.0	R	566	T	23.78	I	491	CB	53.01	I	7.92	I
17H-4, 140-150	155.35	7.97	ISE	9.577	T	35.0	R	567	T	24.60	I	492	CB	53.68	I	7.81	I
18H-4, 140-150	164.85	7.96	ISE	9.561	T	35.0	R	567	T	24.83	I	489	CB	55.22	I	8.03	I
19H-3, 140-150	172.85	7.95	ISE	9.413	T	35.0	R	567	T	24.09	I	487	CB	55.77	I	7.52	I
20H-3, 140-150	182.35	7.95	ISE	9.509	T	35.0	R	567	T	22.61	I	490	CB	53.36	I	7.34	I
21H-4, 140-150	192.98	7.98	ISE	9.440	T	35.5	R	568	T	24.27	I	493	CB	53.98	I	7.27	I
22H-3, 140-150	201.35	7.94	ISE	9.193	T	35.0	R	567	T	23.58	I	491	CB	53.60	I	7.35	I
23H-3, 140-150	210.85	7.91	ISE	9.084	T	35.0	R	565	T	24.51	I	495	CB	52.16	I	6.93	I
24H-4, 140-150	221.54	7.92	ISE	8.979	T	35.0	R	567	T	23.68	I	494	CB	52.46	I	7.04	I
25H-4, 140-150	231.35	8.03	ISE	8.980	T	35.0	R	568	T	24.10	I	493	CB	53.31	I	7.17	I
26H-4, 140-150	240.85	7.80	ISE	8.741	T	35.0	R	566	T	23.05	I	488	CB	53.58	I	7.43	I
27H-4, 140-150	250.35	8.02	ISE	9.173	T	35.0	R	565	T	22.68	I	492	CB	51.74	I	6.96	I
28H-4, 140-150	259.85	7.99	ISE	9.404	T	35.0	R	565	T	21.58	I	490	CB	51.20	I	7.26	I
29H-4, 140-150	269.35	7.76	ISE	9.154	T	34.5	R	562	T	21.69	I	487	CB	50.85	I	7.75	I
30H-4, 140-150	278.85	7.92	ISE	9.243	T	35.0	R	560	T	22.32	I	488	CB	50.09	I	7.51	I
31H-4, 140-150	288.35	7.82	ISE	9.477	T	34.5	R	560	T	21.84	I	486	CB	50.41	I	7.66	I
32H-3, 140-150	296.35	7.72	ISE	9.298	T	34.5	R	560	T	21.48	I	484	CB	51.23	I	7.79	I
33H-4, 140-150	307.35	7.71	ISE	9.036	T	34.5	R	558	T	23.85	I	484	CB	51.35	I	8.39	I

Note: Method abbreviations: ISE = ion selective electrode, T = titration, R = refractometer, I = ion chromatography, CB = charge balance calculation, S = spectrophotometry, AAS = atomic absorption spectrometry, AES = atomic emission spectrometry.

Table T13 (continued).

Core, section, interval (cm)	Depth (mbsf)	K (mM)	Method	H_4SiO_4 (µM)	Method	NH_4 (µM)	Method	HPO_4 (µM)	Method	Sr (µM)	Method	Fe (µM)	Method	Mn (µM)	Method	Li (µM)	Method
177-1091A-																	
1H-3, 145-150	4.48	11.32	I	823	S	83	S	17	S	89	AAS	1.3	AAS	24.4	AAS	23.1	AES
2H-3, 145-150	11.38	11.56	I	744	S	336	S	40	S	88	AAS	-0.1	AAS	82.2	AAS	21.1	AES
3H-4, 145-150	22.38	11.53	I	823	S	464	S	47	S	88	AAS	0.3	AAS	89.4	AAS	20.7	AES
4H-4, 145-150	31.88	11.37	I	853	S	512	S	47	S	89	AAS		AAS	85.2	AAS	21.0	AES
5H-4, 145-150	41.38	11.13	I	788	S	597	S	43	S	88	AAS	2.6	AAS	67.0	AAS	21.1	AES
6H-4, 145-150	50.88	10.95	I	916	S	641	S	39	S	88	AAS	4.1	AAS	54.9	AAS	21.6	AES
7H-4, 145-150	59.32	10.57	I	836	S	667	S	42	S	89	AAS		AAS	68.8	AAS	21.3	AES
8H-4, 145-150	69.88	11.08	I	749	S	809	S	40	S	87	AAS	3.5	AAS	69.2	AAS	21.3	AES
9H-4, 145-150	79.38	11.28	I	1017	S	843	S	43	S	86	AAS		AAS	62.8	AAS	21.6	AES
10H-4, 145-150	88.88	10.76	I	766	S	903	S	46	S		AAS		AAS	48.4	AAS	21.9	AES
11H-4, 145-150	98.38	11.17	I	890	S	940	S	41	S	85	AAS	6.2	AAS	47.2	AAS	22.2	AES
12H-4, 145-150	107.88	10.22	I	886	S	915	S	41	S	88	AAS	3.7	AAS	55.2	AAS	22.2	AES
13H-4, 145-150	117.38	10.73	I	844	S	957	S	43	S	88	AAS	1.4	AAS	50.5	AAS	22.6	AES
14H-4, 140-150	126.85	10.35	I	792	S	976	S	32	S	87	AAS	4.3	AAS	37.5	AAS	23.0	AES
15H-4, 140-150	136.35	10.62	I	801	S	1109	S	24	S	89	AAS	1.2	AAS	23.4	AAS	23.4	AES
16H-4, 140-150	145.85	10.09	I	929	S	1062	S	36	S	91	AAS	2.3	AAS	26.3	AAS	23.8	AES
17H-4, 140-150	155.35	10.67	I	875	S	1086	S	34	S	89	AAS		AAS	29.0	AAS	24.1	AES
18H-4, 140-150	164.85	10.64	I	897	S	1068	S	35	S	88	AAS	3.2	AAS	28.4	AAS	24.6	AES
19H-3, 140-150	172.85	10.38	I	790	S	973	S	31	S	89	AAS	2.0	AAS	26.8	AAS	24.7	AES
20H-3, 140-150	182.35	10.35	I	820	S	990	S	36	S	90	AAS	0.5	AAS	26.9	AAS	25.2	AES
21H-4, 140-150	192.98	10.20	I	866	S	951	S	36	S	89	AAS	0.1	AAS	30.4	AAS	25.7	AES
22H-3, 140-150	201.35	10.33	I	958	S	943	S	32	S	89	AAS	1.4	AAS	28.4	AAS	26.1	AES
23H-3, 140-150	210.85	10.04	I	921	S	971	S	26	S	90	AAS		AAS	15.8	AAS	26.9	AES
24H-4, 140-150	221.54	10.42	I	1102	S	1083	S	29	S	90	AAS	2.3	AAS	19.0	AAS	27.6	AES
25H-4, 140-150	231.35	10.63	I	1008	S	1027	S	28	S	91	AAS	2.4	AAS	25.7	AAS	28.2	AES
26H-4, 140-150	240.85	10.65	I	921	S	1106	S	28	S	88	AAS	0.8	AAS	27.8	AAS	29.9	AES
27H-4, 140-150	250.35	9.98	I	947	S	948	S	24	S	89	AAS	2.8	AAS	28.8	AAS	31.0	AES
28H-4, 140-150	259.85	10.07	I	969	S	924	S	24	S	89	AAS	-0.0	AAS	34.7	AAS	32.9	AES
29H-4, 140-150	269.35	10.23	I	1004	S	975	S	18	S	90	AAS	3.9	AAS	46.5	AAS	35.1	AES
30H-4, 140-150	278.85	10.82	I	1093	S	948	S	16	S	90	AAS	5.7	AAS	57.4	AAS	38.9	AES
31H-4, 140-150	288.35	10.92	I	1121	S	915	S	15	S	89	AAS	8.8	AAS	46.3	AAS	41.2	AES
32H-3, 140-150	296.35	10.61	I	1038	S	847	S	15	S	90	AAS	10.8	AAS	50.3	AAS	43.6	AES
33H-4, 140-150	307.35	10.95	I	1047	S	788	S	11	S	88	AAS	9.5	AAS	47.6	AAS	45.6	AES

Table T14. Analytical results of inorganic carbon, calculated calcium carbonate, total carbon, total organic carbon, total nitrogen, total sulfur, and TOC/TN at Site 1091. (Continued on next page.)

Core, section, interval (cm)	Depth (mbsf)	IC (wt%)	$CaCO_3$ (wt%)	TC (wt%)	TOC (wt%)	TN (wt%)	TS (wt%)	TOC/TN
177-1091A-								
1H-1, 84-85	0.84	0.217	1.8	0.68	0.46	0.10	0.21	4.8
1H-3, 77-78	3.78	3.172	26.4					
1H-4, 120-121	5.70	1.036	8.6					
2H-2, 28-29	8.68	7.069	58.9	7.56	0.49	0.07	0.00	6.9
2H-4, 70-71	12.10	0.048	0.4					
3H-1, 72-73	17.12	0.069	0.6	0.80	0.73	0.14	0.46	5.4
3H-3, 19-20	19.60	0.026	0.2					
3H-5, 75-76	23.16	0.025	0.2					
4H-1, 76-77	26.66	0.027	0.2	0.78	0.76	0.11	0.38	6.6
4H-3, 76-77	29.66	0.058	0.5					
4H-5, 76-77	32.66	0.038	0.3					
5H-1, 89-90	36.30	0.059	0.5	0.84	0.78	0.13	0.43	6.2
5H-3, 75-76	39.16	0.073	0.6					
5H-5, 122-123	42.62	0.074	0.6					
6H-2, 21-22	46.62	0.129	1.1	0.90	0.77	0.12	0.32	6.3
6H-4, 74-75	50.14	0.083	0.7					
6H-6, 75-76	53.16	0.052	0.4					
7H-2, 74-75	55.58	0.069	0.6	0.63	0.56	0.10	0.19	5.4
7H-4, 74-75	58.58	0.052	0.4					
7H-6, 74-75	61.58	0.085	0.7					
8H-2, 70-71	66.10	0.050	0.4	0.22	0.17	0.10	0.35	1.7
8H-3, 67-68	67.58	0.891	7.4					
9H-1, 122-123	74.62	0.044	0.4	0.94	0.89	0.13	0.44	6.8
9H-3, 109-110	77.50	0.085	0.7					
9H-4, 124-125	79.14	2.480	20.7					
10H-2, 112-114	85.53	4.361	36.3	5.00	0.64	0.08	0.32	7.9
10H-4, 115-116	88.56	0.029	0.2					
10H-6, 123-124	91.64	2.137	17.8					
11H-1, 108-109	93.48	0.097	0.8	0.95	0.85	0.13	0.36	6.8
11H-3, 98-99	96.38	5.624	46.8					
11H-5, 116-117	99.56	0.076	0.6					
12H-1, 109-110	103.00	0.114	1.0	1.02	0.91	0.12	0.45	7.2
12H-3, 103-104	105.94	0.084	0.7					
12H-5, 29-30	108.20	1.666	13.9					
13H-1, 123-124	112.64	0.062	0.5	0.74	0.67	0.15	0.81	4.6
13H-3, 69-70	115.10	0.066	0.6					
13H-5, 69-70	118.10	0.065	0.5					
13H-7, 4-5	120.44	3.270	27.2					
14H-1, 70-71	121.60	1.191	9.9	1.66	0.47	0.08	0.30	5.6
14H-3, 70-71	124.60	0.316	2.6					
14H-6, 71-72	129.12	0.205	1.7					
15H-1, 73-74	131.14	0.257	2.1	1.14	0.88	0.12	0.45	7.4
15H-3, 71-72	134.12	0.254	2.1					
15H-5, 72-73	137.12	1.343	11.2					
16H-3, 70-71	143.60	0.087	0.7	0.90	0.81	0.12	0.41	6.8
16H-4, 70-71	145.10	0.417	3.5					
17H-2, 72-73	151.62	0.081	0.7	0.86	0.78	0.12	0.40	6.5
17H-4, 19-20	154.10	1.774	14.8					
17H-6, 49-50	157.40	2.134	17.8					
18H-2, 72-73	161.12	0.286	2.4	0.72	0.43	0.08	0.19	5.4
18H-4, 73-74	164.14	1.796	15.0					
19H-2, 32-33	170.22	0.200	1.7	0.81	0.61	0.10	0.34	5.8
19H-3, 75-76	172.16	2.573	21.4					
19H-5, 20-21	174.60	0.075	0.6					
20H-1, 110-111	179.00	0.978	8.1	1.79	0.81	0.11	0.29	7.1
20H-3, 86-87	181.76	0.106	0.9					
20H-5, 29-30	184.20	0.766	6.4					
21H-1, 76-77	188.16	0.069	0.6	0.24	0.18	0.08	0.22	2.2
21H-3, 108-109	191.12	0.098	0.8					
21H-5, 109-110	194.12	0.058	0.5					
23H-1, 19-20	206.60	0.437	3.6	1.01	0.57	0.09	0.53	6.4
23H-3, 29-30	209.70	2.059	17.1					
23H-5, 28-29	212.68	0.288	2.4					
25H-6, 112-113	234.02	0.093	0.8	0.56	0.47	0.08	0.15	5.8

Table T14 (continued).

Core, section, interval (cm)	Depth (mbsf)	IC (wt%)	$CaCO_3$ (wt%)	TC (wt%)	TOC (wt%)	TN (wt%)	TS (wt%)	TOC/TN
26H-2, 72-73	237.12	0.054	0.4	0.64	0.58	0.10	0.23	5.7
26H-4, 54-55	239.94	0.631	5.3					
26H-6, 112-113	243.52	0.320	2.7					
27H-4, 38-39	249.28	0.170	1.4	0.36	0.19	0.10	0.18	2.0
27H-6, 28-29	252.18	0.073	0.6					
28H-2, 69-70	256.10	0.080	0.7	0.89	0.81	0.13	1.33	6.4
28H-4, 98-99	259.38	2.893	24.1					
28H-6, 98-99	262.38	0.131	1.1					
29H-1, 99-100	264.40	0.071	0.6	0.70	0.63	0.10	0.63	6.3
29H-4, 69-70	268.60	0.532	4.4					
29H-6, 28-29	271.18	0.069	0.6					
30H-1, 71-72	273.62	0.072	0.6	0.58	0.50	0.11	0.12	4.7
30H-3, 109-110	277.00	1.189	9.9					
30H-5, 71-72	279.62	0.074	0.6					
31H-1, 89-90	283.30	0.050	0.4	0.55	0.50	0.11	0.15	4.7
31H-3, 73-74	286.14	0.069	0.6					
31H-5, 29-30	288.70	0.317	2.6					
32H-1, 73-74	292.64	0.067	0.6	0.32	0.25	0.10	0.07	2.5
32H-3, 71-72	295.62	0.056	0.5					
32H-5, 59-60	298.50	0.266	2.2					
33H-2, 74-75	303.64	0.056	0.5	0.46	0.40	0.09	0.00	4.3
33H-5, 30-31	307.70	0.067	0.6					

Note: IC = inorganic carbon, $CaCO_3$ = calcium carbonate, TC = total carbon, TOC = total organic carbon, TN = total nitrogen, TS = total sulfur.

Table T15. Summary of physical properties measurements conducted at Site 1091.

Measurement	Core 177-1091A-	Core 177-1091B-	Core 177-1091C-	Core 177-1091D-	Core 177-1091E-
GRA sample spacing	1H-24H: 2 cm; 25H-33H: 4 cm	1H-29H: 4 cm	1H: 4 cm	1H-22H: 4 cm	1H-6H: 4 cm
MS sample spacing	1H-24H: 2 cm; 25H-33H: 4 cm	1H-29H: 4 cm	1H: 4 cm	1H-22H: 4 cm	1H-6H: 4 cm
NGR sample spacing	1H-23H: 2 cm; 24H-33H: 4 cm	3H-29H: 4 cm	1H: 4 cm	3H-13H4: 4 cm; 13H5-15H3: 8 cm	—
PWL sample spacing	1H-24H: 2 cm; 25H-33H: 4 cm	3H-29H: 4 cm	1H: 4 cm	3H-22H: 4 cm	4H-6H: 4 cm
OSU-SCAT sample spacing	1H-17H3: 4 cm; 17H4-33H: 6 cm	1H-29H: 6cm	—	—	—
CM-2002 sample spacing	—	—	1H: 5 cm	1H-22H: 5 cm	1H-6H: 5 cm
PWS3	*N* = 311	*N* = 126	—	—	—
MAD	*N* = 172	*N* = 50	—	—	—
TC	*N* = 31	*N* = 28	—	*N* = 22	—

Note: GRA = gamma-ray attenuation, MS = magnetic susceptibility, NGR = natural gamma radiation, PWL = *P*-wave logger, OSU-SCAT = Oregon State University Split Core Analysis Track, CM-2002 = Minolta spectrophotometer, PWS3 = *P*-wave velocity sensor 3 for split cores, MAD = moisture and density, TC = thermal conductivity.

Table T16. Thermal conductivity measurements at Site 1091. (See table note. Continued on next two pages.)

Core, section, interval (cm)	Depth (mbsf)	Depth (mcd)	TC (W/[m·K])	Start (s)	Length (s)	End (s)
177-1091A-						
1H-3, 50	3.50	3.50	0.686	75.0	26.0	101.0
1H-3, 50	3.50	3.50	0.666	123.0	26.5	149.5
2H-3, 50	10.40	13.32	0.671	51.5	26.0	77.5
2H-3, 50	10.40	13.32	0.647	73.5	25.0	98.5
3H-3, 50	19.90	22.08	0.730	30.0	28.5	58.5
5H-3, 50	38.90	41.21	0.664	66.5	26.5	93.0
6H-3, 50	48.40	51.87	0.695	87.0	25.0	112.0
6H-3, 50	48.40	51.87	0.662	113.5	25.0	138.5
7H-3, 50	56.84	60.65	0.633	115.5	28.0	143.5
7H-3, 50	56.84	60.65	0.630	89.0	26.5	115.5
8H-3, 75	67.65	72.54	0.681	26.5	25.0	51.5
8H-3, 75	67.65	72.54	0.642	113.0	25.0	138.0
9H-3, 50	76.90	81.35	0.705	47.0	25.0	72.0
9H-3, 50	76.90	81.35	0.688	75.0	25.0	100.0
10H-3, 50	86.40	91.79	0.726	91.5	25.0	116.5
10H-3, 50	86.40	91.79	0.743	55.5	28.0	83.5
11H-3, 50	95.90	101.66	0.686	69.0	26.0	95.0
11H-3, 50	95.90	101.66	0.710	33.5	25.0	58.5
12H-3, 50	105.40	112.66	0.703	59.5	25.0	84.5
13H-3, 50	114.90	121.44	0.677	93.0	25.0	118.0
13H-3, 50	114.90	121.44	0.678	109.0	25.0	134.0
14H-3, 50	124.40	133.01	0.698	96.0	25.0	121.0
14H-3, 50	124.40	133.01	0.684	98.5	32.0	130.5
16H-3, 50	143.40	157.26	0.707	57.5	25.0	82.5
17H-3, 50	152.90	165.61	0.694	37.0	25.0	62.0
17H-3, 50	152.90	165.61	0.691	70.0	25.0	95.0
18H-3, 50	162.40	176.89	0.700	106.5	25.0	131.5
18H-3, 50	162.40	176.89	0.704	63.0	25.0	88.0
19H-3, 50	171.90	188.03	0.668	75.5	28.0	103.5
19H-3, 50	171.90	188.03	0.660	120.5	25.0	145.5
20H-3, 50	181.40	198.84	0.646	69.0	27.0	96.0
20H-3, 50	181.40	198.84	0.639	115.0	27.0	142.0
21H-3, 50	190.53	207.42	0.716	103.5	25.0	128.5
22H-3, 50	200.40	219.54	0.636	95.5	25.0	120.5
22H-3, 50	200.40	219.54	0.639	59.0	25.0	84.0
23H-3, 50	209.90	230.30	0.691	109.0	25.0	134.0
23H-3, 50	209.90	230.30	0.682	124.0	25.0	149.0
24H-3, 50	219.09	240.56	0.718	88.0	25.0	113.0
24H-3, 50	219.09	240.56	0.718	99.5	25.0	124.5
25H-3, 50	228.90	250.37	0.711	58.5	26.5	85.0
26H-3, 50	238.40	260.09	0.683	41.5	25.0	66.5
26H-3, 50	238.40	260.09	0.666	94.0	25.0	119.0
27H-3, 50	247.90	269.15	0.702	37.5	25.0	62.5
27H-3, 50	247.90	269.15	0.680	77.0	31.0	108.0
28H-3, 50	257.40	279.87	0.668	85.0	25.0	110.0
28H-3, 50	257.40	279.87	0.667	102.5	25.0	127.5
29H-3, 50	266.90	289.11	0.769	50.5	30.5	81.0
30H-3, 50	276.40	298.87	0.696	85.0	25.0	110.0
30H-3, 50	276.40	298.87	0.685	118.5	25.0	143.5
31H-3, 75	286.15	308.62	0.629	104.0	26.0	130.0
31H-3, 75	286.15	308.62	0.632	57.5	25.0	82.5
32H-3, 75	295.65	318.12	0.760	44.0	26.0	70.0
32H-3, 75	295.65	318.12	0.728	120.5	25.0	145.5
33H-3, 75	305.15	327.62	0.745	59.0	30.0	89.0
33H-3, 75	305.15	327.62	0.720	109.0	25.5	134.5
177-1091B-						
1H-3, 50	3.50	3.50	0.685	106.5	25.0	131.5
1H-3, 50	3.50	3.50	0.700	70.5	29.5	100.0
2H-3, 50	11.30	11.52	0.757	106.0	27.0	133.0
2H-3, 50	11.30	11.52	0.764	72.5	25.0	97.5
3H-3, 50	19.41	18.27	0.672	99.0	25.0	124.0
3H-3, 50	19.41	18.27	0.667	117.5	26.0	143.5
4H-3, 50	30.30	29.38	0.666	49.0	26.0	75.0
4H-3, 50	30.30	29.38	0.637	113.5	25.0	138.5
5H-3, 50	39.80	38.94	0.617	121.0	26.5	147.5

Table T16 (continued).

Core, section, interval (cm)	Depth (mbsf)	Depth (mcd)	TC (W/[m·K])	Start (s)	Length (s)	End (s)
5H-3, 50	39.80	38.94	0.624	86.0	27.0	113.0
6H-3, 50	49.30	48.33	0.673	77.5	25.0	102.5
6H-3, 50	49.30	48.33	0.652	108.0	25.0	133.0
7H-3, 75	59.05	57.86	0.721	44.5	25.0	69.5
7H-3, 75	59.05	57.86	0.680	108.5	25.0	133.5
8H-3, 75	68.55	70.46	0.690	50.0	25.0	75.0
8H-3, 75	68.55	70.46	0.663	100.5	28.5	129.0
9H-3, 75	78.05	78.72	0.689	98.0	25.0	123.0
9H-3, 75	78.05	78.72	0.692	79.5	25.0	104.5
10H-3, 75	87.55	88.90	0.455	71.0	30.0	101.0
11H-3, 60	96.90	98.76	0.680	120.0	28.0	148.0
11H-3, 60	96.90	98.76	0.667	124.0	25.5	149.5
12H-3, 60	106.40	108.45	0.698	113.5	25.5	139.0
12H-3, 60	106.40	108.45	0.700	111.0	29.5	140.5
13H-3, 60	115.90	118.01	0.736	30.5	25.0	55.5
14H-3, 60	125.40	128.92	0.712	88.0	25.0	113.0
14H-3, 60	125.40	128.92	0.740	38.5	25.0	63.5
15H-3, 60	134.90	137.61	0.649	84.5	25.0	109.5
15H-3, 60	134.90	137.61	0.647	59.5	33.0	92.5
16H-3, 75	144.55	149.56	0.721	53.5	25.0	78.5
16H-3, 75	144.55	149.56	0.706	72.0	26.0	98.0
17H-3, 75	154.05	160.27	0.696	84.0	25.0	109.0
17H-3, 75	154.05	160.27	0.670	123.0	26.5	149.5
18H-3, 75	163.55	172.15	0.694	102.0	28.0	130.0
18H-3, 75	163.55	172.15	0.705	87.0	26.5	113.5
19H-3, 60	172.90	184.11	0.686	120.5	25.5	146.0
19H-3, 60	172.90	184.11	0.685	91.5	25.0	116.5
20H-3, 75	182.55	195.67	0.685	68.0	25.0	93.0
20H-3, 75	182.55	195.67	0.685	67.0	29.0	96.0
21H-3, 75	192.05	205.52	0.693	68.5	25.0	93.5
21H-3, 75	192.05	205.52	0.675	111.0	25.0	136.0
22H-3, 60	201.40	216.42	0.631	102.5	30.0	132.5
23H-3, 60	210.90	225.48	0.635	116.5	25.0	141.5
23H-3, 60	210.90	225.48	0.630	33.0	25.0	58.0
24H-1, 75	217.55	233.13	0.679	75.5	26.0	101.5
25H-3, 60	229.90	245.13	0.688	83.0	26.5	109.5
25H-3, 60	229.90	245.13	0.683	82.5	25.0	107.5
26H-3, 75	239.55	256.82	0.617	48.5	25.0	73.5
26H-3, 75	239.55	256.82	0.605	83.0	25.0	108.0
27H-3, 75	249.05	268.02	0.705	72.0	29.5	101.5
27H-3, 75	249.05	268.02	0.695	97.5	25.5	123.0
29H-3, 75	268.05	284.22	0.709	93.5	25.5	119.0
29H-3, 75	268.05	284.22	0.697	95.5	25.0	120.5
177-1091D-						
1H-2, 75	2.25	10.24	0.684	87.0	29.0	116.0
1H-2, 75	2.25	10.24	0.687	57.5	25.0	82.5
2H-2, 75	5.85	17.77	0.673	99.0	25.5	124.5
2H-2, 75	5.85	17.77	0.654	108.5	25.0	133.5
3H-3, 75	16.85	27.26	0.654	101.0	25.5	126.5
3H-3, 75	16.85	27.26	0.650	92.5	27.0	119.5
4H-3, 75	26.35	36.13	0.672	87.5	25.0	112.5
4H-3, 75	26.35	36.13	0.654	120.0	25.0	145.0
5H-3, 75	35.85	47.64	0.657	76.0	27.5	103.5
5H-3, 75	35.85	47.64	0.670	48.5	25.0	73.5
6H-3, 75	45.35	54.35	0.724	62.5	26.5	89.0
6H-3, 75	45.35	54.35	0.708	114.5	25.0	139.5
7H-3, 75	54.85	63.43	0.686	94.5	25.0	119.5
7H-3, 75	54.85	63.43	0.691	65.0	25.0	90.0
8H-3, 75	64.35	71.25	0.732	50.0	25.0	75.0
8H-3, 75	64.35	71.25	0.731	75.5	25.0	100.5
9H-3, 60	73.70	83.49	0.648	121.5	25.0	146.5
9H-3, 60	73.70	83.49	0.655	102.0	28.0	130.0
10H-3, 75	83.35	95.51	0.679	90.0	25.0	115.0
10H-3, 75	83.35	95.51	0.683	75.0	25.5	100.5
11H-3, 75	92.85	105.50	0.717	66.0	26.0	92.0
11H-3, 75	92.85	105.50	0.713	68.0	25.0	93.0
11H-3, 75	92.85	105.50	0.707	93.0	26.0	119.0
11H-3, 75	92.85	105.50	0.708	86.5	26.5	113.0
12H-3, 75	102.35	115.16	0.684	49.5	25.0	74.5

Table T16 (continued).

Core, section, interval (cm)	Depth (mbsf)	Depth (mcd)	TC (W/[m·K])	Start (s)	Length (s)	End (s)
12H-3, 75	102.35	115.16	0.651	115.5	30.0	145.5
13H-3, 75	111.85	125.50	0.696	110.0	25.0	135.0
13H-3, 75	111.85	125.50	0.685	124.0	25.5	149.5
14H-3, 75	121.35	135.15	0.701	58.5	25.0	83.5
14H-3, 75	121.35	135.15	0.692	74.5	25.0	99.5
15H-3, 60	130.70	146.17	0.767	93.0	26.5	119.5
16H-3, 75	140.35	156.32	0.731	124.0	25.0	149.0
16H-3, 75	140.35	156.32	0.730	102.0	25.0	127.0
17H-3, 75	149.85	167.57	0.652	89.5	34.0	123.5
17H-3, 75	149.85	167.57	0.643	108.5	26.0	134.5
18H-3, 75	159.35	178.26	0.726	38.5	25.0	63.5
19H-3, 75	168.85	189.54	0.693	43.0	25.0	68.0
19H-3, 75	168.85	189.54	0.674	84.5	25.0	109.5
20H-3, 75	178.35	200.78	0.670	115.0	25.0	140.0
20H-3, 75	178.35	200.78	0.668	97.0	25.0	122.0
21H-3, 75	187.85	211.55	0.660	106.0	26.0	132.0
21H-3, 75	187.85	211.55	0.654	117.5	25.5	143.0
22H-3, 75	197.35	221.68	0.750	100.0	25.5	125.5

Notes: TC = thermal conductivity. Start, Length, and End refer to the interval of the time-temperature series used for the determination of thermal conductivity. This table is also available in ASCII format in the **TABLES** directory.